6 FLAW TOLERANCE CHARTS

6.1 INTRODUCTION

The flaw tolerance charts were developed using the stress analysis of each of the penetration locations as discussed in Section 5. The crack growth law developed for San Onofre Units 2 & 3 in Section 4.2 was used for each case, and several flaw tolerance charts were developed for each penetration location. The first series of charts characterizes the growth of a part through flaw and is used in predicting remaining service life of the penetration nozzle. The second series of charts, which characterizes the growth of a through-wall flaw below the J-groove weld, can be used to determine the minimum required inspection coverage to ensure that any flaws initiated below the weld in the un-inspected region of the penetration nozzle would not reach the bottom of the weld in less than one operating fuel cycle. All times resulting from these calculations are Effective Full Power Years, since crack growth will only occur at operating temperatures.

6.2 OVERALL APPROACH

The results of the three-dimensional stress analysis of the penetration locations were used directly in the flaw tolerance evaluation.

The crack growth evaluation for the part-through flaws was based on the worst stress distribution through the penetration wall at the location of interest of the penetration. The highest stressed location was found to be in the immediate vicinity of the weld for both the center and outermost penetrations.

The stress profile was represented by a cubic polynomial:

$$\sigma(x) = A_0 + A_1 x + A_2 x^2 + A_3 x^3 \tag{6-1}$$

where:

x	=	the coordinate distance into the nozzle wall
σ	=	stress perpendicular to the plane of the crack
A_I	=	coefficients of the cubic polynomial fit

For the surface flaw with length six times its depth, the stress intensity factor expression of Raju and Newman [5A] was used. The stress intensity factor $K_I(\Phi)$ can be calculated anywhere along the crack front. The point of maximum crack depth is represented by $\Phi = 0$, and this location was also found to be the point of maximum K_I for the cases considered here. The following expression is used for calculating $K_I(\Phi)$, where Φ is the angular location around the crack. The units of $K_I(\Phi)$ are $\text{ksi}\sqrt{\text{in}}$.

$$K_I(\Phi) = \left[\frac{\pi a}{Q}\right]^{0.5} \sum_{j=0}^{3} G_j\left(a/c,\ a/t,\ t/R,\ \Phi\right) A_j a^j \tag{6-2}$$

The boundary correction factors G_0 (Φ), G_1 (Φ), G_2 (Φ) and G_3 (Φ) are obtained by the procedure outlined in reference [5A]. The dimension "a" is the crack depth, and "c" is the semi crack length, while "t" is the wall thickness. "R" is the inside radius of the tube, and "Q" is the shape factor.

[

]a,c,e

6.3 AXIAL FLAW PROPAGATION

CEDM and ICI Surface Flaws

The results of the calculated growth for inside surface flaws growing through the wall thickness of the CEDM penetration nozzles are shown in Figures 6-2 through 6-7 for inside surface flaws. For outside surface flaws, the results are shown in Figures 6-9 and 6-10. Based on the discussion in MRP-55 report [4H], the use of stress intensity factors less than $15\,\mathrm{MPa}\sqrt{\mathrm{m}}$ involves assumption not currently substantiated by actual CGR data for neither CEDM or ICI nozzle materials. Therefore, these crack growth curves begin at a flaw depth that result in a stress intensity factor of $15\,\mathrm{MPa}\sqrt{\mathrm{m}}$, which exceeds the threshold value of $9\,\mathrm{MPa}\sqrt{\mathrm{m}}$. This may result in curves with different initial flaw sizes, as seen for example in Figure 6-3. Note that results are only provided for the uphill and downhill sides of each penetration nozzle. The stresses for the regions 90 degrees from these locations are in general compressive. If flaws are found in such a location, the results for either the uphill or downhill location, whichever is closer, can be conservatively used.

Each of these figures allows the future allowable service time to be estimated graphically, as discussed in Section 3. Results are shown for each of the penetration nozzles analyzed in each of these figures. The stresses are much higher near the attachment weld than at 0.5 inch below or above it, so separate figures have been provided for these three regions. For more than 0.5 inch below the weld, the crack growth will eventually come to rest since the stresses are compressive as shown for the CEDM/ICI nozzles in Appendix A. Also, the stresses are different on the downhill side of the penetration as opposed to the uphill side, so these two cross sections have also been treated separately.

It should be noted that the hoop stress distribution in Appendix A is determined based on the as-designed J-weld geometry. A comparison of the hoop stress distribution below the weld between the as-designed [6A] and as-built J-weld geometry [16] is shown in Appendix B. The comparison shows that the hoop stress below the weld on the downhill side for the as-built J-weld geometry is in general lower and that the magnitude of the hoop stress drops off faster as a function of distance away from the bottom of the J-weld.

Example problems are provided in section 7 for a range of possible flaw types.

Inspection Coverage of RPV Head Penetration Below the Weld

As a result of NRC Order EA-03-009, nearly all the plants in the United States have encountered problems with the required inspection coverage of the head penetrations below the weld. To support the submittal of relaxation request for less than 100% inspection coverage below the weld, a series of axial through-wall crack growth below the weld charts for the downhill side were prepared for each of the penetrations evaluated. The charts are shown in Figures 6-12 through 6-17.

There is nearly universal agreement that high stresses, on the order of the material yield strength, are necessary to initiate Primary Water Stress Corrosion Cracking (PWSCC). There is no known case of stress corrosion cracking of Alloy 600 below the yield stress [15]. Typical yield strengths

for wrought Alloy 600 head penetration nozzles are in the range of 37 ksi to 65 ksi. Weld metal yield strengths are generally higher. The yield strength of the head penetration nozzles for San Onofre varies from 35 ksi to 59 ksi [11]. The stress level of 20 ksi is a conservative value below which PWSCC initiation is extremely unlikely. Therefore the assumption of any PWSCC crack initiation in the region of the penetration nozzle with a stress level of 20 ksi or less is conservative.

In each of the figures, the location of the upper extremity of the postulated through-wall crack is identified on the charts by the distance measured from the bottom of weld. The initial through-wall flaw size is determined by assuming that the lower extremity of the through-wall flaw is located on the penetration nozzle where both the inside and outside surface hoop stress in the tensile region drops below 20 ksi [13]. If either inside or outside surface hoop stress becomes compressive before the opposite surface drops below 20 ksi, which is the case for the ICI nozzle on the uphill side, the lower extremity of the initial flaw is assumed to be where either the inside or outside surface hoop stress drops below 0 ksi. The time duration required for the upper extremity of an axial through-wall flaw to reach the bottom of the weld can be determined from these charts as illustrated in Example 5 of section 7.

A limiting case for the crack growth below the weld is shown in Appendix C. For this limiting case, the initial through-wall flaw size is determined by assuming that the lower extremity of the flaw is located on the penetration nozzle where either the inside or outside surface hoop stress drops below 0 ksi.

Head Vent

The only flaw tolerance chart that is necessary for the head vent region is for flaws at and above the weld, since there is no portion of the head vent which projects below the weld. Figure 6-8 provides the projected growth of a part through flaw in the head vent just above the attachment weld. The growth through the wall is relatively rapid, because the thickness of the head vent is small.

6.4 CIRCUMFERENTIAL FLAW PROPAGATION

Since circumferentially oriented flaws have been found at five plants (Bugey 3, Oconee 2, Crystal River 3, Davis Besse, and Oconee 3), it is important to consider the possibility of crack extension in the circumferential direction. The first case was discovered as part of the destructive examination of the tube with the most extensive circumferential cracking at Bugey 3. The crack was found to have extended to a depth of 2.25 mm in a wall thickness of 16 mm. The flaw was found at the outside surface of the penetration (number 54) at the downhill side location, just above the weld.

The circumferential flaws in Oconee Unit 3 were discovered during the process of repairing a number of axial flaws, whereas the circumferential flaw in Oconee Unit 2 and Crystal River Unit 3 were discovered by UT. Experience gained from these findings has enabled the development of UT procedures capable of detecting circumferential flaws reliably.

To investigate this issue completely, a series of crack growth calculations were carried out for a postulated surface circumferential flaw located just above the head penetration weld, in a plane parallel to the weld itself. This is the only flaw plane that could result in a complete separation of the penetration nozzle, since all others would result in propagation below the weld, and therefore there is no chance of complete separation because the remaining weld would hold the penetration nozzle in place.

[

]^{a,c,e} The results of this calculation are shown in Figure 6-18. From this figure, it can be seen that the time required for propagation of a circumferential flaw to a point where the integrity of the CEDM penetration nozzle would be affected (330-350 degrees [10]) would be about 27 years. From the same figure, the required time for propagation of a circumferential flaw to a point where the integrity of the ICI penetration nozzles would be affected is about 40 years. Due to the conservatism in the calculations (the time period for a surface flaw to become a through-wall flaw was conservatively ignored) the service life is likely to be even longer. In addition, due to uncertainties in the exact composition of the chemical environment in contact with the nozzle OD, a multiplicative factor of 2.0 is used in the Crack Growth Rate (CGR) for all

circumferential surface flaws on the OD of the head penetration nozzles located above the elevation of the J-groove weld.

6.5 FLAW ACCEPTANCE CRITERIA

Now that the projected crack growth curves have been developed, the question remains as to what flaw size would be acceptable for further service.

Acceptance criteria have been developed for indications found during inspection of reactor vessel upper head penetration as part of an industry program coordinated by NEI (formerly NUMARC). Such criteria are normally found in Section XI of the ASME Code, but Section XI does not require in-service inspection of these regions and therefore acceptance criteria are not available. In developing the enclosed acceptance criteria, the approach used was very similar to that used by Section XI, in that an industry consensus was reached using input from both operating utility technical staff and each of the three PWR vendors. The criteria developed are applicable to all PWR plant designs.

Since the discovery of the leaks at Oconee and ANO-1, the acceptance criteria have been revised slightly to cover flaws on the outside diameter of the penetration below the attachment weld, and flaws in the attachment weld. These revised criteria are now formally endorsed by the NRC [12], and will be used in these evaluations. Portions of the acceptance criteria will be noted below.

The criteria presented herein are limits on flaw sizes, which are acceptable. The criteria are to be applied to inspection results. It should be noted that determination of the future service during which the criteria are satisfied is plant-specific and dependent on flaw geometry and loading conditions.

It has been previously demonstrated by each of the owners groups that the penetration nozzles are very tolerant of flaws and there is only a small likelihood of flaw extensions to larger sizes. Therefore, it was concluded that complete fracture of the penetration nozzle is highly unlikely. The approach used here is more conservative than that used in Section XI applications where the acceptable flaw size is calculated by placing a margin on the critical flaw size. For the current application, the critical flaw size would be far too large to allow a practical application of the approach used in Section XI applications, so protection against leakage is the priority.

The acceptance criteria presented herein apply to all the flaw types regardless of orientation and shape. Similar to the approach used in Section XI, flaws are first characterized according to established rules and then compared with acceptance criteria.

Flaw Characterization

Flaws detected must be characterized by the flaw length and preferably flaw depth. The proximity rules of Section XI for considering flaws as separate, may be used directly (Section XI, Figure IWA 3400-1). This figure is reproduced here as Figure 6-19.

When a flaw is detected, its projections in both the axial and circumferential directions must be determined. Note that the axial direction is always the same for each penetration, but the

circumferential direction will be different depending on the angle of intersection of the penetration nozzle with the vessel head. The "circumferential" direction of interest here is along the top of the attachment weld, as illustrated in Figure 6-20. It is this angle which will change for each penetration nozzle and the top of the attachment weld is also the plane which could cause separation of the penetration nozzle from the vessel head. The location of the flaw relative to both the top and bottom of the partial penetration attachment weld must also be determined since a potential leak path exists when a flaw propagates through the penetration nozzle wall and up the penetration nozzle past the attachment weld. Schematic of a typical weld geometry is shown in Figure 6-21.

Flaw Acceptance Criteria

The maximum allowable depth (a_f) for axial flaws on the inside surface of the penetration nozzle, at or above the weld is 75 percent of the penetration wall thickness. The term a_f is defined as the maximum size to which the detected flaw is calculated to grow in a specified time period. This 75 percent limitation was selected to be consistent with the maximum acceptable flaw depth in Section XI and to provide an additional margin against through wall penetration. There is no concern about separation of the penetration nozzle from the vessel head, unless the flaw is above the attachment weld and oriented circumferentially. Calculations have been completed to show that the geometry of all penetrations can support a continuous circumferential flaw with a depth of 75 percent of the wall thickness.

Axial inside surface flaws found below the weld are acceptable regardless of depth as long as their upper extremity does not reach the bottom of the weld during the period of service until the next inspection. Axial flaws that extend above the weld are limited to 75 percent of the wall thickness.

Axial flaws on the outside surface of the penetration nozzle below the attachment weld are acceptable regardless of depth, as long as they do not extend into the attachment weld during the period of service until next inspection. Outside surface flaws above the attachment weld must be evaluated on a case by case basis, and must be discussed with the regulatory authority.

Circumferential flaws located below the weld are acceptable regardless of their depth, provided the length is less than 75 percent of the penetration nozzle circumference for the period of service until the next inspection. Circumferential flaws detected in this area have no structural significance except that loose parts must be avoided. To this end, intersecting axial and circumferential flaws shall be removed or repaired. Circumferential flaws at and above the weld must be discussed with the regulatory authority on a case by case basis.

Surface flaws located in the attachment welds themselves are not acceptable regardless of their depth. This is because the crack growth rate of the weld material is several times faster than that of the Alloy 600 material, and also because depth sizing capability does not yet exist for indications in the attachment weld.

The flaw acceptance criteria are summarized in Table 6-1. Flaws that exceed these criteria must be repaired unless analytically justified for further service. These criteria have been reviewed and endorsed by the NRC, as documented in references [7, 8, 12].

It is expected that the use of these criteria and crack growth curves will provide conservative predictions of the allowable service time.

Table 6-1 Summary of R.V. Head Penetration Flaw Acceptance Criteria

Location	Axial		Circumferential	
	a_f	ℓ	a_f	ℓ
Below Weld (ID)	t	no limit	t	.75 circ.
At and Above Weld (ID)	0.75 t	no limit	repair	repair
Below Weld (OD)	t	no limit	t	.75 circ.
Above Weld (OD)	repair	repair	repair	repair

Note: Surface flaws of any size in the attachment weld are not acceptable.

a_f = Flaw Depth
ℓ = Flaw Length
t = Wall Thickness

Table 6-2 San Onofre Units 2 & 3 Penetration Geometries

Penetration Type	Wall Thickness (in.)	Penetration OD (in.)
CEDM	0.661	4.050
ICI	0.469*	5.563
ICI Counterbore	0.407*	5.563
Head Vent	0.154	1.05

*ICI counterbore wall thickness shall be used when evaluating ICI nozzle flaws at all time.

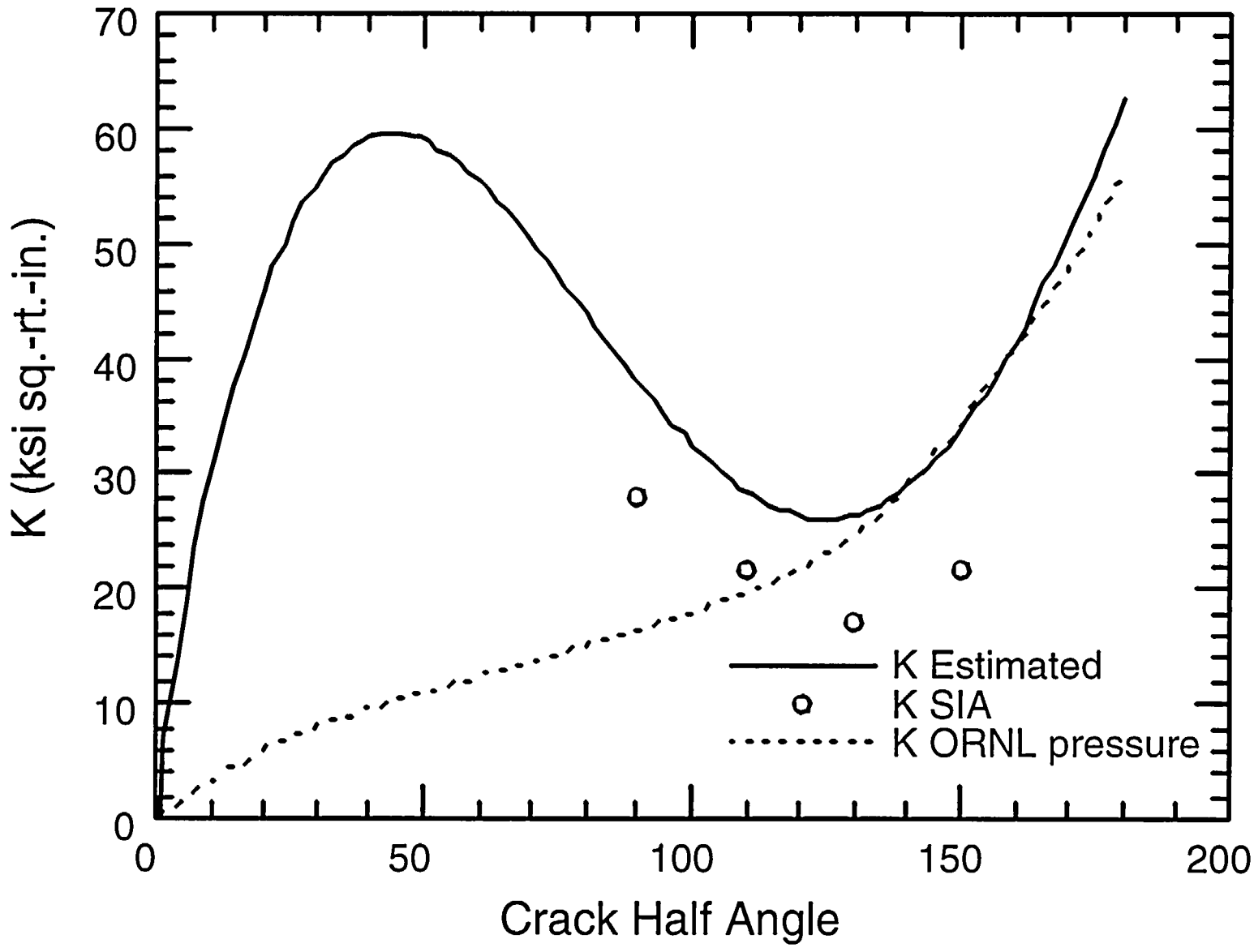

Figure 6-1 Stress Intensity Factor for a Through-Wall Circumferential Flaw in a Head Penetration

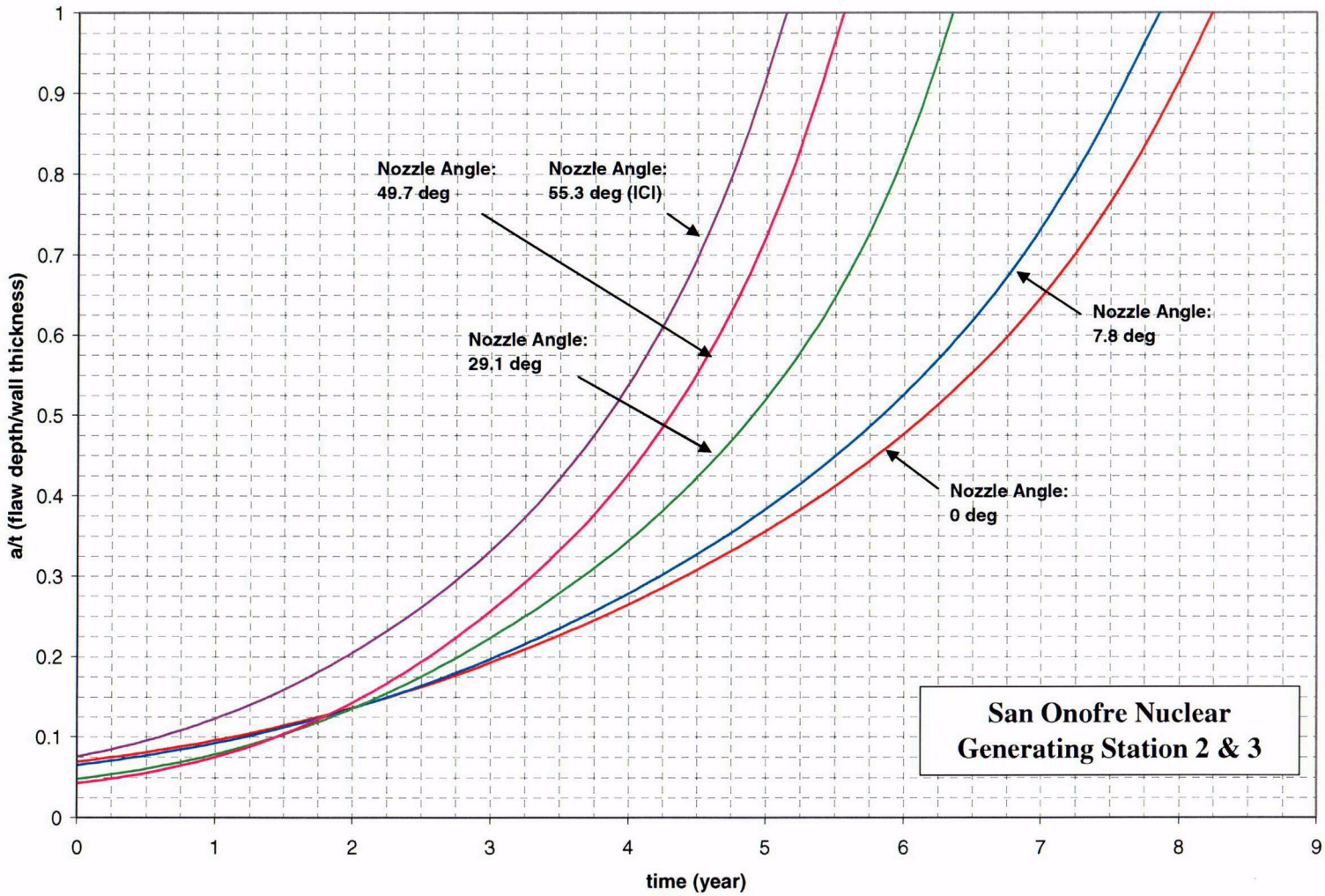

Figure 6-2 **Inside, Axial Surface Flaws, .5" Below the Attachment Weld, Nozzle Uphill Side - Crack Growth Predictions for San Onofre Units 2 & 3**

C11

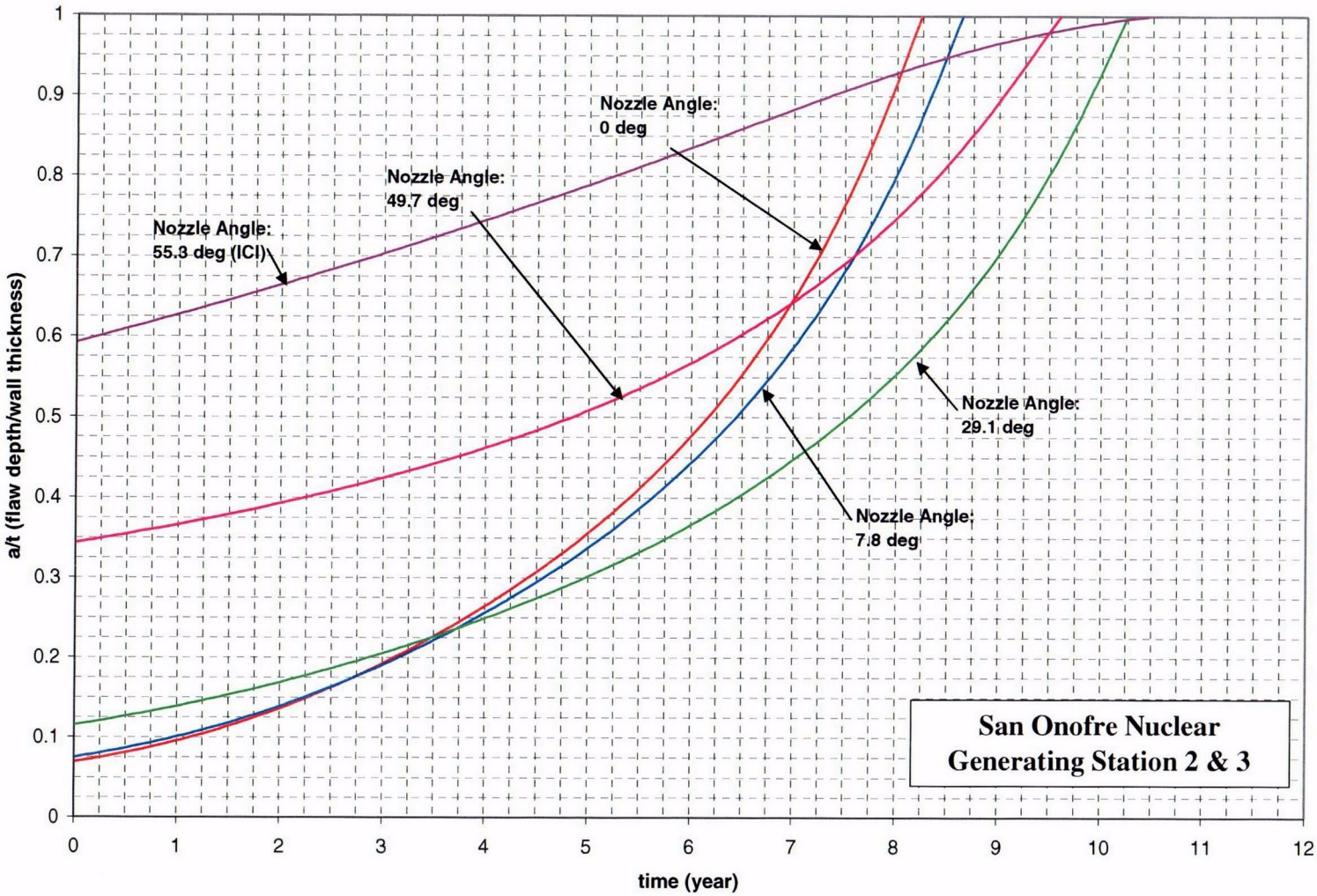

Figure 6-3 **Inside, Axial Surface Flaws, .5" Below the Attachment Weld, Nozzle Downhill Side - Crack Growth Predictions for San Onofre Units 2 & 3**

C12

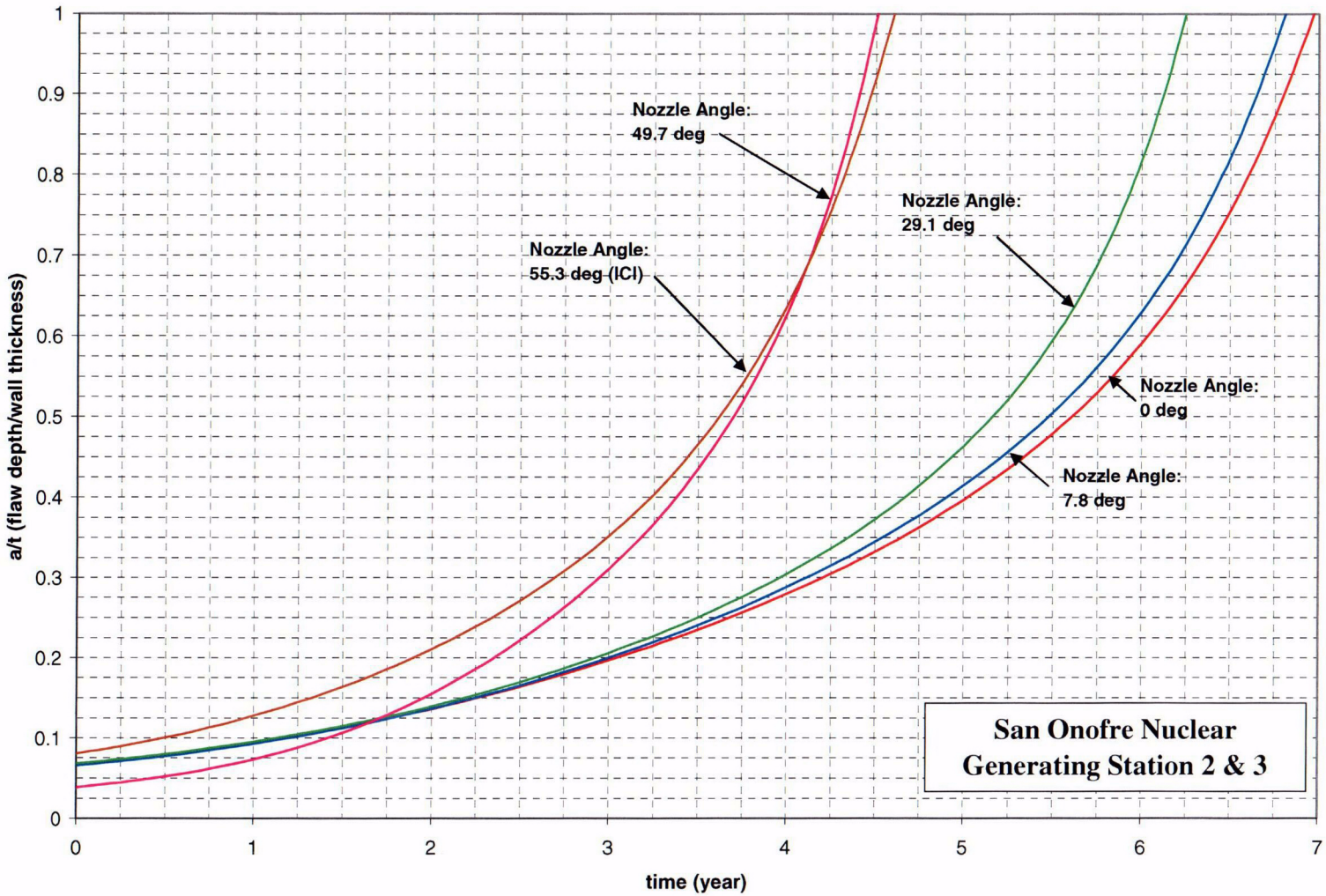

Figure 6-4 **Inside, Axial Surface Flaws, At the Attachment Weld, Nozzle Uphill Side - Crack Growth Predictions for San Onofre Units 2 & 3**

C13

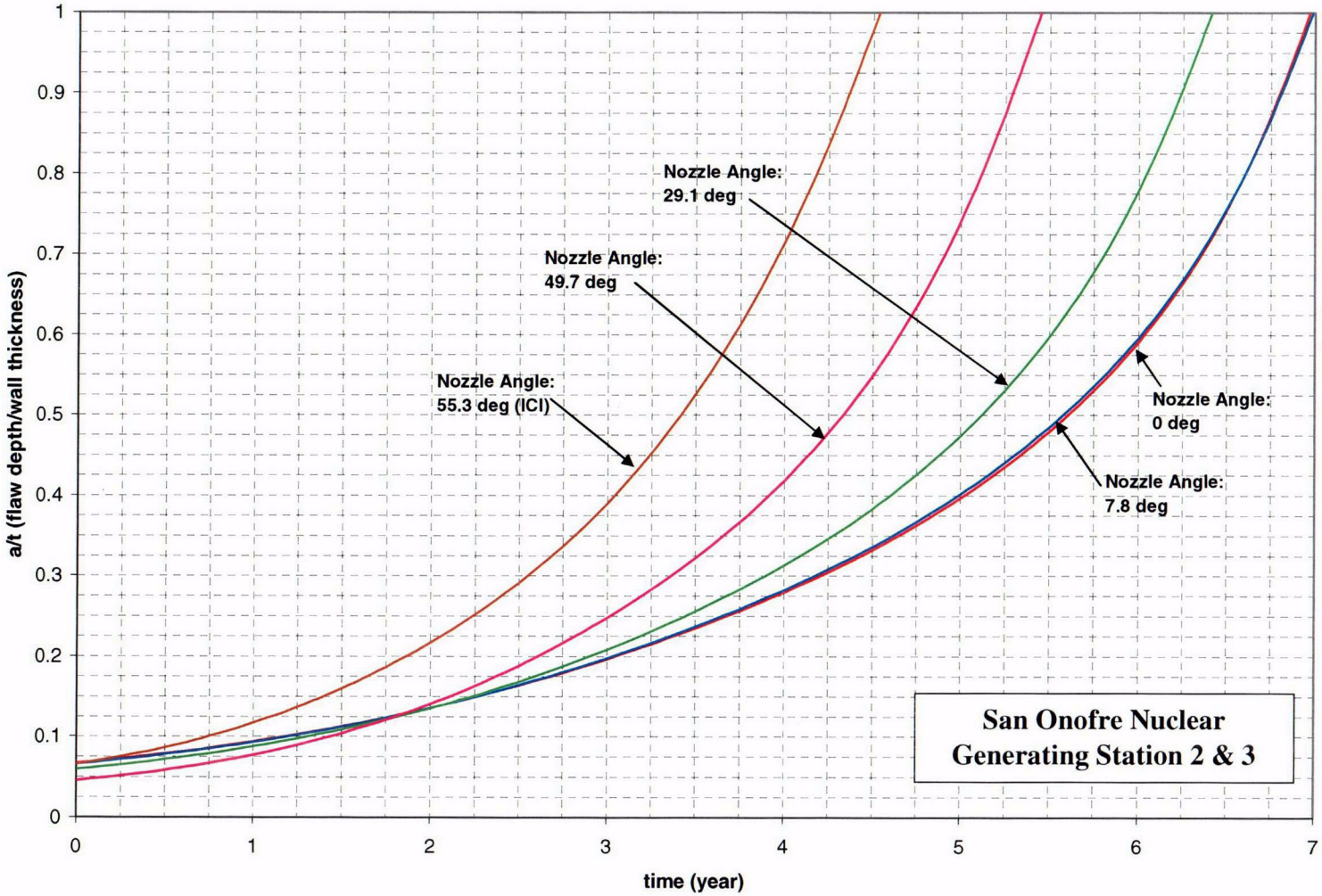

Figure 6-5 **Inside, Axial Surface Flaws, At the Attachment Weld, Nozzle Downhill Side - Crack Growth Predictions for San Onofre Units 2 & 3**

C14

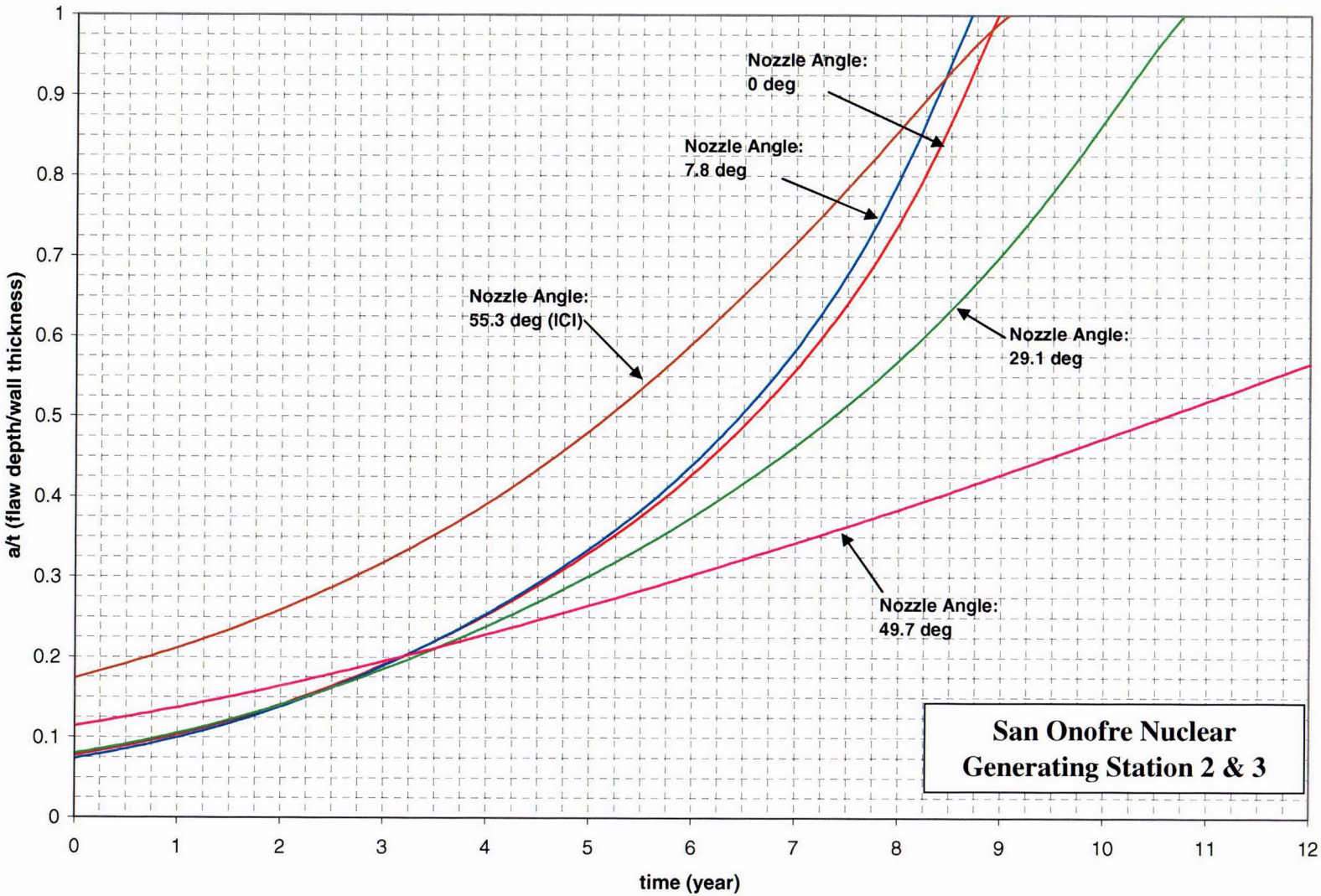

Figure 6-6 **Inside, Axial Surface Flaws, .5" Above the Attachment Weld, Nozzle Uphill Side - Crack Growth Predictions for San Onofre Units 2 & 3**

C15

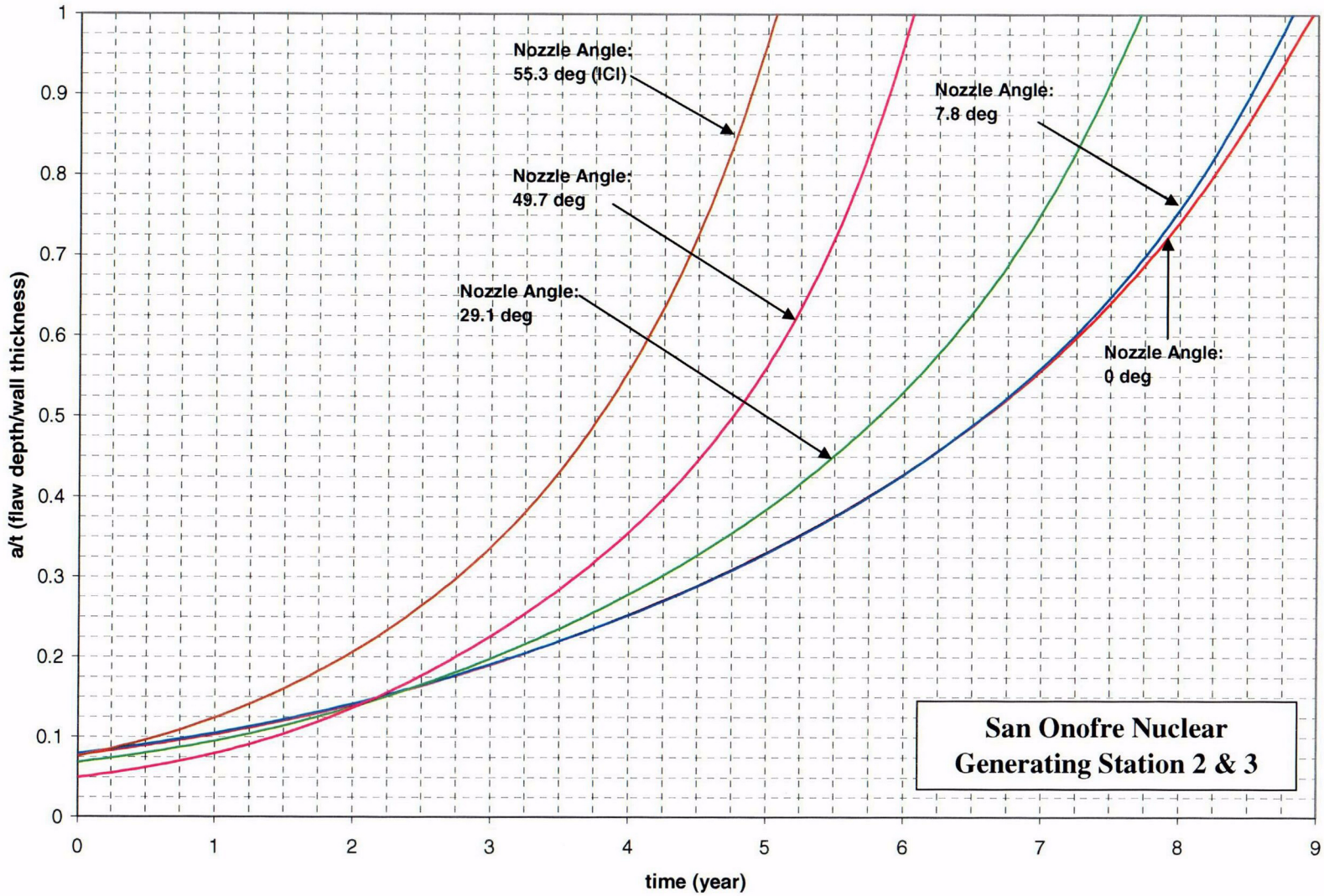

Figure 6-7 **Inside, Axial Surface Flaws, .5" Above the Attachment Weld, Nozzle Downhill Side - Crack Growth Predictions for San Onofre Units 2 & 3**

C16

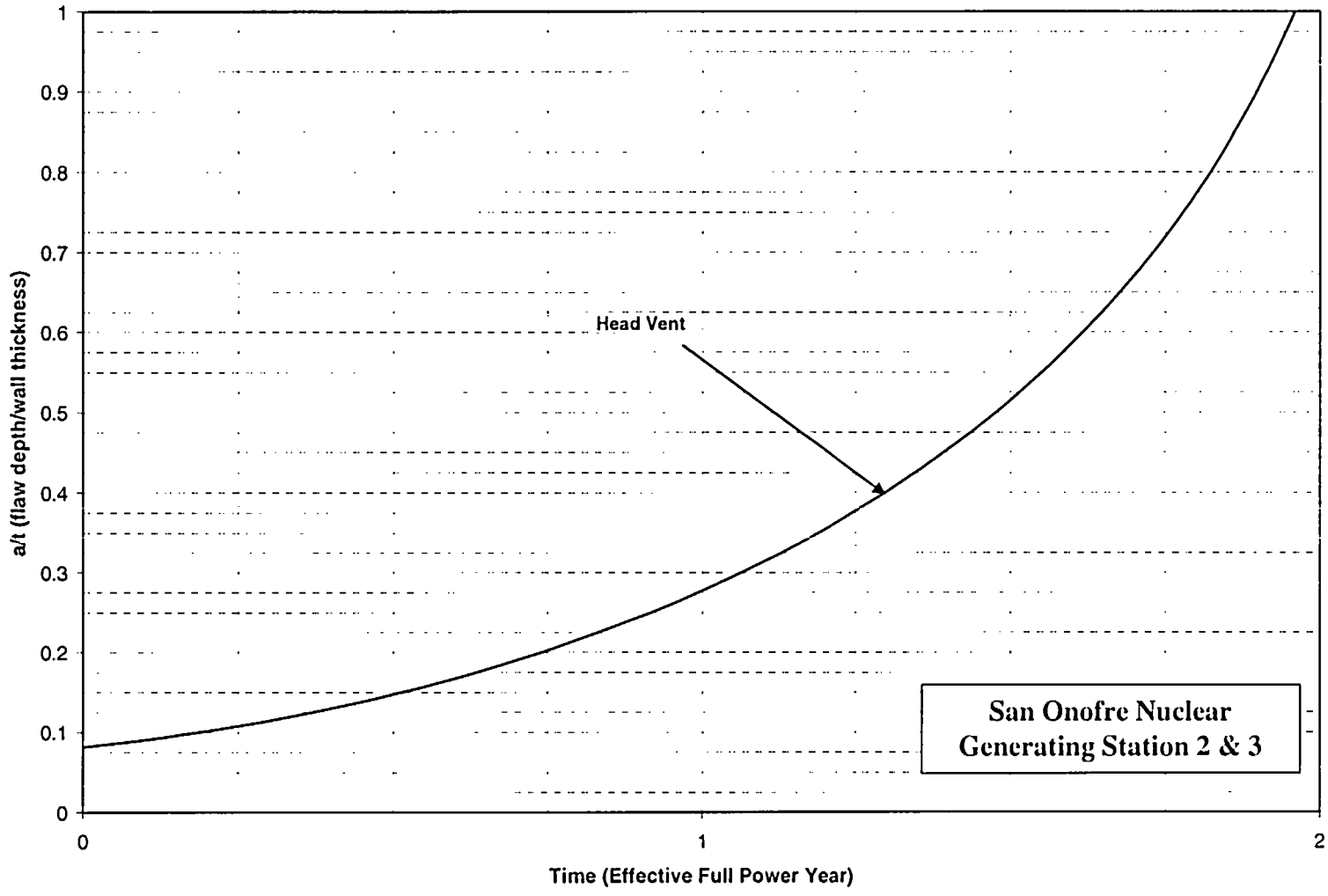

Figure 6-8 Inside, Axial Surface Flaws, At the Attachment Weld, Head Vent- Crack Growth Predictions for San Onofre Units 2 & 3

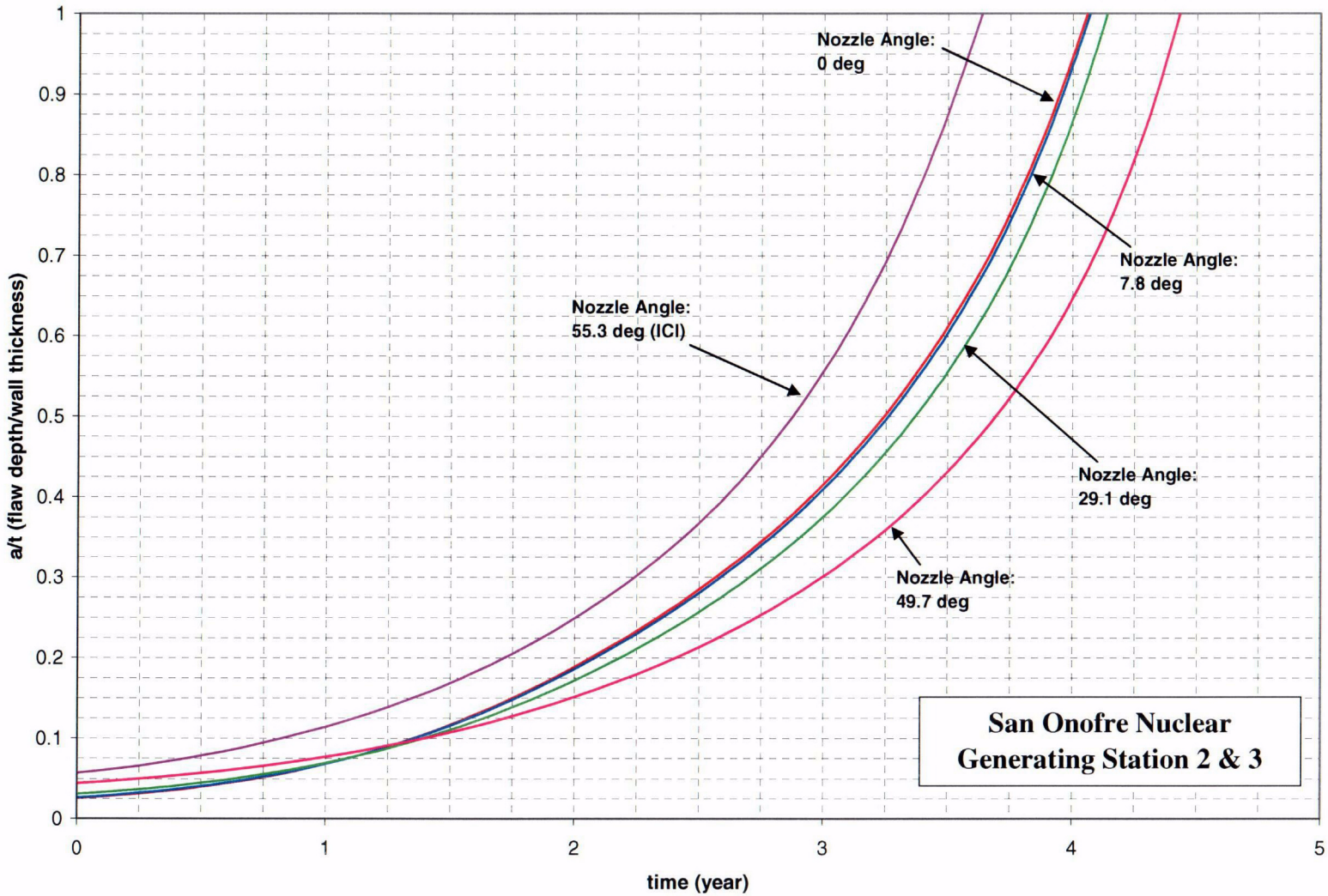

Figure 6-9 **Outside, Axial Surface Flaws, Below the Attachment Weld, Nozzle Uphill Side - Crack Growth Predictions for San Onofre Units 2 & 3**

C17

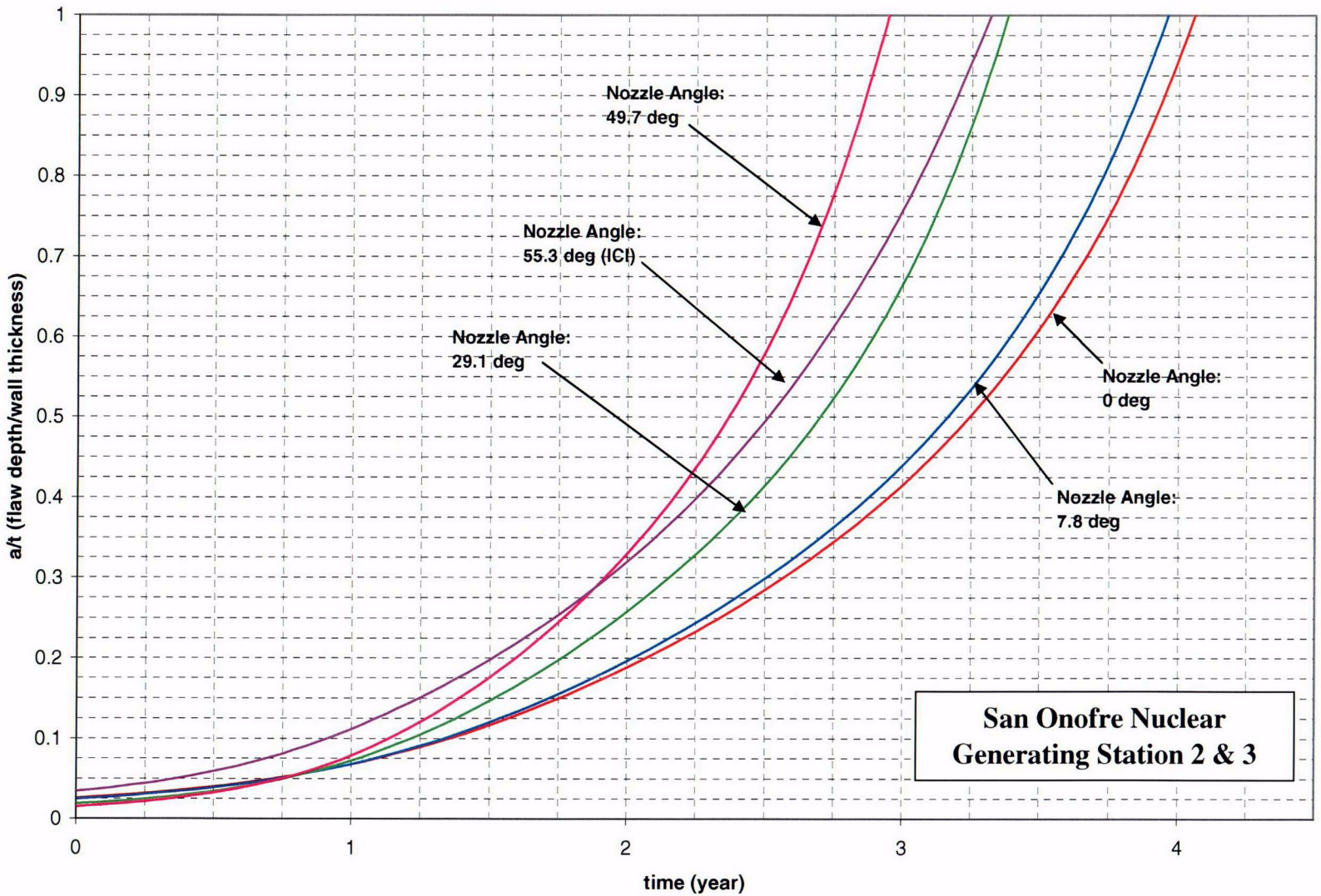

Figure 6-10 **Outside, Axial Surface Flaws, Below the Attachment Weld, Nozzle Downhill Side - Crack Growth Predictions for San Onofre Units 2 & 3**

C18

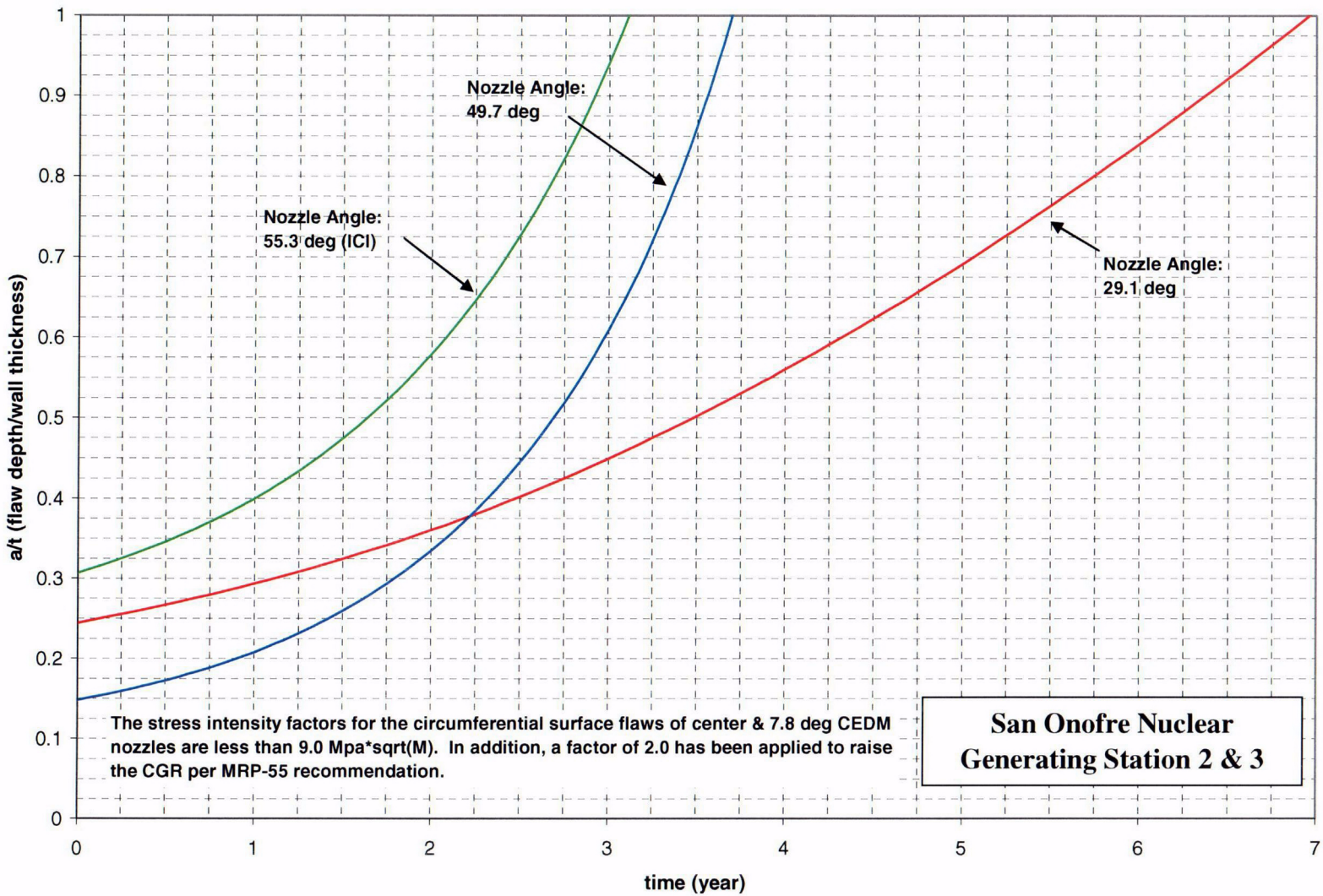

Figure 6-11 **Outside, Circumferential Surface Flaws, Along the Top of the Attachment Weld - Crack Growth Predictions for San Onofre Units 2 & 3 (MRP Factor of 2.0 Included)**

C19

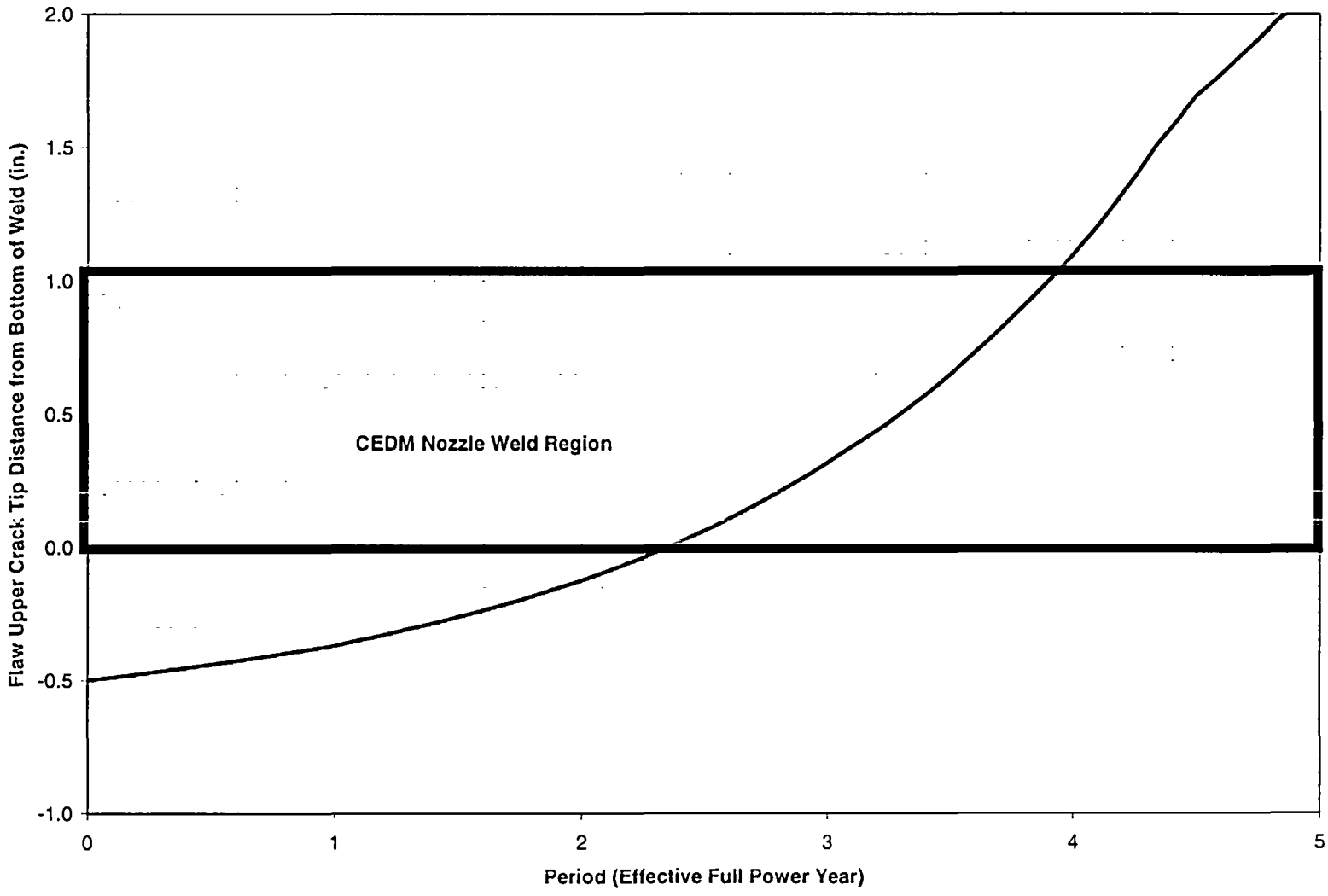

Figure 6-12 Through-Wall Axial Flaws Located in the Center CEDM (0.0 Degrees) Penetration - Crack Growth Predictions for San Onofre Units 2 & 3

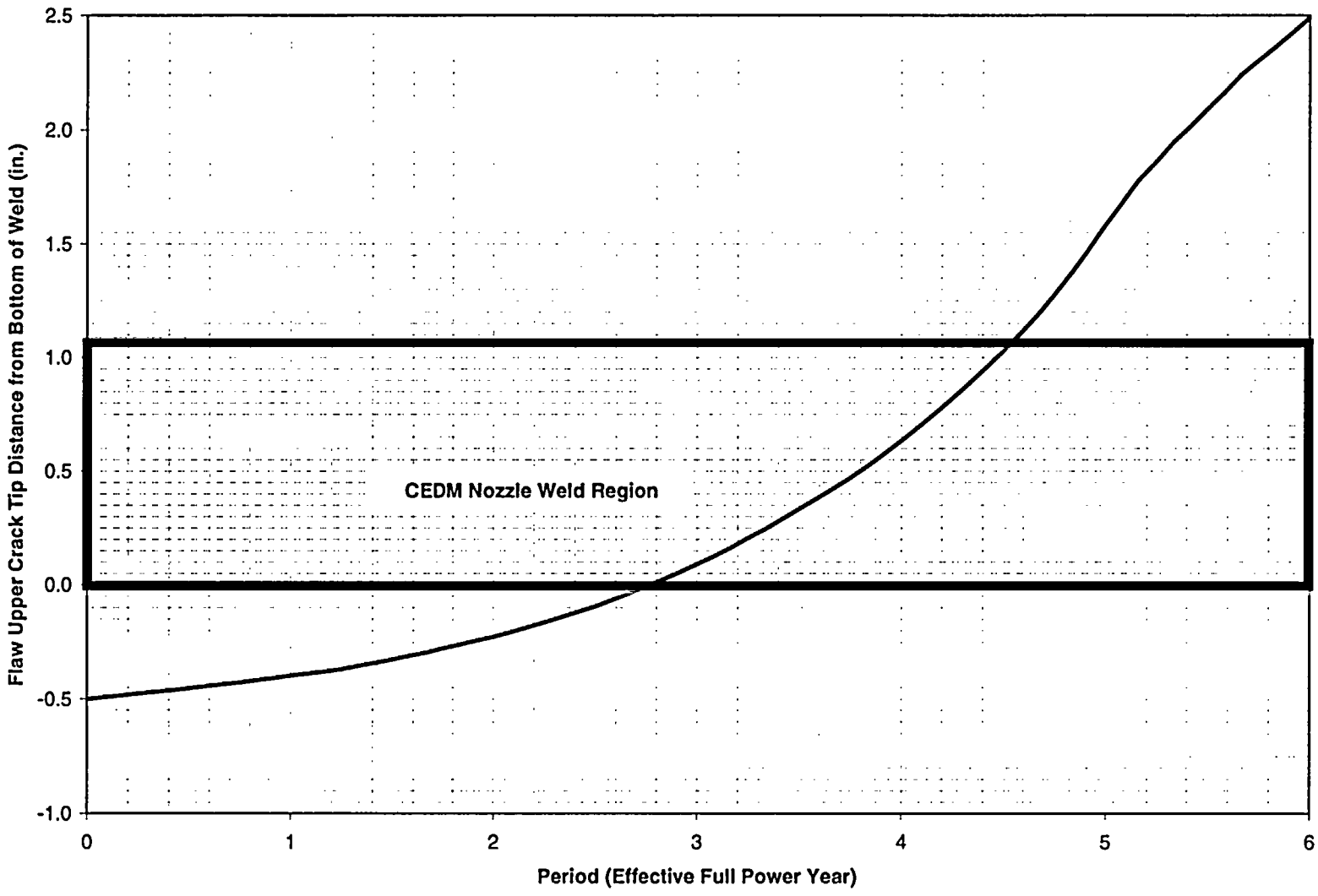

Figure 6-13 Through-Wall Axial Flaws Located in the 7.8 Degrees CEDM Row of Penetrations, Downhill Side - Crack Growth Predictions for San Onofre Units 2 & 3

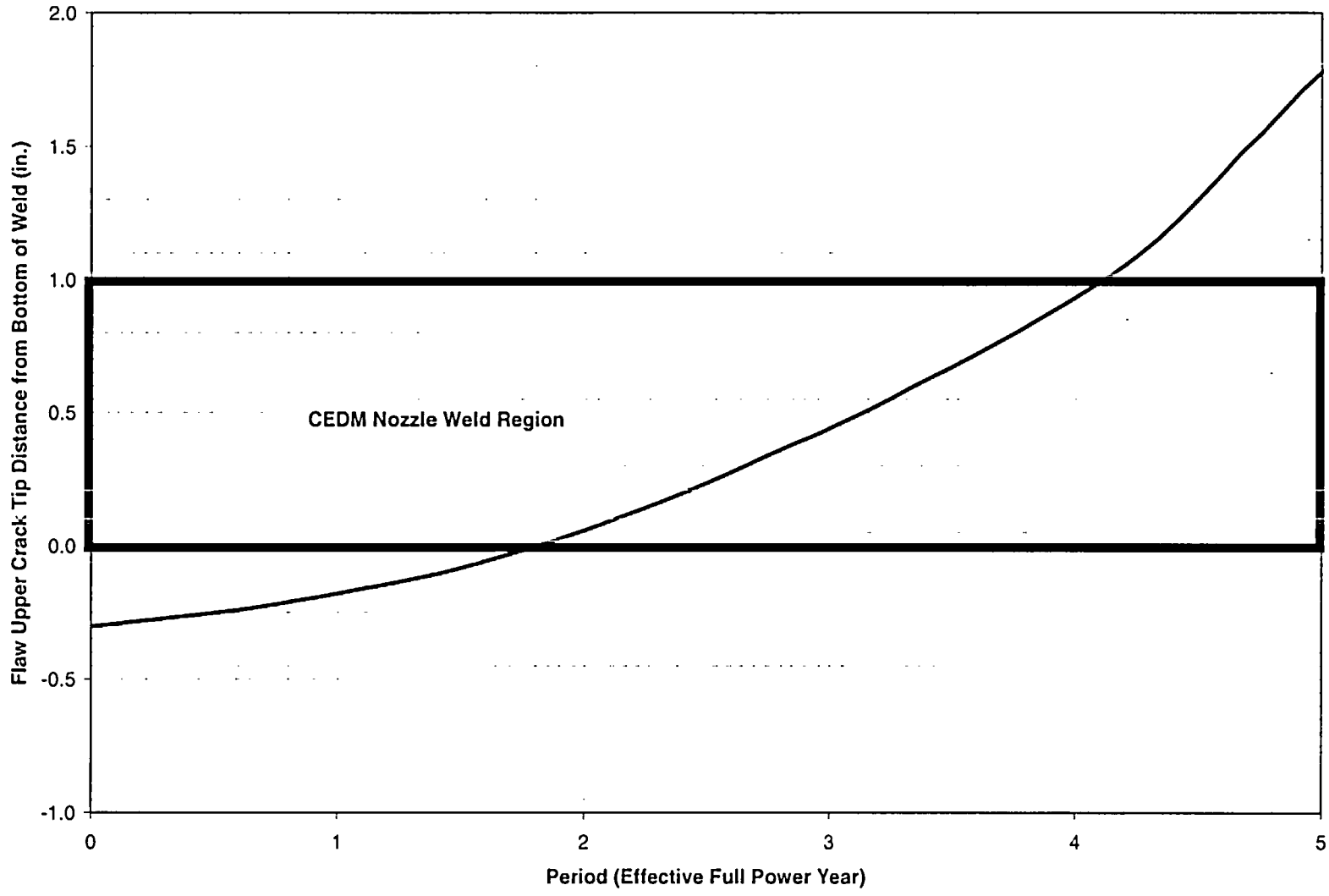

Figure 6-14 Through-Wall Axial Flaws Located in the 29.1 Degrees (CEDM) Row of Penetrations, Downhill Side - Crack Growth Predictions for San Onofre Units 2 & 3

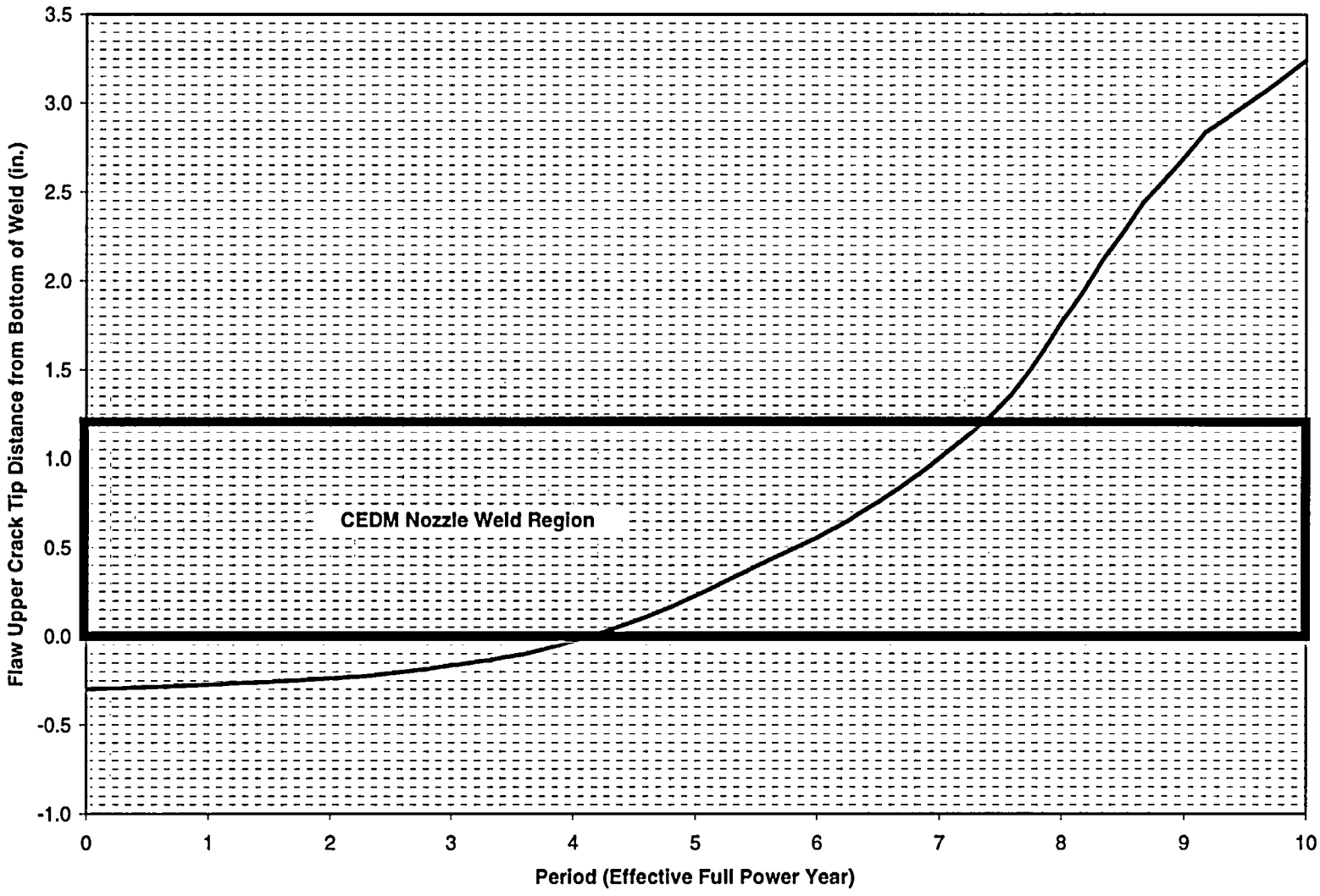

Figure 6-15 Through-Wall Axial Flaws Located in the 49.7 Degrees (CEDM) Row of Penetrations, Downhill Side - Crack Growth Predictions for San Onofre Units 2 & 3

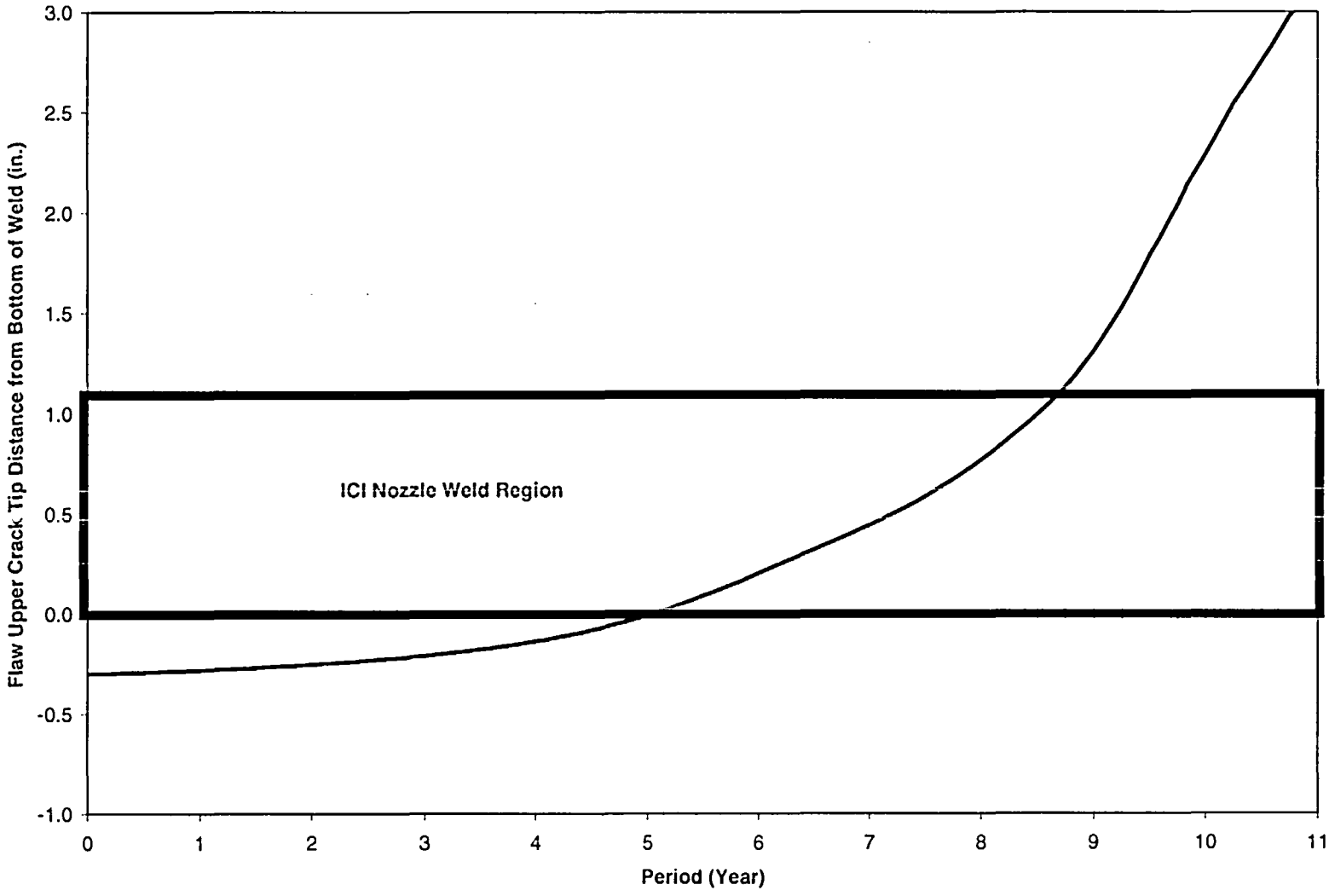

Figure 6-16 Through-Wall Axial Flaws Located in the 55.3 Degrees (ICI) Row of Penetrations, Downhill Side - Crack Growth Predictions for San Onofre Units 2 & 3

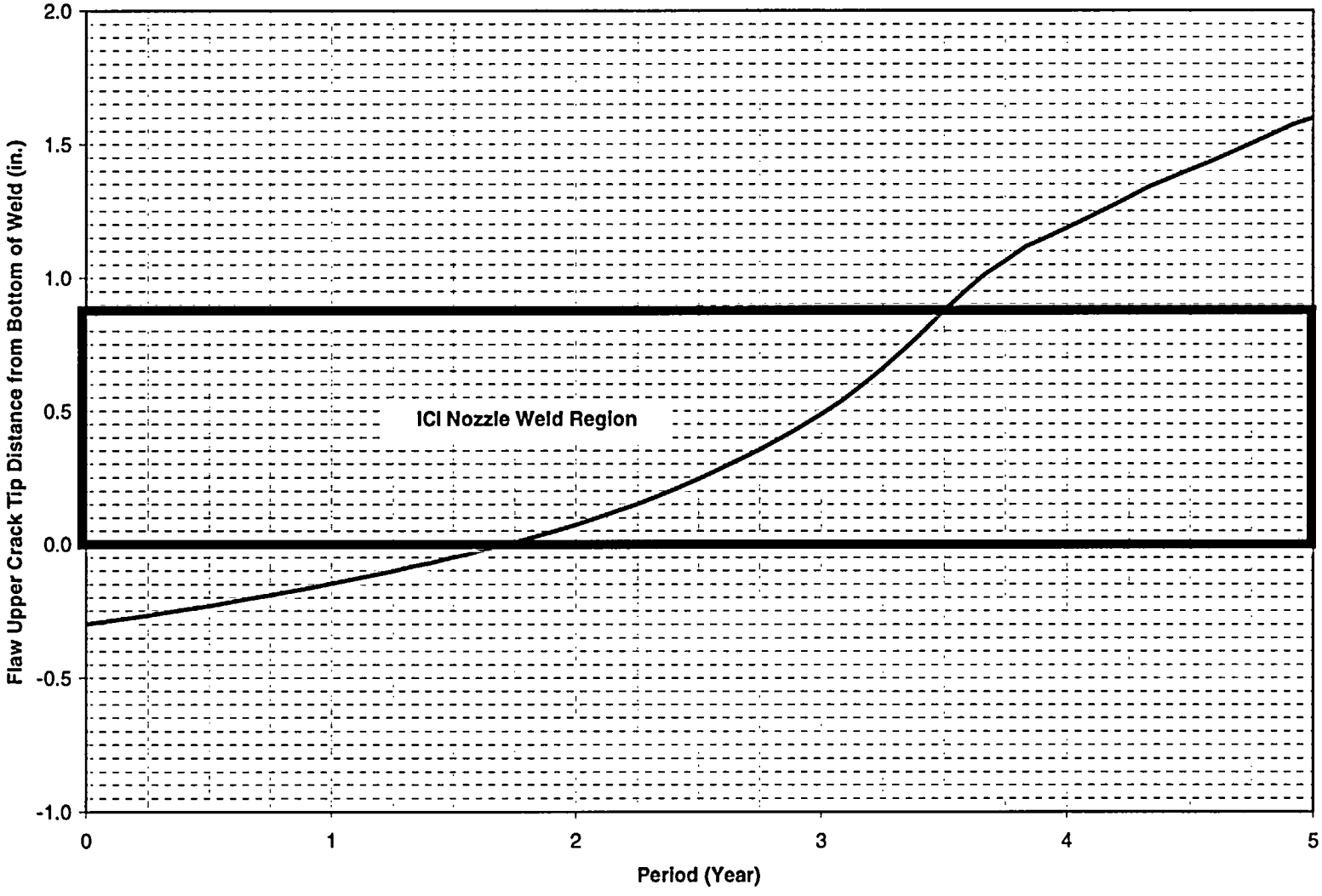

Figure 6-17 Through-Wall Axial Flaws Located in the 55.3 Degrees (ICI) Row of Penetrations, Uphill Side - Crack Growth Predictions for San Onofre Units 2 & 3

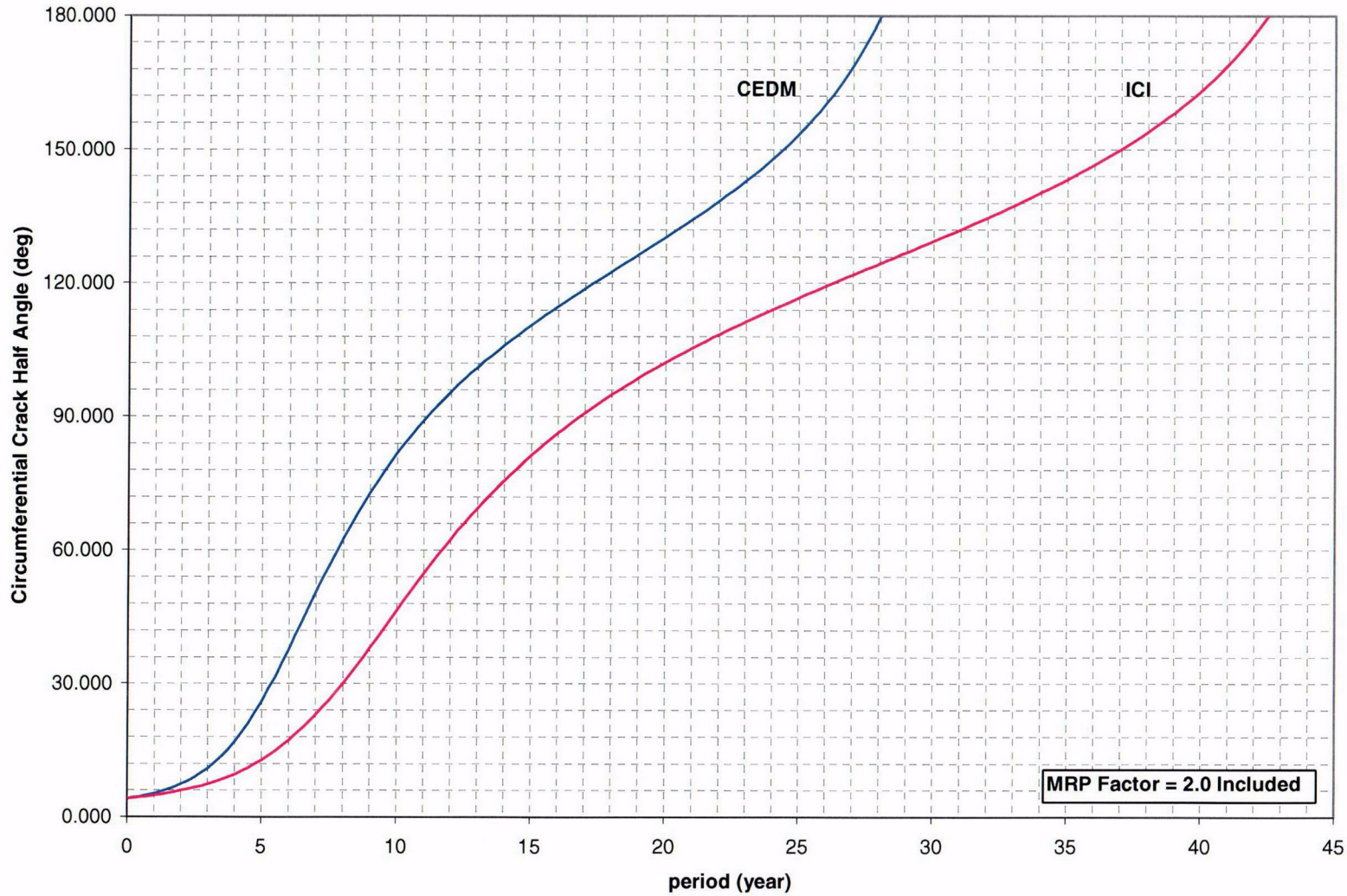

Figure 6-18 Through-Wall Circumferential Flaws Near the Top of the Attachment Weld for CEDM and ICI Nozzles - Crack Growth Predictions for San Onofre Units 2 & 3 (MRP Factor of 2.0 Included)

C20

THIS PAGE IS LEFT INTENTIONALLY BLANK

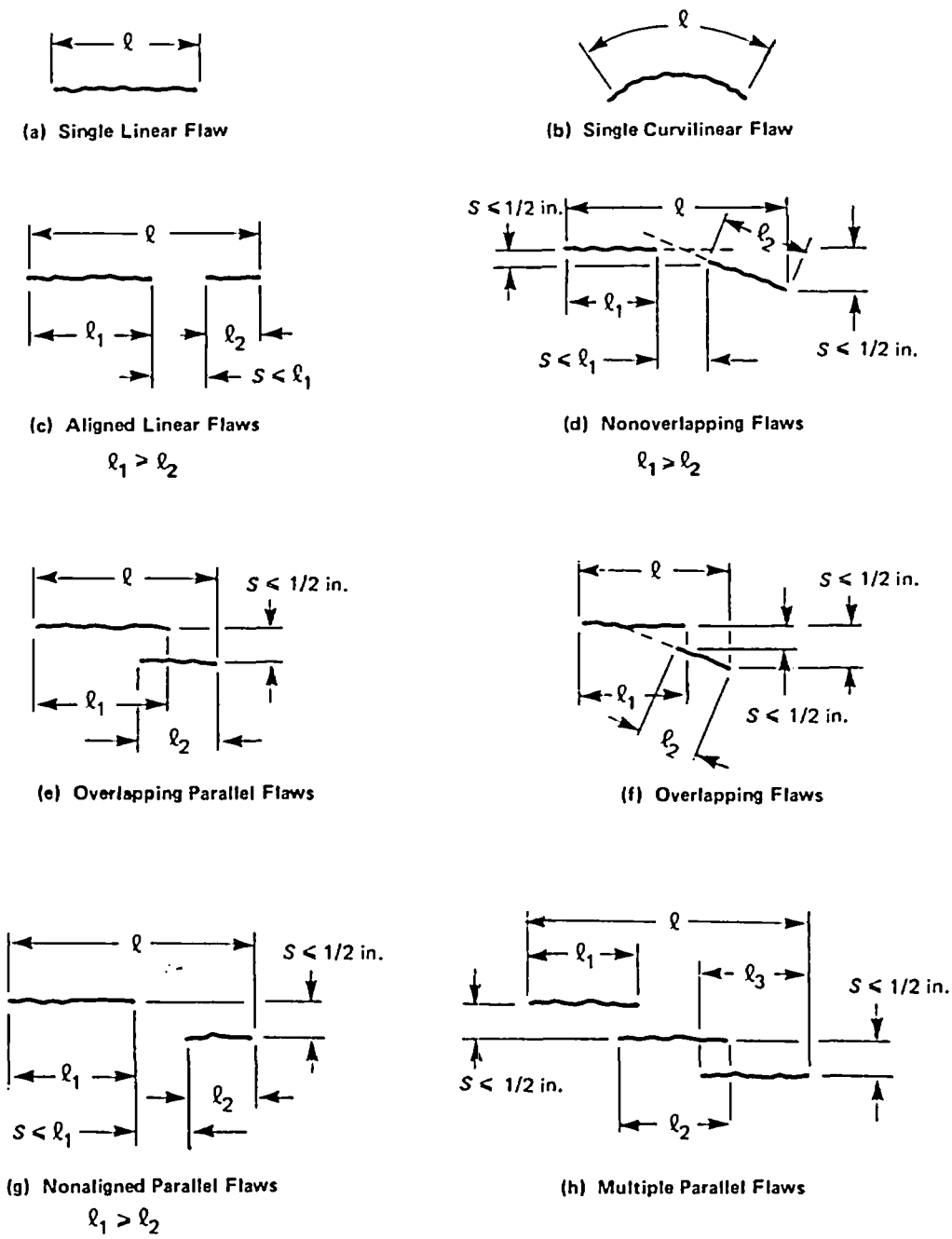

Figure 6-19 Section XI Flaw Proximity Rules for Surface Flaws (Figure IWA-3400-1)

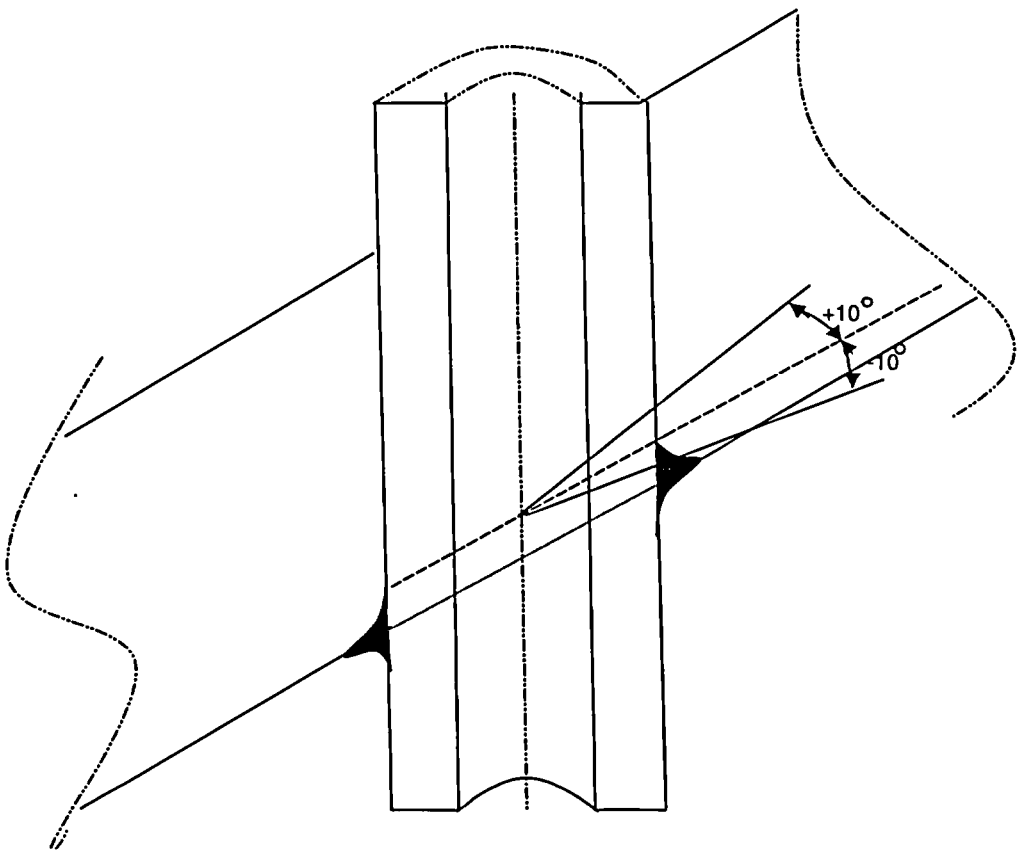

Figure 6-20 Definition of "Circumferential"

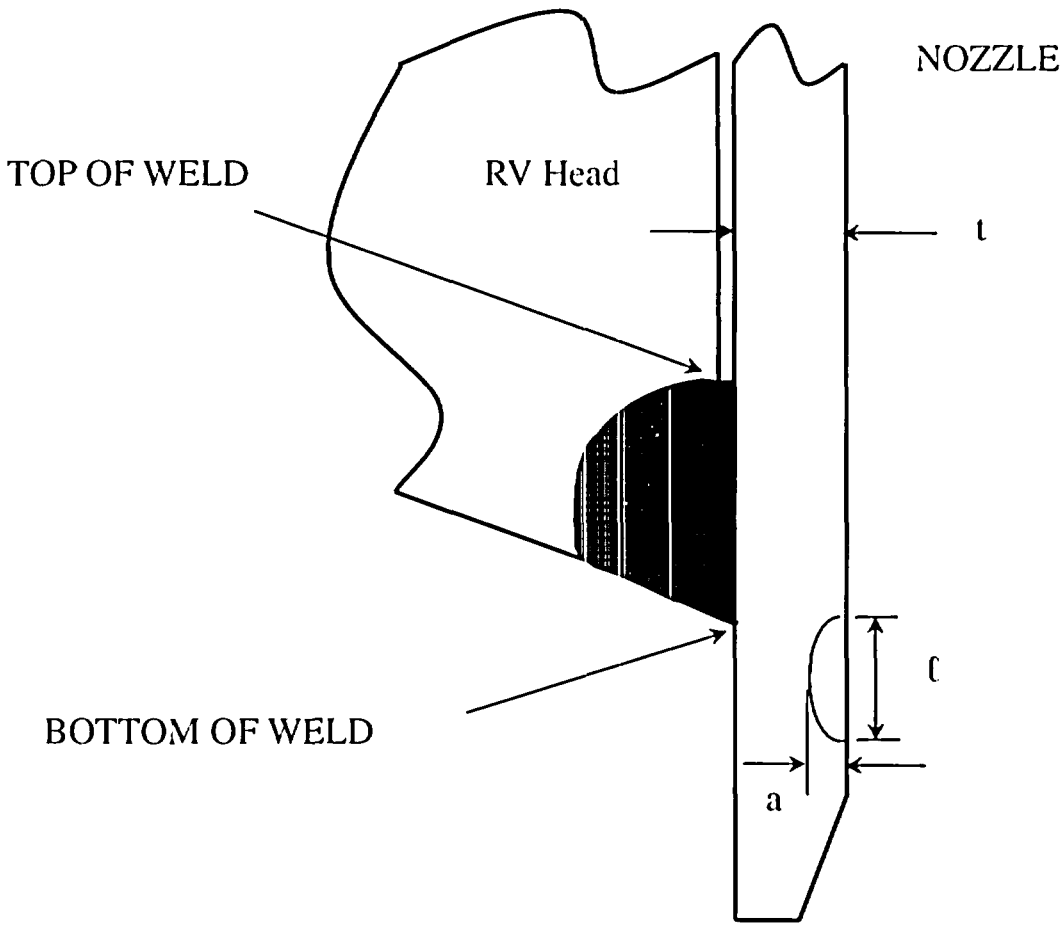

Figure 6-21 Schematic of Head Penetration Geometry

7 SUMMARY AND EXAMPLE PROBLEMS

An extensive evaluation has been carried out to characterize the loadings and stresses, which exist in the head penetrations at San Onofre Units 2 & 3 reactor vessel head. Three-dimensional finite element models were constructed [6], and all pertinent loadings on the penetrations were analyzed. These loadings included internal pressure and thermal expansion effects typical of steady state operation. In addition, residual stresses due to the welding of the penetrations to the vessel head were considered.

Results of the analyses reported here are consistent with the axial orientation and location of flaws which have been found in service in a number of plants and that the largest stress component is the hoop stress, and the maximum stresses were found to exist at the attachment weld. The most important loading conditions were found to be those which exist on the penetration for the majority of the time, which are the steady state loading and the residual stresses.

These stresses are important because the cracking observed to date in operating plants has been determined to result from primary water stress corrosion cracking (PWSCC). These stresses were used in the fracture calculations to predict the future growth of flaws postulated to exist in the head penetrations. A crack growth law was developed specifically for the operating temperature of the head at San Onofre Units 2 & 3 reactor pressure vessel, based on the EPRI recommendation, which is consistent with laboratory data as well as crack growth results for operating plants.

The crack growth predictions contained in Section 6 show that the future growth of cracks which might be found in the penetrations will be typically moderate, however, a number of effective full power years would be required for any significant extensions.

7.1 SAFETY ASSESSMENT

It is appropriate to examine the safety consequences of an indication which might be found. The indication, even if it were to propagate through the penetration nozzle wall, would have only minor consequences, since the pressure boundary would not be broken, unless it were to propagate above the weld.

Further propagation of the indication would not change its orientation, since the hoop stresses in the penetration nozzle are much larger than the axial stresses. Therefore, it is extremely unlikely that the head penetration would be severed.

If the indication were to propagate to a position above the weld, a leak could result, but the magnitude of such a leak would be very small, because the crack could not open significantly due to the tight fit between the penetration nozzle and the vessel head. Such a leak would have no immediate impact on the structural integrity of the system, but could lead to wastage in the ferritic steel of the vessel head, as the borated primary water concentrates due to evaporation. Davis Besse has demonstrated the consequence of ignoring such leaks.

Any indication is unlikely to propagate very far up the penetration nozzle above the weld, because the hoop stresses decrease in this direction, and this will cause it to slow down, and to stop before it reaches the outside surface of the head.

The high likelihood that the indication will not propagate up the penetration nozzle beyond the vessel head ensures that no catastrophic failure of the head penetration will occur, since the indication will be enveloped in the vessel head itself, which precludes the opening of the crack and limits leakage.

It should be noted that the objective of the acceptance criteria shown in Table 6-1 is to prevent leakage. Therefore, even though a small leak may have no immediate impact on the structural integrity of the system, it is not acceptable to the NRC and nozzle repair is required.

7.2 EXAMPLE PROBLEMS

The flaw tolerance charts in Figures 6-2 through 6-18 can be used with the acceptance criteria of Section 6.5 to determine the available service life. In this section, a few examples will be presented to illustrate the use of these figures. The example cases are listed in Table 7-1.

Example 1. Determine the service life of an axially oriented inside surface flaw whose upper extremity is located 1.25" below the weld on the uphill side of penetration no. 40. First, the penetration locality angle is obtained from Table 1-1 and, in this case, the locality angle is 29.1 degrees. The initial flaw depth, $a_{initial}$, is 0.078" and the initial flaw length, $2c_{initial}$, is 0.195". Assuming that the initial aspect ratio of 2.5:1 is maintained throughout the time that the inside surface flaw becomes a through-wall flaw, the final length of the flaw ($2c_{final}$) will be 1.653". The upper extremity of the flaw is now located 0.521" below the weld and validates the use of a single crack growth curve. The crack growth curve for the 29.1 degrees nozzle angle of Figure 6-2 is applicable and Figure 6-2 has been reproduced as Figure 7-1. The flaw is initially 11.8 percent of the wall thickness, and a straight line is drawn horizontally at a/t = 0.118 that intersects the crack growth curve. Using the acceptance criteria in Table 6-1, the service life can then be determined as the remaining time for this flaw to grow to the limit of 100 percent of the wall thickness or approximately 4.6 years (labeled as "Service Life" in Figure 7-1)

Example 2. In this case, the flaw is identical in size to that used in Example 1, but located on the outside surface and on the downhill side of penetration no. 40. This flaw, just as the flaw in Example 1, will not cross into the weld region. The applicable curve to use is Figure 6-10. The ratio a/t and initial reference time are likewise found using the same approach as used in Example 1. Using the acceptance criteria in Table 6-1, the determination of service life is illustrated in Figure 7-2, where we can see that the result is approximately 2.0 years.

Example 3. An axial inside surface flaw is located at the weld and on the downhill side of penetration no. 90. The initial length of the flaw is 0.250" and the initial depth is 0.05". From Table 1-1, the angle of this penetration nozzle is 49.7 degrees. The applicable curve is Figure 6-5 and is reproduced here as Figure 7-3. In this case, the initial flaw depth is 7.6 percent of the wall thickness. The initial reference time can be found by drawing a horizontal line at a/t = 0.076. Using the acceptance criteria in Table 6-1, the allowable service life can then be determined as the

time for the flaw to reach a depth of 75 percent of the wall thickness. The final reference time is found through a horizontal line drawn at a/t = 0.75. The service life can be determined through the intersection points of these lines and the crack growth curve. The resulting service life is approximately 4.0 years, as shown in Figure 7-3.

Example 4. In this case, we have postulated an axial inside surface flaw with an upper extremity located 1.0 inch below the attachment weld on the uphill side of penetration no. 90 (49.7 degrees). The flaw has an initial depth of 0.079" and an initial length of 0.395". Assuming that the initial aspect ratio of 0.395" / 0.079" or 5:1 is maintained as the flaw propagates into the nozzle wall, the final length of a through-wall flaw would be 0.661" x 5 = 3.305" long. The location of the upper extremity of this flaw would have reached within 0.5 inch below the weld as it propagates into the nozzle wall (1.0 – ((3.305" / 2) – (0.395" / 2)) = -0.455). Therefore the evaluation will require the use of two flaw charts. The first step is to estimate the time required for the initial flaw to grow to within 0.5 inch from the weld. This can be accomplished with the use of Figure 6-2 and is reproduced here as Figure 7-4a. The upper extremity is 1 inch below the weld and is assumed to grow until the extremity is 0.5 inches below the weld. The final half-length of the flaw when it reaches 0.5 inches below the weld will be the sum of the initial half-length and the 0.5 inches it has grown or 0.395" / 2 + 0.5" = 0.6975". Multiplying this by two and then dividing by the aspect ratio gives the flaw depth when the upper extremity is 0.5 inches below the weld: 2 x 0.6975" / 5.0 = 0.279". Figure 7-4a can be used to find the time it takes to grow from 12.0% through-wall (a/t = 0.079" / 0.661" = 0.120) to 42.2% through-wall (a/t = 0.279" /0.661" = 0.422). The time is estimated as 2.2 years. Using the flaw depth calculated previously (a/t = 0.422) as the initial flaw depth, the curves in Figure 6-4 reproduced here as Figure 7-4b for inside surface flaws near the weld can be used to determine the remaining service time before the flaw depth reaches the allowable flaw size (a/t = 0.75). Using the acceptance criteria in Table 6-1, Figure 7-4b shows an additional 0.8 years of service life for a total of 3.0 years.

As shown above, flaws whose upper extremities grow within 0.5 inch below weld require the use of both the 0.5 inch below weld and "at the attachment weld" flaw tolerance charts. To avoid the use of these two charts, the "at the weld" chart may solely be used in determining the service life. This shall provide a conservative estimate of the crack growth due to larger stress field.

Example 5. This case is an axial through-wall flaw with its upper extremity located 0.40 inches below the weld region of penetration no. 3. This would be the case where inspection can only be performed from 2 inch above the J-weld to only 0.4 inches below the weld on the downhill side. The objective is to determine the remaining service life for a flaw in the un-inspected region below the weld to reach the bottom of the J-weld. The angle of the penetration nozzle is 7.8 degrees as shown in Table 1-1. The crack growth curve of Figure 6-13 is applicable and has been reproduced as Figure 7-5. The initial reference time is found by drawing a horizontal line 0.40 inches below the line representing the bottom of the weld, then dropping a vertical line to the x axis. The final reference time is found by drawing a vertical line where the crack growth curve intersects the bottom of the weld horizontal line. If inspection can only be performed from 2 inch above the J-weld to only 0.4 inches below the weld, it would take approximately 1.8 years for a flaw in the un-inspected region below the weld to reach the weld bottom.

Several guidelines are important to understand when using these flaw evaluation charts.

1. If a flaw is found in a penetration nozzle for which no specific analysis was performed and there is a uniform trend as a function of penetration nozzle angle, interpolation between penetration nozzle is the best approach.

2. If a flaw is found in a penetration nozzle for which no specific analysis was performed and there is no apparent trend as a function of penetration nozzle angle, the result for the penetration nozzle with the closest angle should be used.

3. If a flaw is found which has a depth smaller than any depth shown for the penetration nozzle angle of interest, the initial flaw depth should be assumed to be the same as the smallest depth analyzed for that particular penetration nozzle.

4. The flaw evaluation charts are applicable for aspect ratio of 6 or less. Consult with Westinghouse if the as-found flaw has an aspect ratio larger than 6.0.

5. All references to service life are in Effective Full Power Years.

6. Results are only provided for the uphill and downhill sides of the selected penetration nozzles. If flaws are found in locations between the uphill and downhill side, use the results for either the uphill or downhill location, whichever is closer.

Table 7-1 Example Problem Inputs: Initial Flaw Sizes and Locations

Example No.	Orientation	Vertical Location	Circumferential Location	Penetration Row	Length	Depth	Penetration No.	Source Figure
1	Axial - Inside Surface	1.25" Below Weld	Uphill	29.1°	0.195"	0.078"	40	6-2
2	Axial - Outside Surface	1.25" Below Weld	Downhill	29.1°	0.195"	0.078"	40	6-10
3	Axial - Inside Surface	At Weld	Downhill	49.7°	0.250"	0.05"	90	6-5
4	Axial - Inside Surface	1.0" Below Weld	Uphill	49.7°	0.395"	0.079"	90	6-2, 6-4
5	Axial Through-Wall	0.4" Below Weld	Downhill	7.8°	--	--	3	6-13

Example No.	Orientation	Crack Tip Location	Circumferential Location	Penetration Row	Length (2c)	Depth (a)	Wall Thickness	a/t	Penetration No.	Source Figure
1	Axial – Inside Surface	1.25" Below Weld	Uphill	29.1°	0.195"	0.078"	0.661"	0.118	40	6-2

Locality Angle from Table 1-1:

Nozzle No.	Type	Angle
40	CEDM	29.1

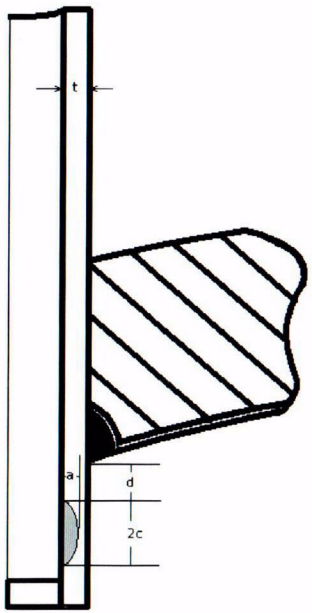

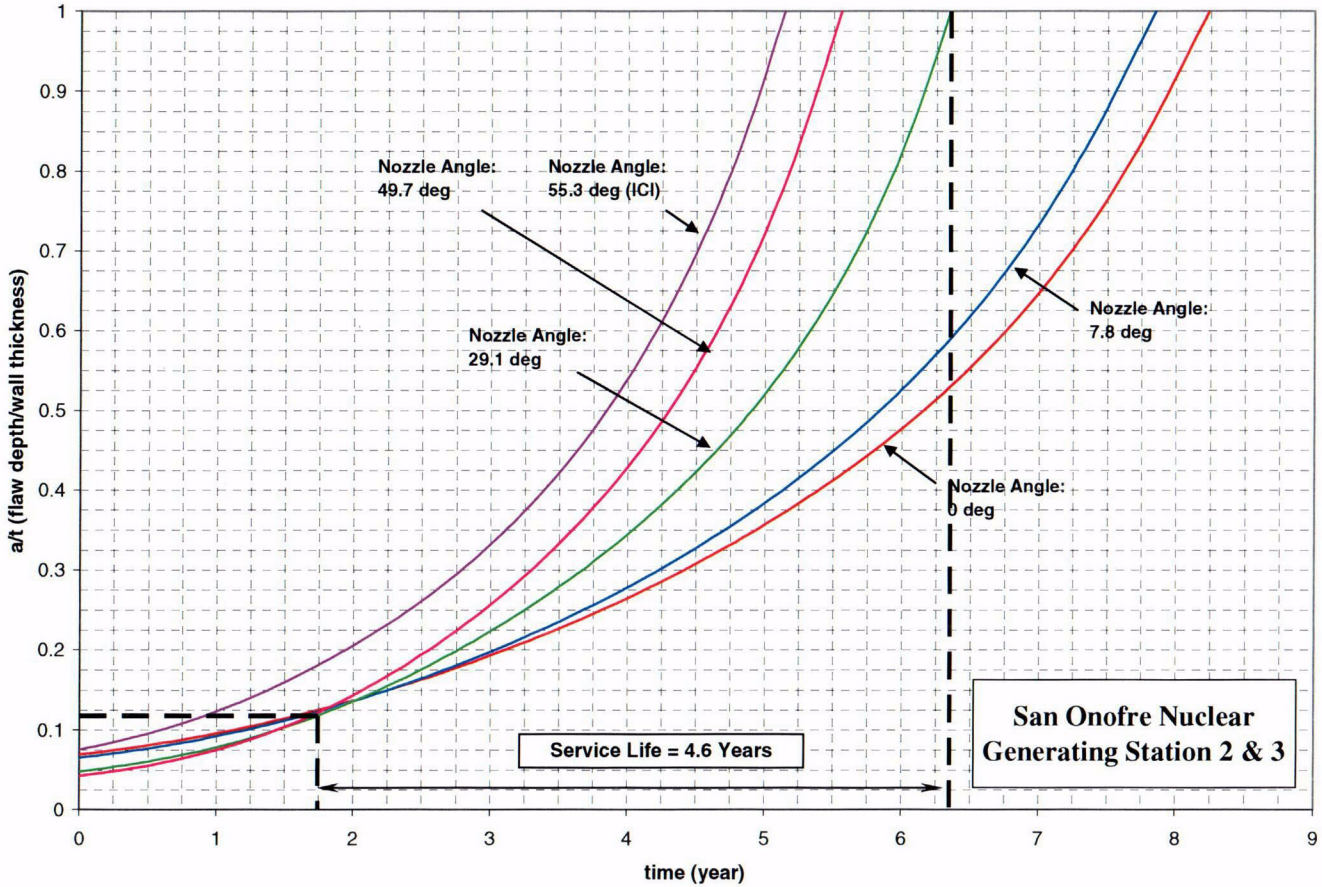

Figure 7-1 Example Problem 1

CZ1

Example No.	Orientation	Crack Tip Location	Circumferential Location	Penetration Row	Length (2c)	Depth (a)	Wall Thickness	a/t	Penetration No.	Source Figure
2	Axial – Outside Surface	1.25" Below Weld	Downhill	29.1°	0.195"	0.078"	0.661"	0.118	40	6-10

Locality Angle from Table 1-1:

Nozzle No.	Type	Angle
40	CEDM	29.1

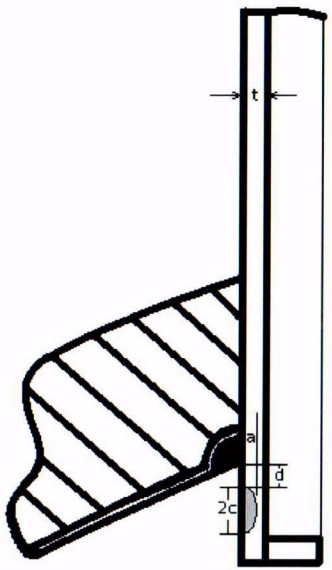

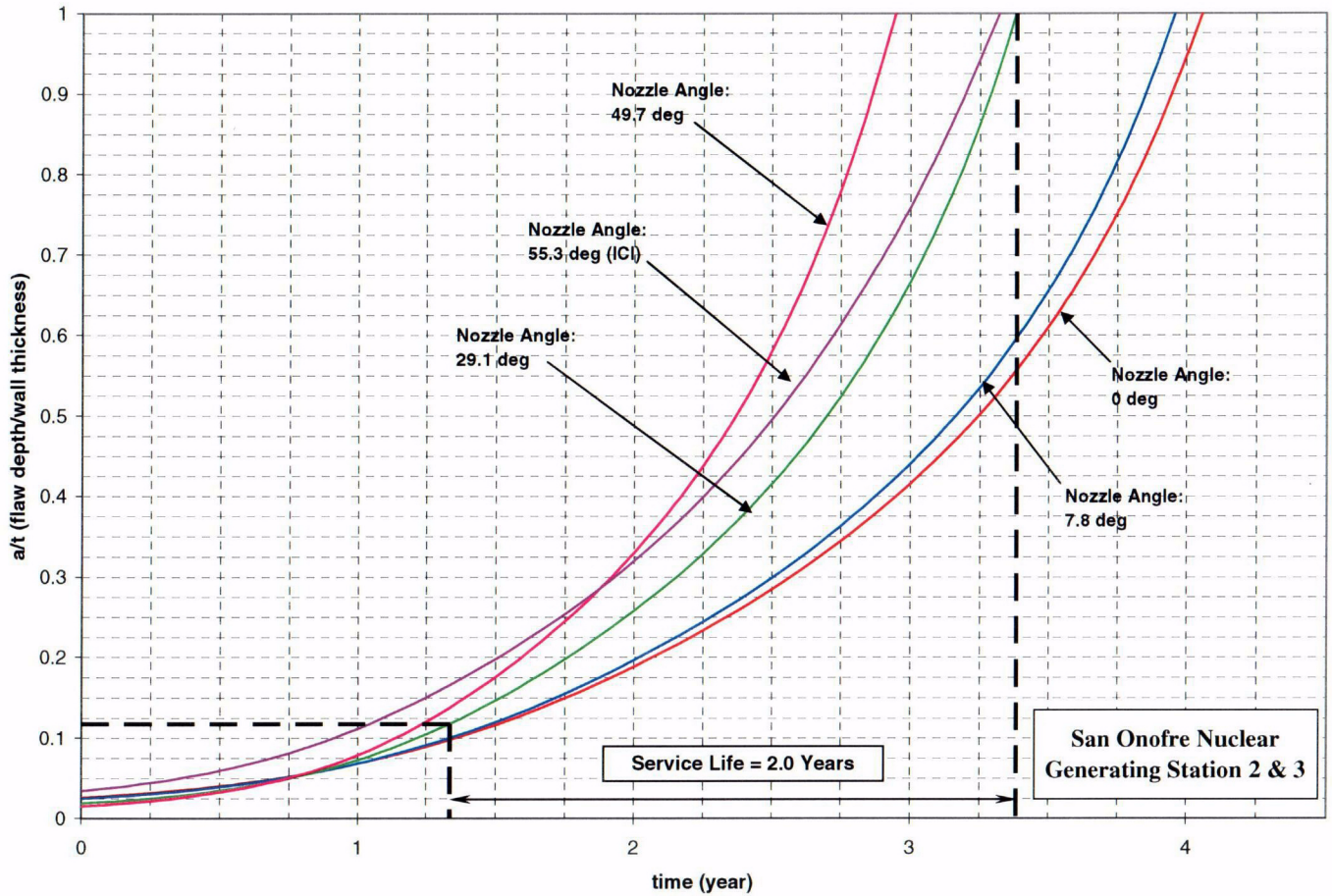

Figure 7-2 Example Problem 2

C22

Example No.	Orientation	Crack Tip Location	Circumferential Location	Penetration Row	Length (2c)	Depth (a)	Wall Thickness	a/t	Penetration No.	Source Figure
3	Axial – Inside Surface	At Weld	Downhill	49.7°	0.250"	0.05"	0.661"	0.076	90	6-5

Locality Angle from Table 1-1:

Nozzle No.	Type	Angle
90	CEDM	49.7

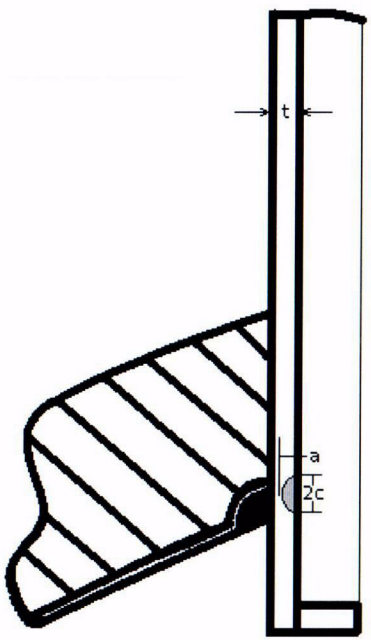

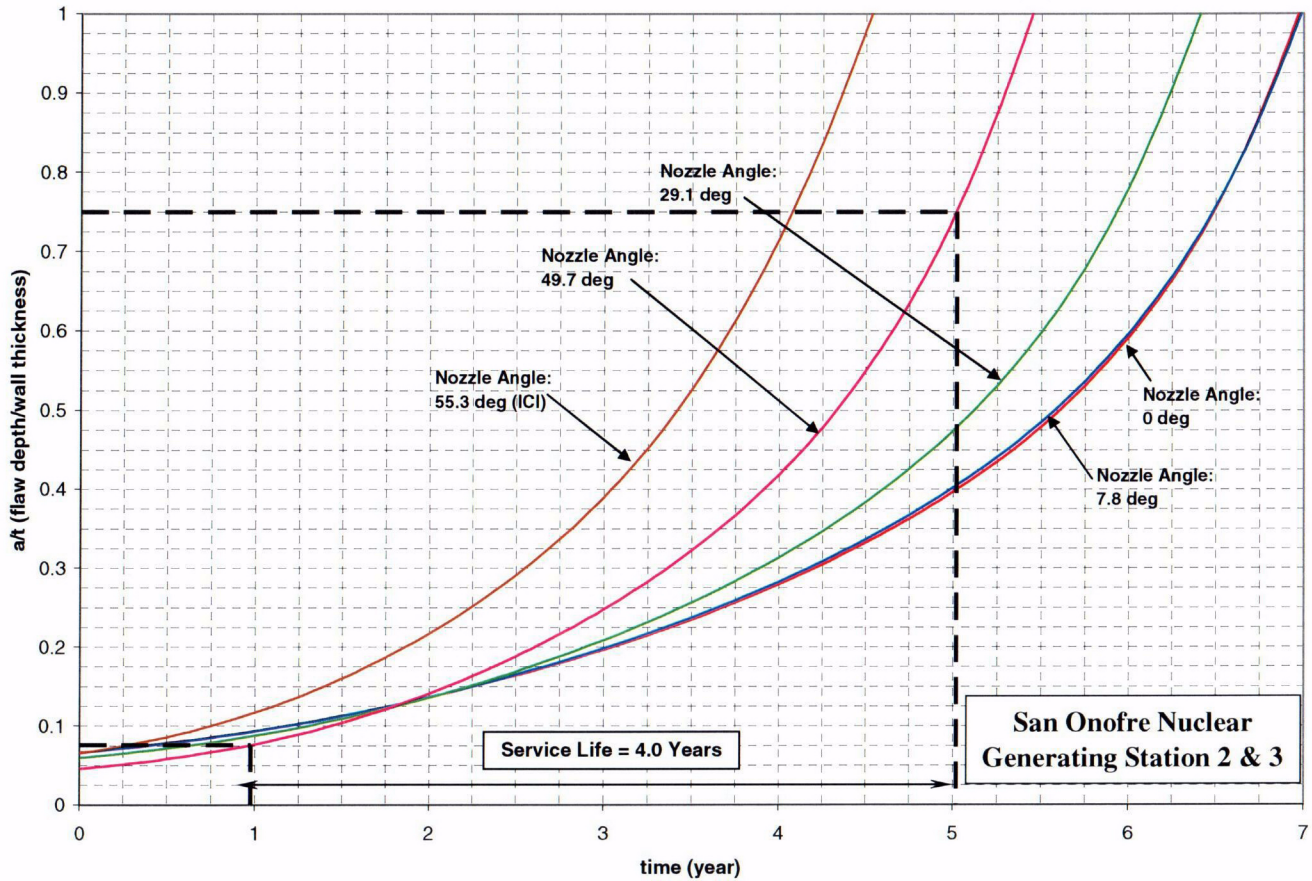

Figure 7-3 Example Problem 3

C23

Example No.	Orientation	Crack Tip Location	Circumferential Location	Penetration Row	Length (2c)	Depth (a)	Wall Thickness	a/t	Penetration No.	Source Figure
4	Axial – Inside Surface	1.00" Below Weld	Uphill	49.7°	0.395"	0.079"	0.661"	0.12	90	6-2, 6-4

Locality Angle from Table 1-1:

Nozzle No.	Type	Angle
90	CEDM	49.7

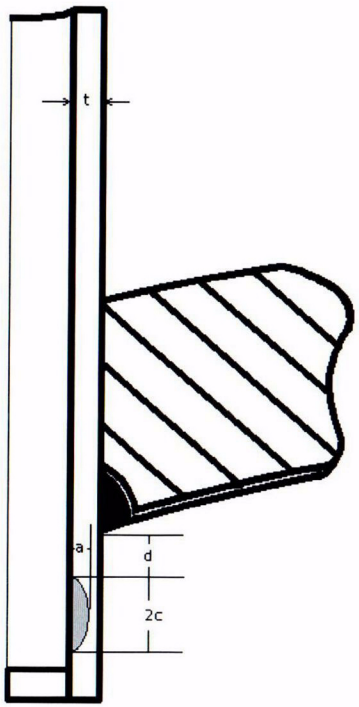

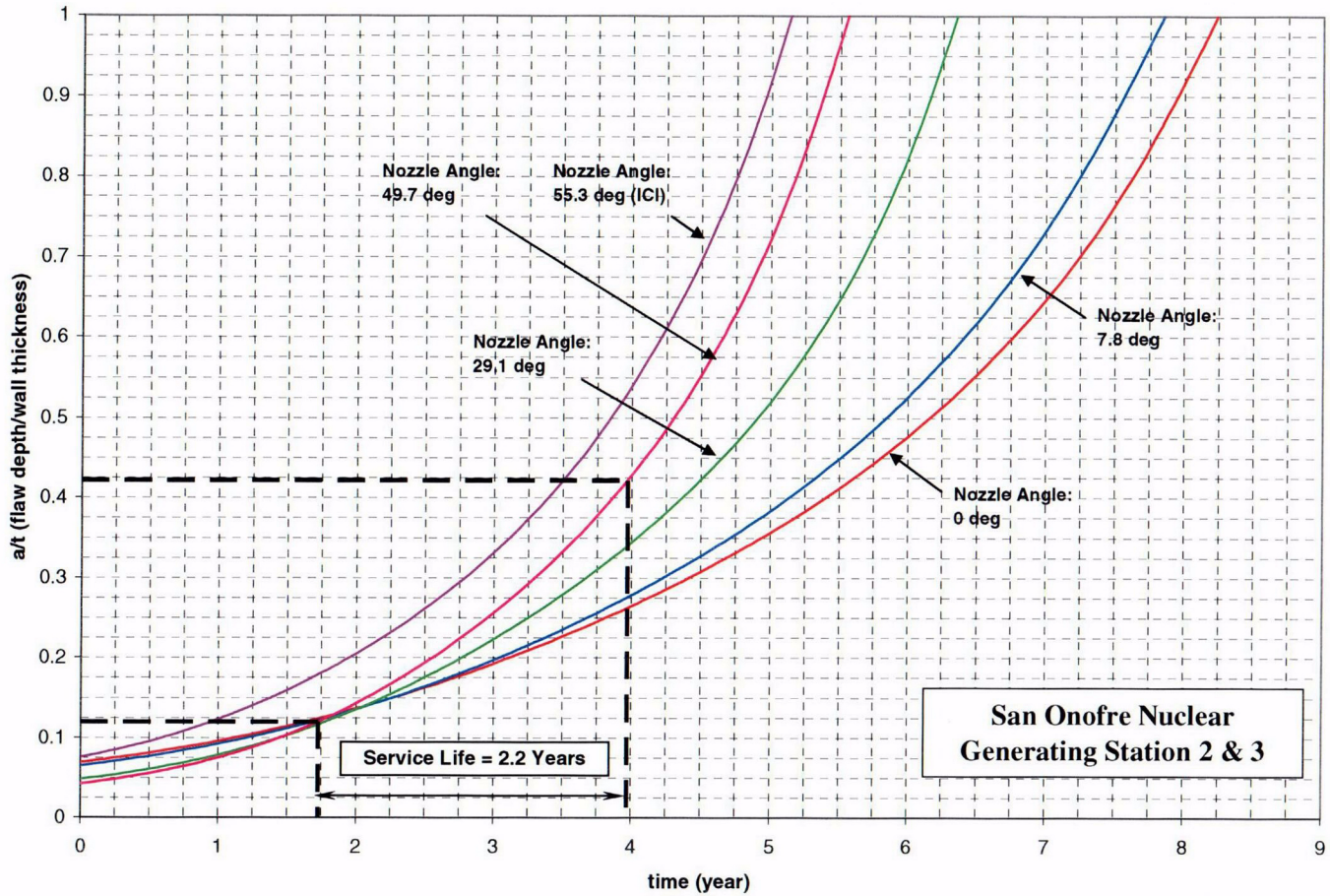

Figure 7-4a Example Problem 4 (See also Figure 7-4b)

C24

Example No.	Orientation	Crack Tip Location	Circumferential Location	Penetration Row	Length (2c)	Depth (a)	Wall Thickness	a/t	Penetration No.	Source Figure
4	Axial – Inside Surface	1.00" Below Weld	Uphill	49.7°	0.395"	0.079"	0.661"	0.12	90	6-2, 6-4

Locality Angle from Table 1-1:

Nozzle No.	Type	Angle
90	CEDM	49.7

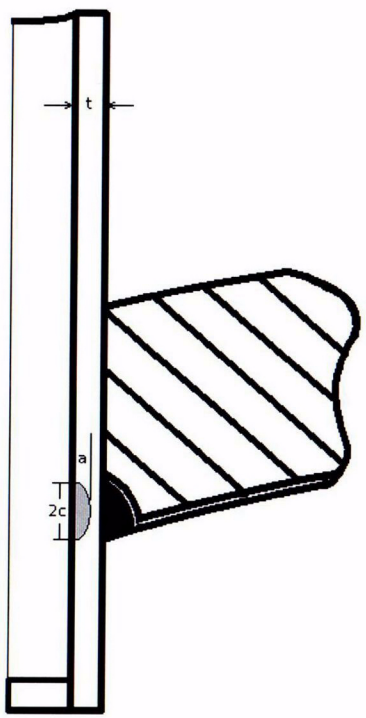

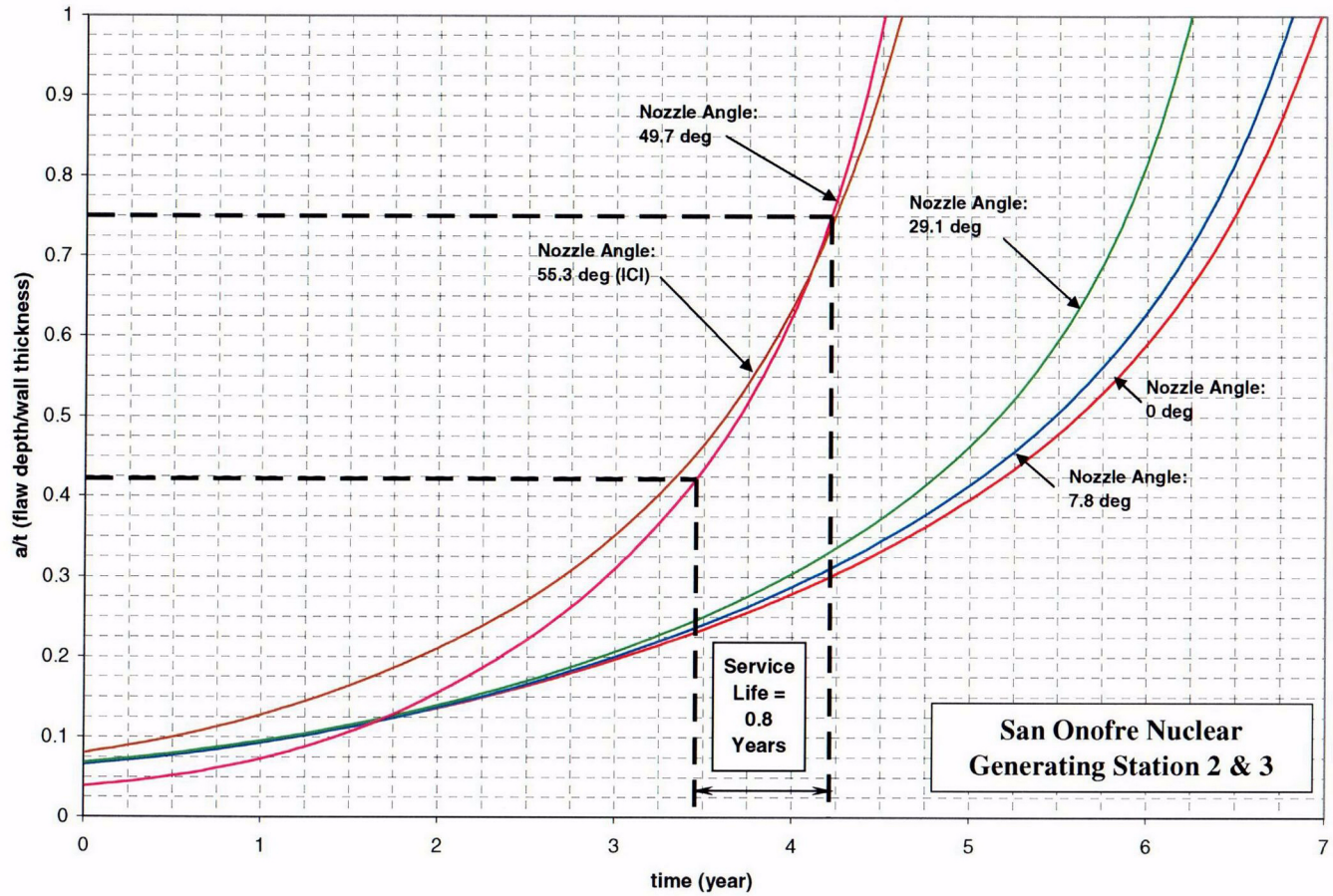

Figure 7-4b Example Problem 4 (See also Figure 7-4a)

C25

Example No.	Orientation	Crack Tip Location	Circumferential Location	Penetration Row	Length (2c)	Depth (a)	Wall Thickness	a/t	Penetration No.	Source Figure
5	Axial – Through-Wall	0.4" Below Weld	Downhill	7.8°	N/A	N/A	0.661"	N/A	3	6-13

Locality Angle from Table 1-1:

Nozzle No.	Type	Angle
3	CEDM	7.8

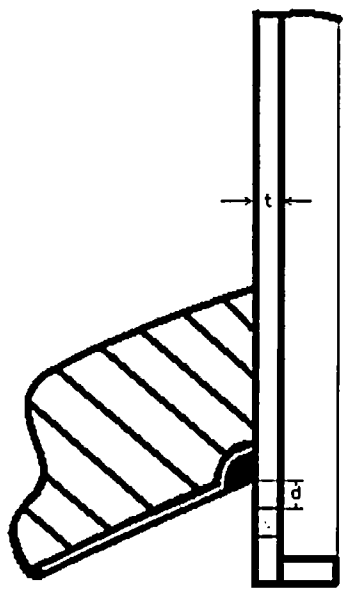

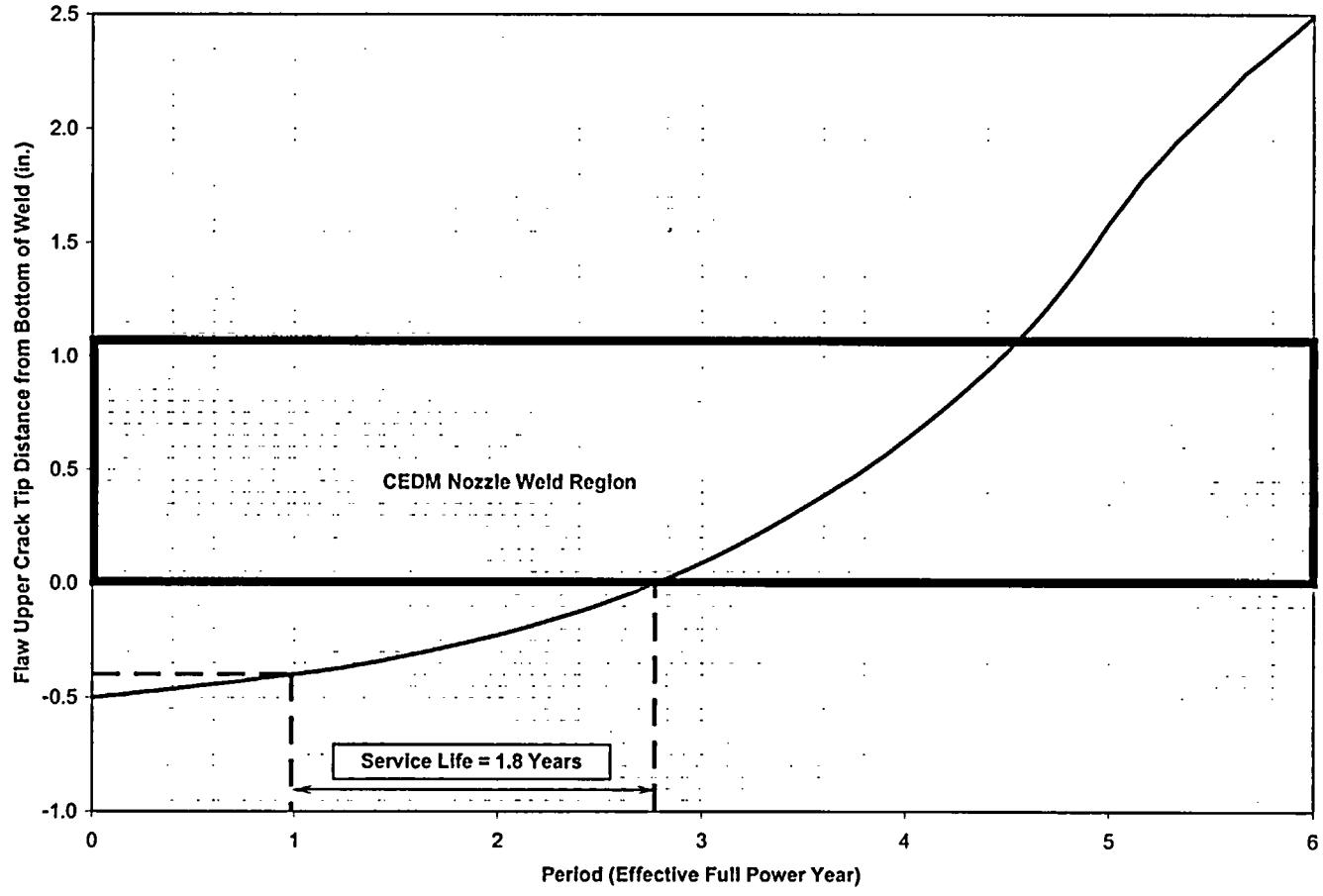

Figure 7-5 Example Problem 5

8 REFERENCES

1. Scott, P. M., "An Analysis of Primary Water Stress Corrosion Cracking in PWR Steam Generators," in Proceedings, Specialists Meeting on Operating Experience With Steam Generators, Brussels Belgium, Sept. 1991, pages 5, 6.

2. McIlree, A. R., Rebak, R. B., Smialowska, S., "Relationship of Stress Intensity to Crack Growth Rate of Alloy 600 in Primary Water," Proceedings International Symposium Fontevraud II, Vol, 1, p. 258-267, September 10-14, 1990.

3. Cassagne, T., Gelpi, A., "Measurements of Crack Propagation Rates on Alloy 600 Tubes in PWR Primary Water, in Proceedings of the 5th International Symposium on Environmental Degradation of Materials in Nuclear Power Systems-Water Reactors," August 25-29, 1991, Monterey, California.

4A. *Crack Growth and Microstructural Characterization of Alloy 600 PWR Vessel Head Penetration Materials,* EPRI, Palo Alto, CA. 1997. TR-109136.

4B. Vaillant, F. and C. Amzallag. "Crack Growth Rates of Alloy 600 in Primary Water," Presentation to the EPRI-MRP Crack Growth Rate (CGR) Review Team, Lake Tahoe, NV, presented August 10, 2001, and revised October 11, 2001

4C. Vaillant, F. and S. Le Hong. *Crack Growth Rate Measurements in Primary Water of Pressure Vessel Penetrations in Alloy 600 and Weld Metal 182,* EDF, April 1997. HT-44/96/024/A.

4D. Framatome laboratory data provided by C. Amzallag (EDF) to MRP Crack Growth Rate Review Team, October 4, 2001 (Proprietary to EDF).

4E. Cassagne, T., D. Caron, J. Daret, and Y. Lefevre. "Stress Corrosion Crack Growth Rate Measurements in Alloys 600 and 182 in Primary Water Loops Under Constant Load," *Ninth International Symposium on Environmental Degradation of Materials in Nuclear Power Systems-Water Reactors* (Newport Beach, CA, August 1-5, 1999), Edited by F. P. Ford, S. M. Bruemmer, and G. S. Was, The Minerals, Metals & Materials Society (TMS), Warrendale, PA, 1999.

4F. Studsvik laboratory data provided by Anders Jenssen (Studsvik) to MRP Crack Growth Rate Review Team, October 3, 2001 (Proprietary to Studsvik).

4G. [ ]a,c,e

4H. "Materials Reliability Program (MRP) Crack Growth Rates for Evaluating Primary Water Stress Corrosion Cracking (PWSCC) of Thick Wall Alloy 600 Material (MRP-55) Revision 1," EPRI, Palo Alto, CA:, November 2002. 1006695.

4I. "Crack Growth Rate Tests of Alloy 600 in Primary PWR Conditions," Communication from M. L. Castaño (CIEMAT) to J. Hickling (EPRI), March 25, 2002.

4J. Gómez-Briceño, D., J. Lapeña, and F. Blázquez. "Crack Growth Rates in Vessel Head Penetration Materials," *Proceedings of the International Symposium Fontevraud III: Contribution of Materials Investigation to the Resolution of Problems Encountered in Pressurized Water Reactors* (Chinton, France, September 12-16, 1994), French Nuclear Energy Society, Paris, 1994, pp. 209-214.

4K. Gómez-Briceño, D. and J. Lapeña. "Crack Growth Rates in Vessel Head Penetration Materials." *Proceedings: 1994 EPRI Workshop on PWSCC of Alloy 600 in PWRs* (Tampa, FL, November 15-17, 1994), EPRI, Palo Alto, CA, TR-105406, August 1995, pp. E4-1 through E4-15.

4L. Gómez-Briceño, D., et al. "Crack Propagation in Inconel 600 Vessel Head Penetrations." Eurocorr 96, Nice, France, September 24-26, 1996.

4M. Castaño, M. L., D. Gómez-Briceño, M. Alvarez-de-Lara, F. Blázquez, M. S. Garcia, F. Hernández, and A. Largares. "Effect of Cationic Resin Intrusions on IGA/SCC of Alloy 600 Under Primary Water Conditions." *Proceedings of the International Symposium Fontevraud IV: Contribution of Materials Investigation to the Resolution of Problems Encountered in Pressurized Water Reactors* (France, September 14-18, 1998), French Nuclear Energy Society, Paris, 1998, Volume 2, pp. 925-937.

5A. Newman, J. C. and Raju, I. S., "Stress Intensity Factor Influence Coefficients for Internal and External Surface Cracks in Cylindrical Vessels," in Aspects of Fracture Mechanics in Pressure Vessels and Piping, PVP Vol. 58, ASME, 1982, pp. 37-48.

5B. Hiser, Allen, "Deterministic and Probabilistic Assessments," presentation at NRC/Industry/ACRS meeting, November 8, 2001.

6A. [ ]a,c,e

6B. [ ]a,c,e

7. USNRC Letter, W. T. Russell to W. Raisin, NUMARC, "Safety Evaluation for Potential Reactor Vessel Head Adapter Tube Cracking," November 19, 1993.

8. USNRC Letter, A. G. Hansen to R. E. Link, "Acceptance Criteria for Control Rod Drive Mechanism Penetrations at Point Beach Nuclear Plant, Unit 1," March 9, 1994.

9. Materials Reliability Program Response to NRC Bulletin 2001-01 EPRI MRP Report 48 (TP 1006284), August 2001.

10. "CEOG Report # CEN-614, "Safety Evaluation of the Potential for and Consequences of Reactor Vessel Head Penetration Alloy 600 OD initiated Nozzle Cracking", December 1993.

11. "CEOG Program to Address Alloy 600 Cracking of CEDM Penetrations Subtask 1 Nozzle Evaluation," CE NSPD-903-P, CEOG Task 730, Combustion Engineering Owners Group (CEOG), February 1993.

12. USNRC Letter, R. Barrett to A. Marion, "Flaw Evaluation Guidelines," April 11, 2003

13. "Materials Reliability Program Generic Evaluation of Examination Coverage Requirements for Reactor Pressure Vessel Head Penetration Nozzles (MRP-95)," EPRI, Palo Alto, CA:, September 2003, 1009129.

14. "The Stress Analysis of Cracks Handbook", Hiroshi Tada, 2nd Edition.

15. "Effect of Strain Rate on SCC in High Temperature Primary Water, Comparison between Alloys 690 and 600, ANS 11th Environmental Degradation Meeting, August 2003, K. M. Boursier et al (EDF).

16. [

]a,c,e

APPENDIX A

CEDM/ICI HOOP STRESS VS DISTANCE FROM BOTTOM OF WELD PLOTS

In this section, CEDM and ICI hoop stresses are plotted against corresponding distance from the bottom of weld for 55.3 degrees, 49.7 degrees, 29.1 degrees, 7.8 degrees and the center location penetration rows on both the downhill and uphill sides.

Figure A-1
Hoop Stress Distribution Below the Weld Downhill and Uphill Side
(0° CEDM Penetration Nozzle)

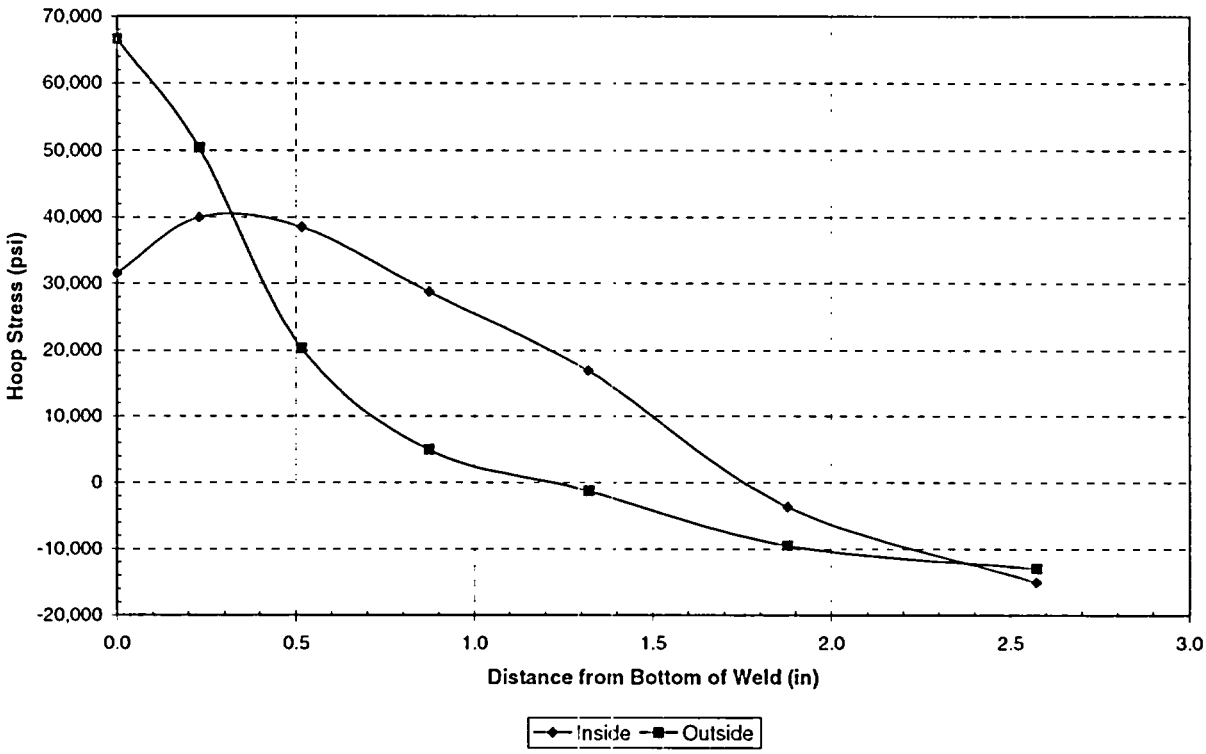

Figure A-2
Hoop Stress Distribution Below the Weld Downhill Side
(7.8° CEDM Penetration Nozzle)

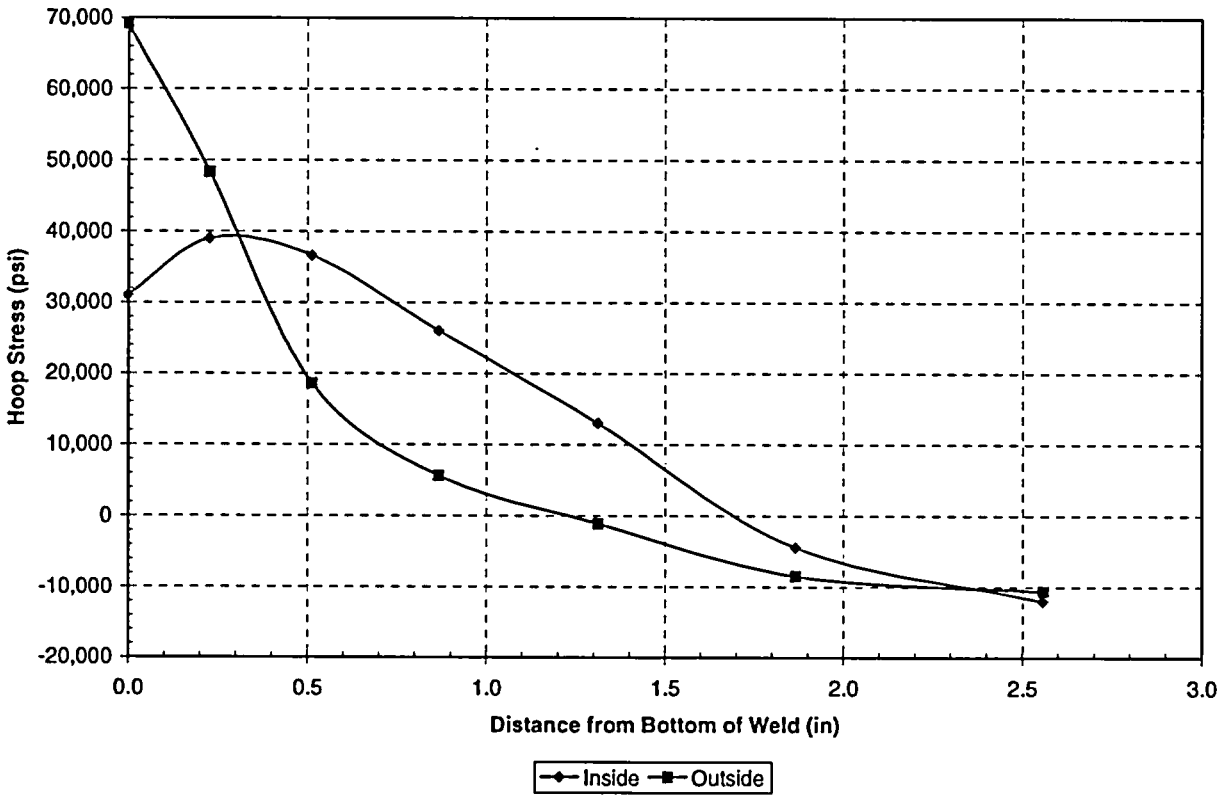

Figure A-3
Hoop Stress Distribution Below the Weld Uphill Side
(7.8° CEDM Penetration Nozzle)

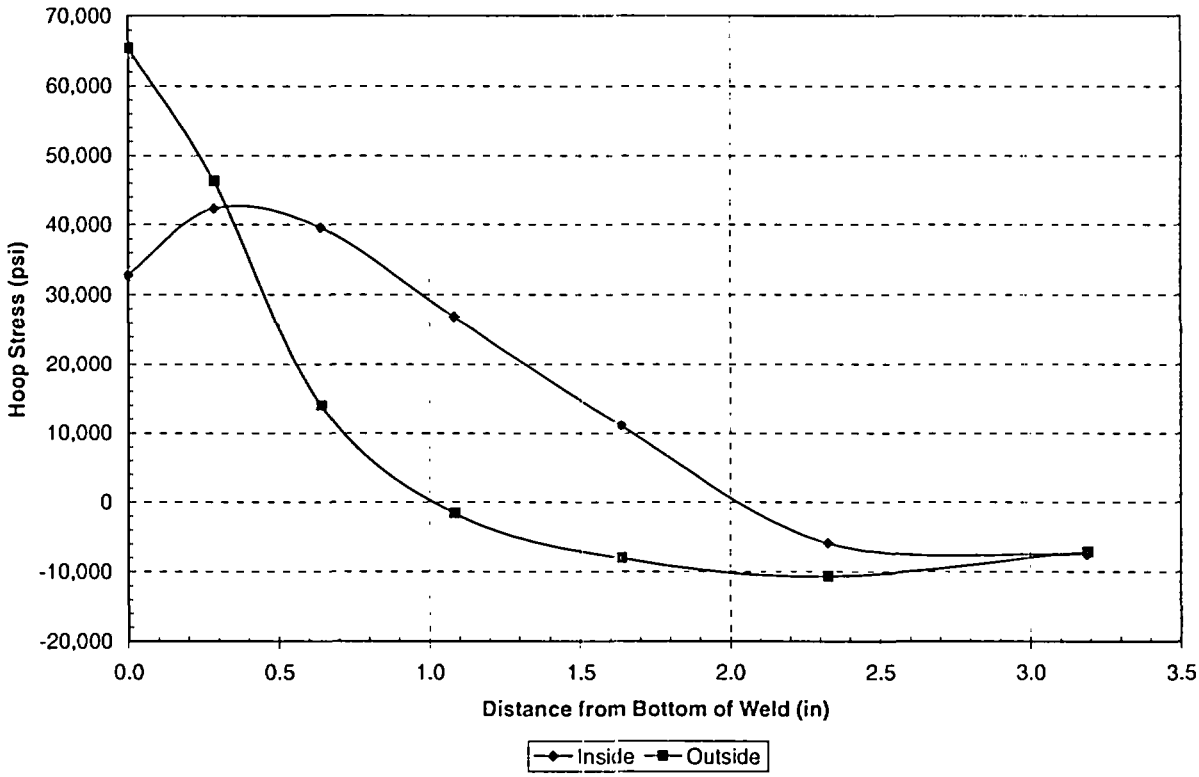

Figure A-4
Hoop Stress Distribution Below the Weld Downhill Side
(29.1° CEDM Penetration Nozzle)

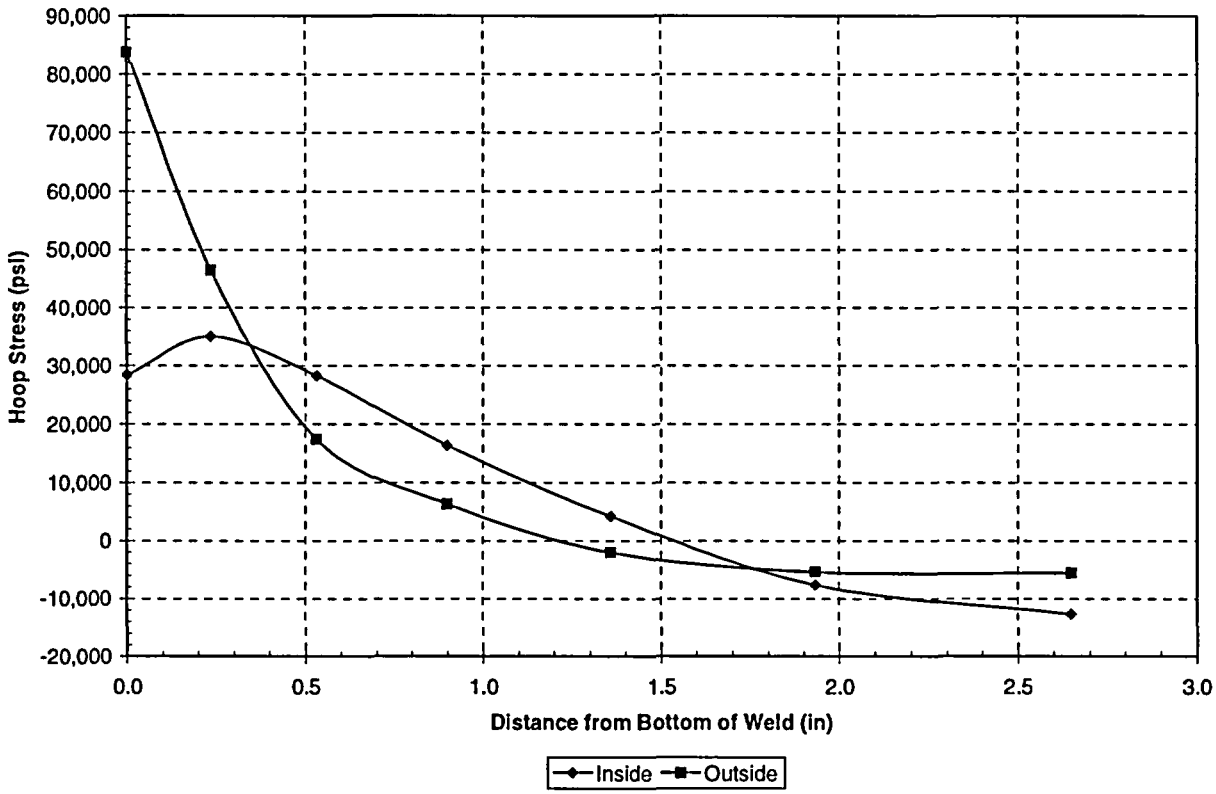

Figure A-5
Hoop Stress Distribution Below the Weld Uphill Side
(29.1° CEDM Penetration Nozzle)

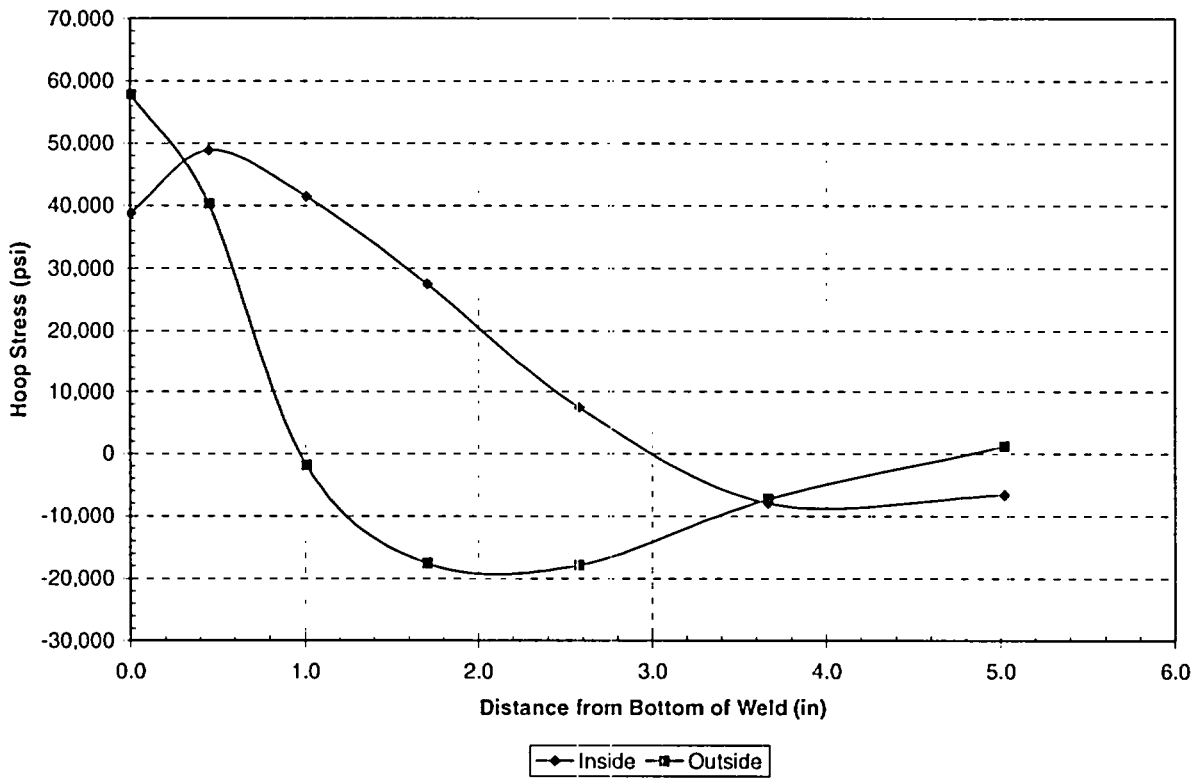

Figure A-6
Hoop Stress Distribution Below the Weld Downhill Side
(49.7° CEDM Penetration Nozzle)

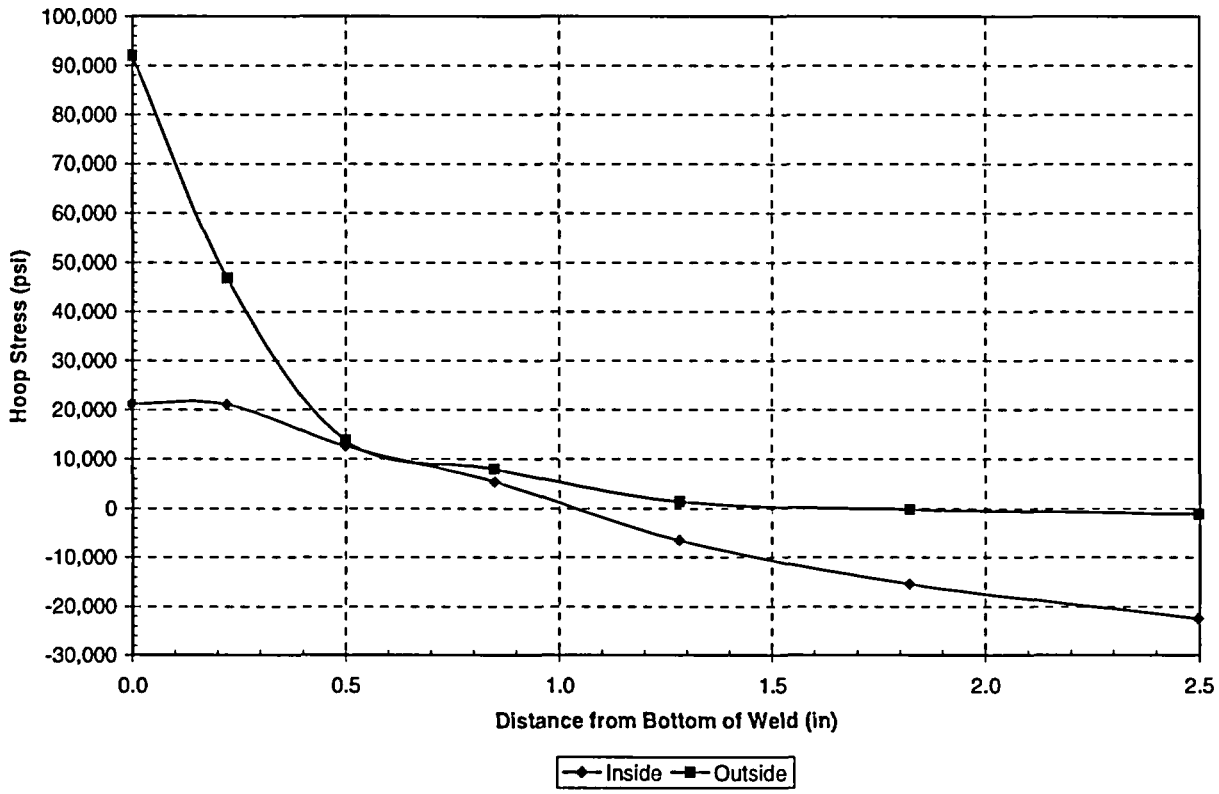

Figure A-7
Hoop Stress Distribution Below the Weld Uphill Side
(49.7° CEDM Penetration Nozzle)

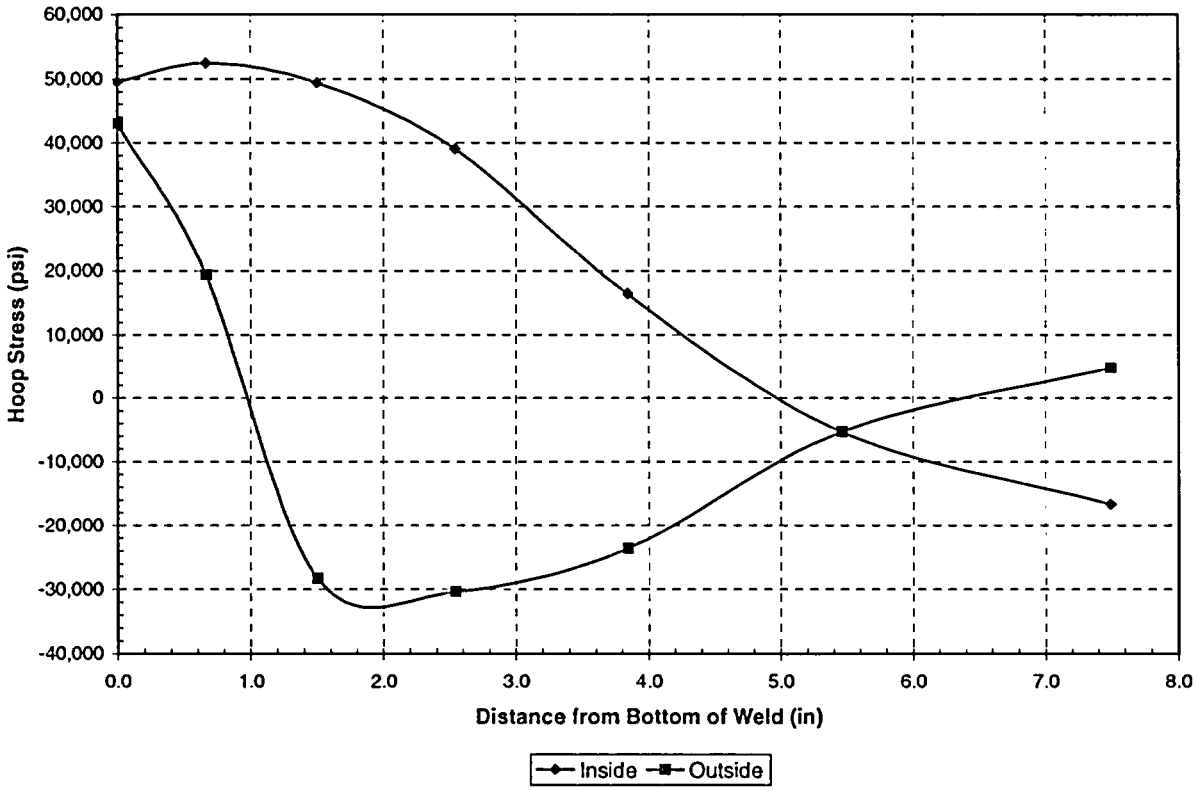

Figure A-8
Hoop Stress Distribution Below the Weld Downhill Side
(55.3° ICI Penetration Nozzle)

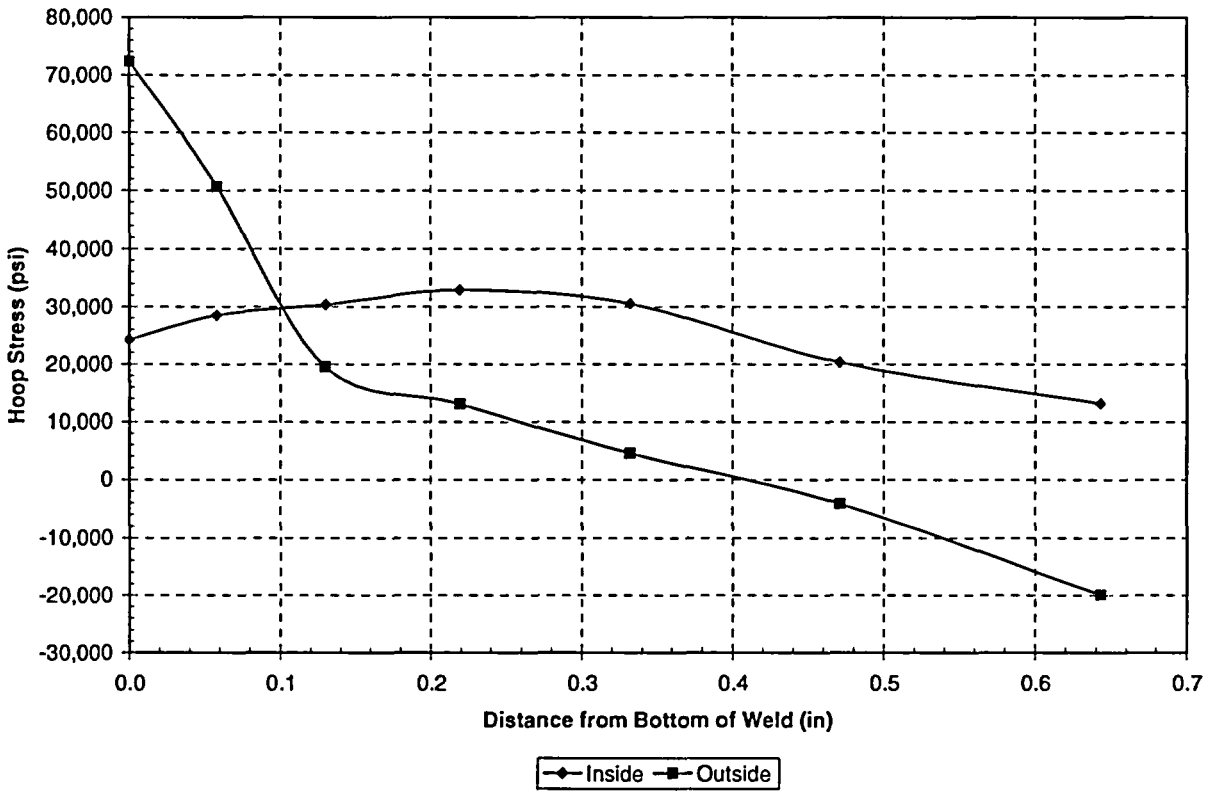

Figure A-9
Hoop Stress Distribution Below the Weld Uphill Side
(55.3° ICI Penetration Nozzle)

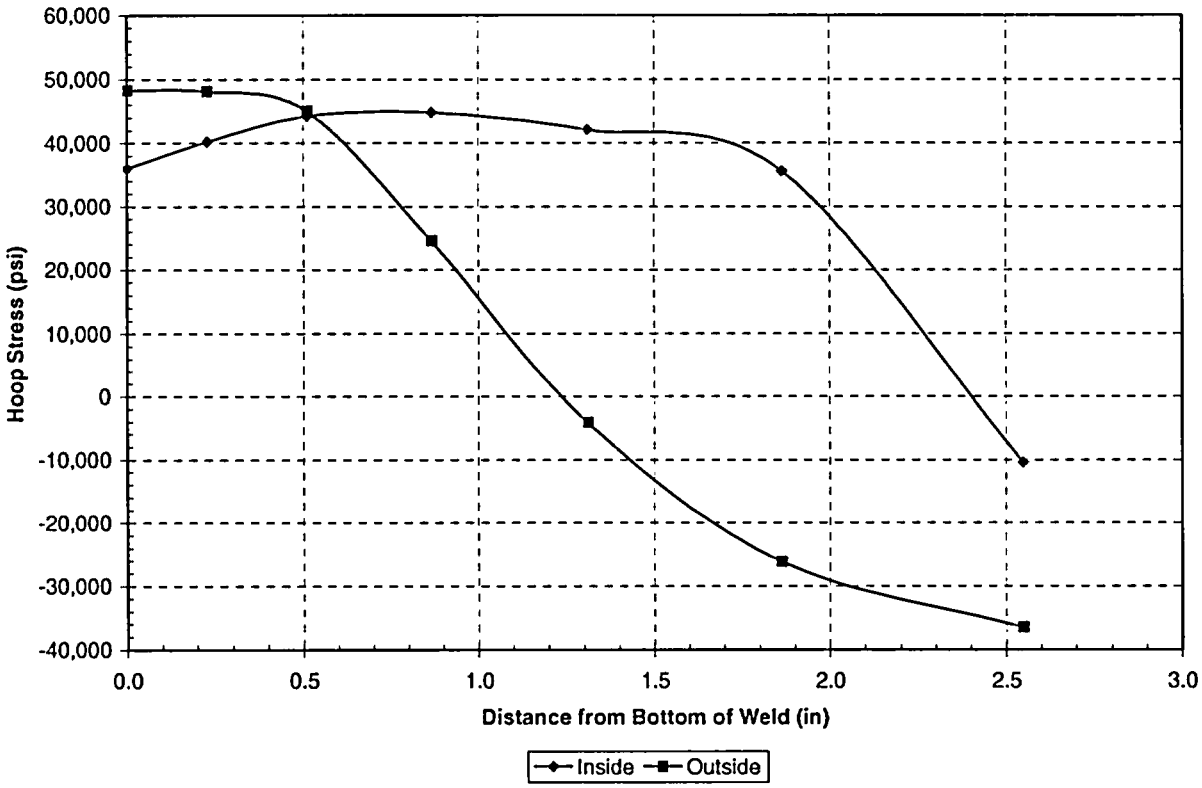

APPENDIX B

COMPARISON OF THE HOOP STRESS DISTRIBUTION BELOW THE WELD BETWEEN THE AS-BUILT AND AS-DESIGNED J-WELD GEOMETRY [16]

Figure B-1
Nozzle ID and OD Hoop Stress (0° CEDM Nozzle Downhill and Uphill Case)

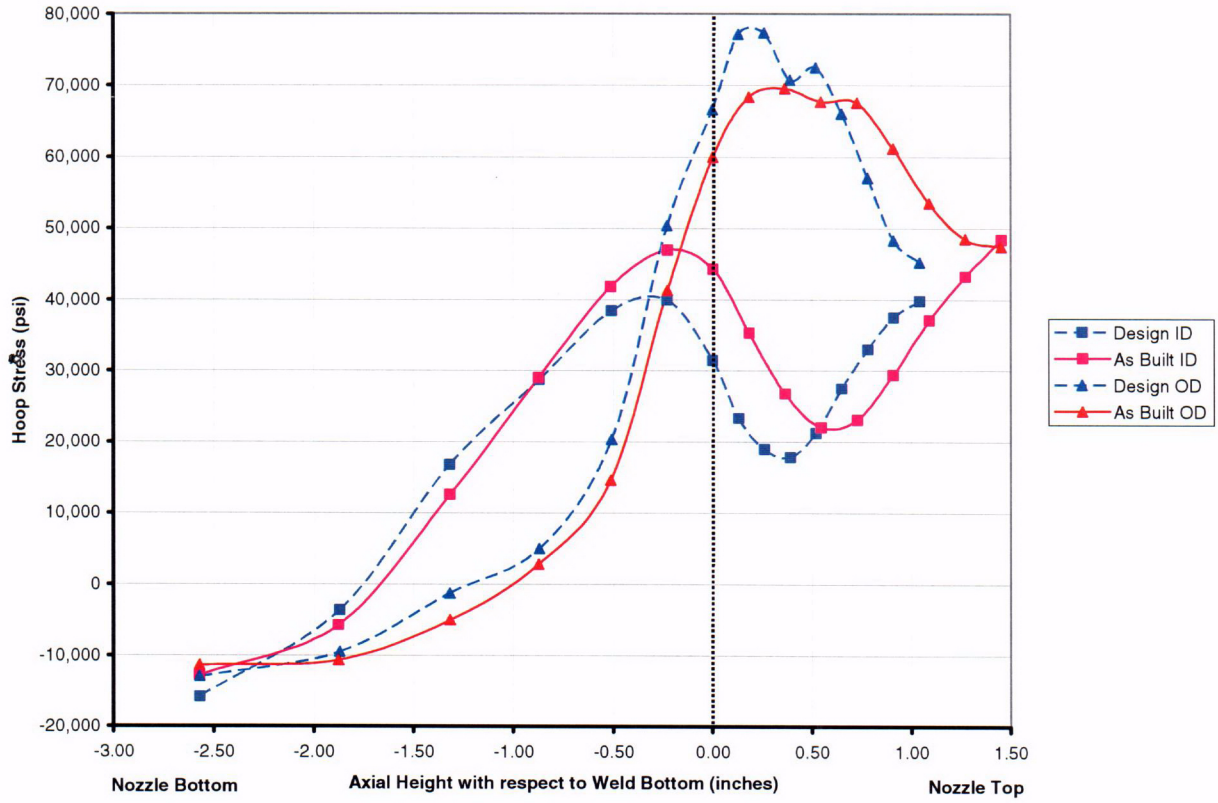

Figure B-2
Nozzle ID and OD Hoop Stress (7.8° CEDM Nozzle Downhill Case)

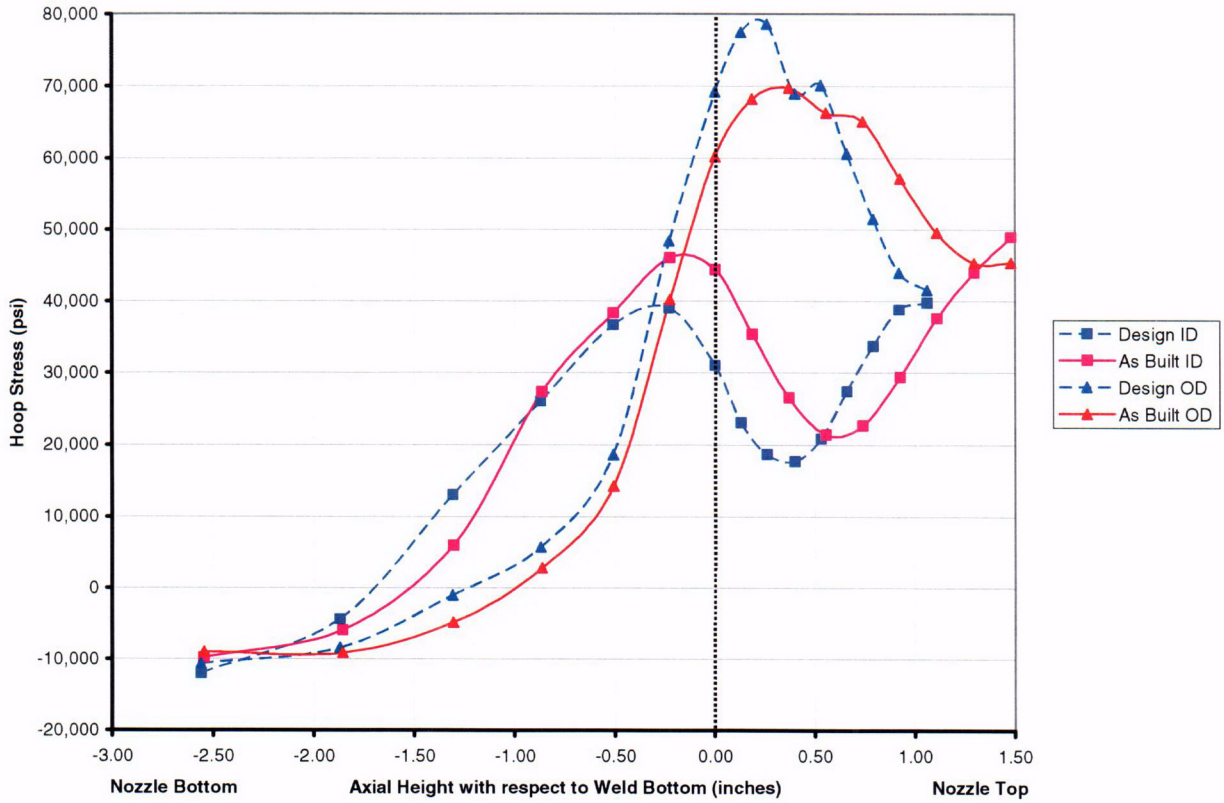

C27

Figure B-3
Nozzle ID and OD Hoop Stress (7.8° CEDM Nozzle Uphill Case)

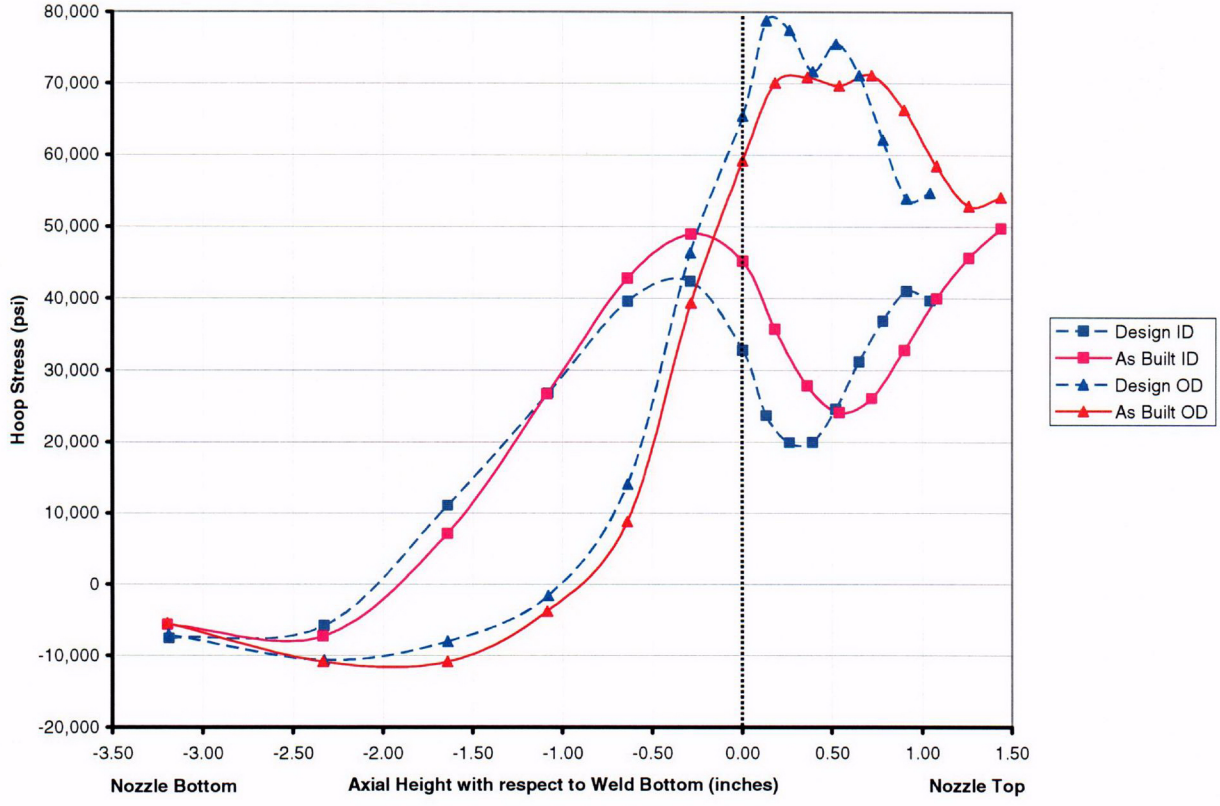

CZ8

Figure B-4
Nozzle ID and OD Hoop Stress (29.1° CEDM Nozzle Downhill Case)

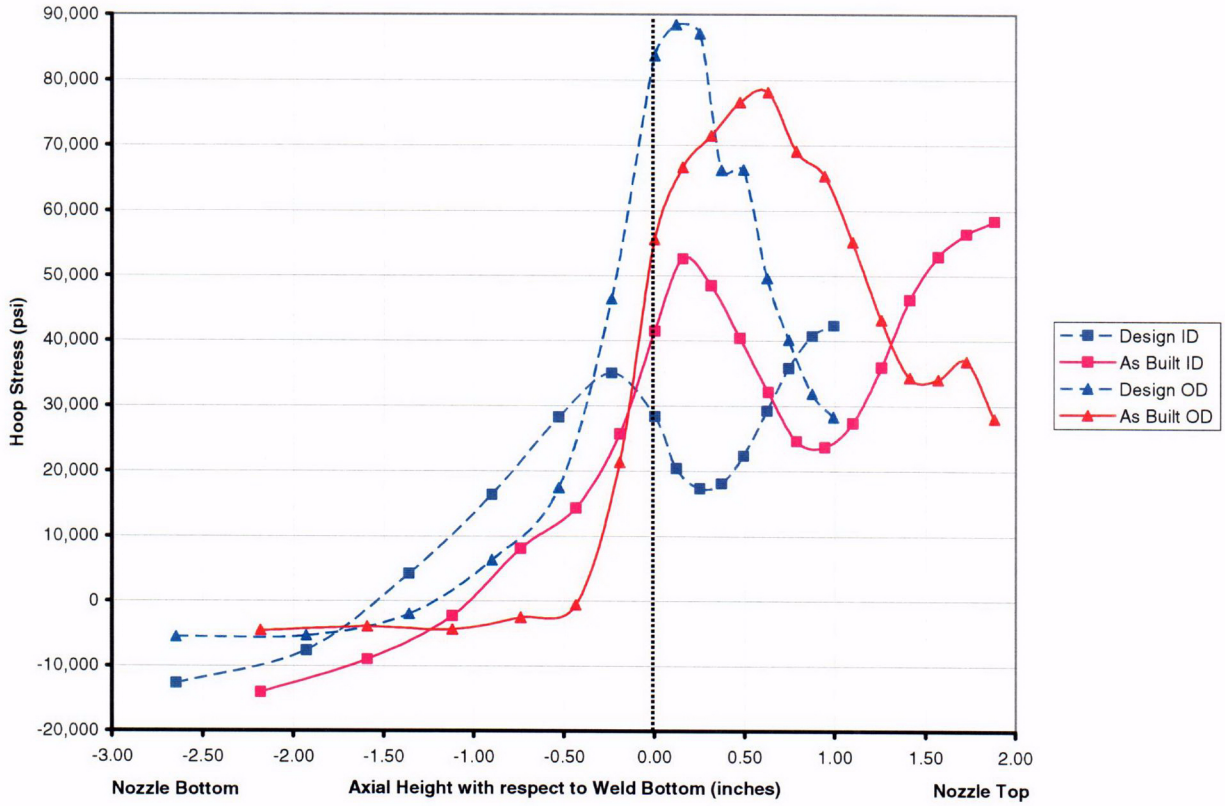

C29

Figure B-5
Nozzle ID and OD Hoop Stress (29.1° CEDM Nozzle Uphill Case)

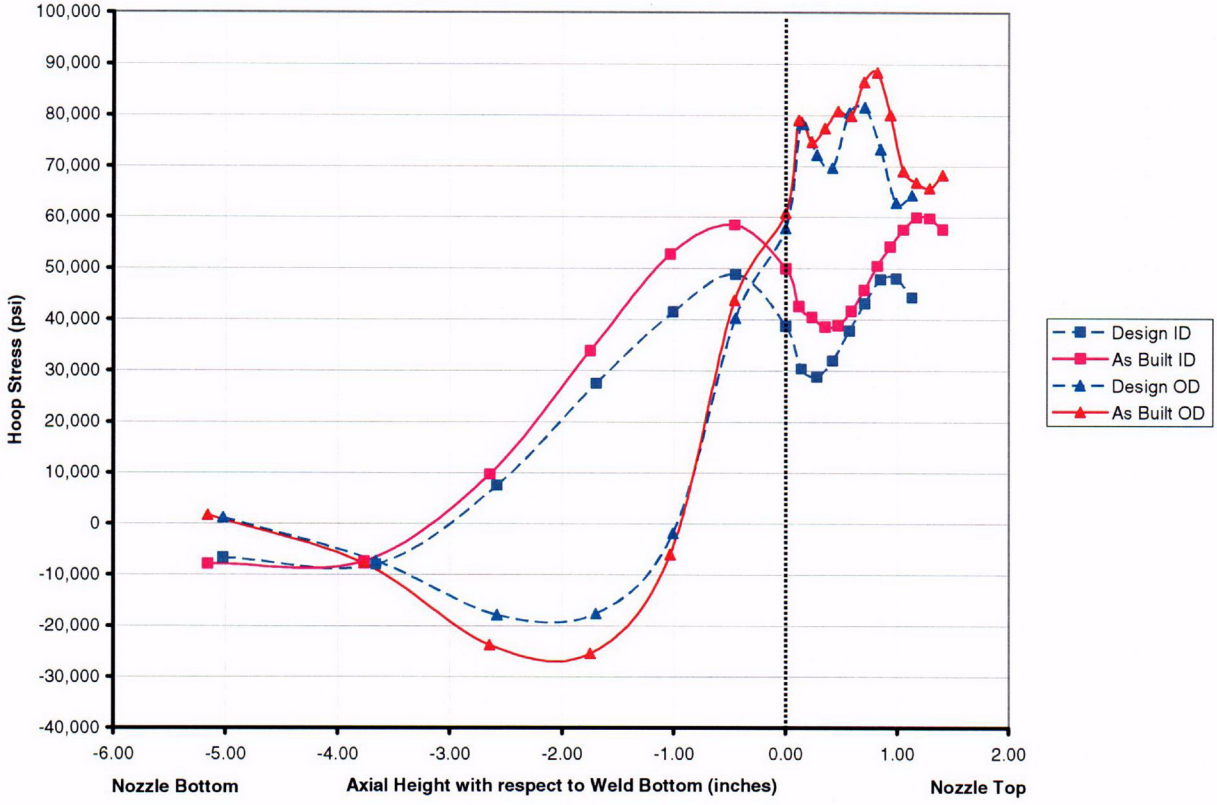

C39

Figure B-6
Nozzle ID and OD Hoop Stress (49.7° CEDM Nozzle Downhill Case)

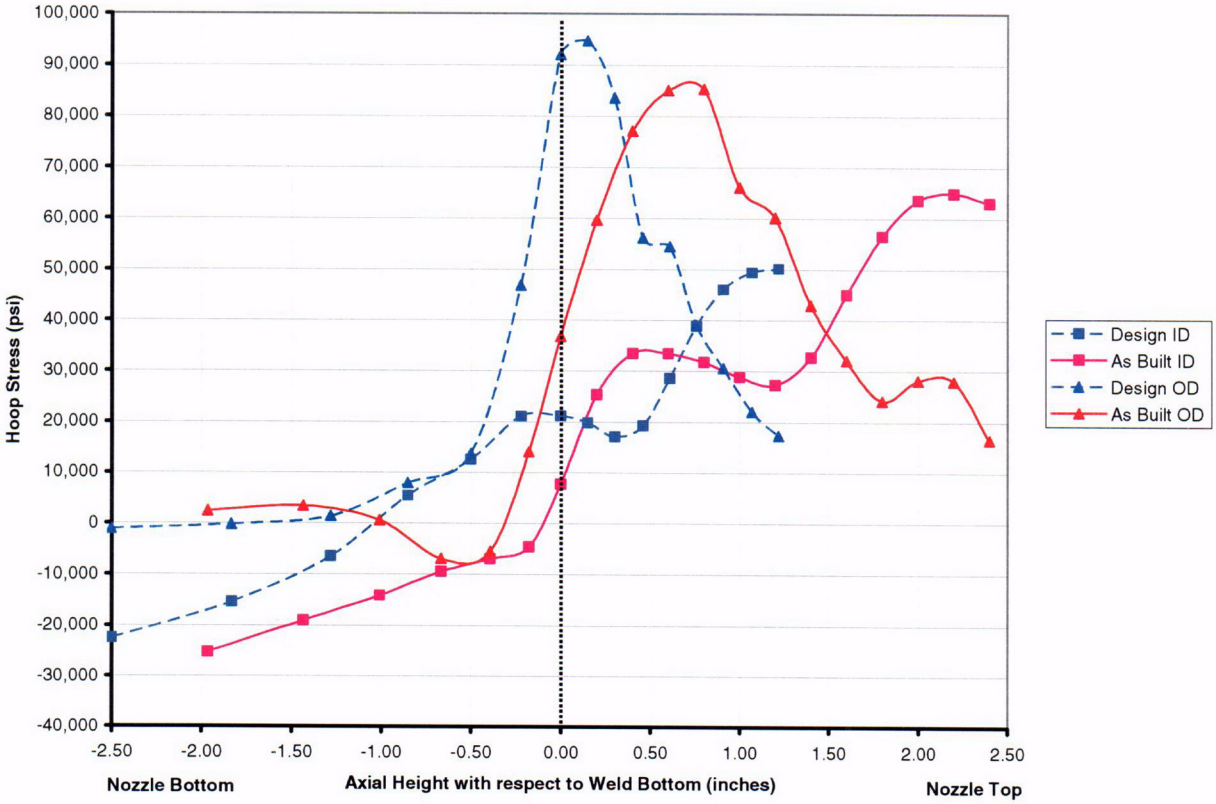

C31

Figure B-7
Nozzle ID and OD Hoop Stress (49.7° CEDM Nozzle Uphill Case)

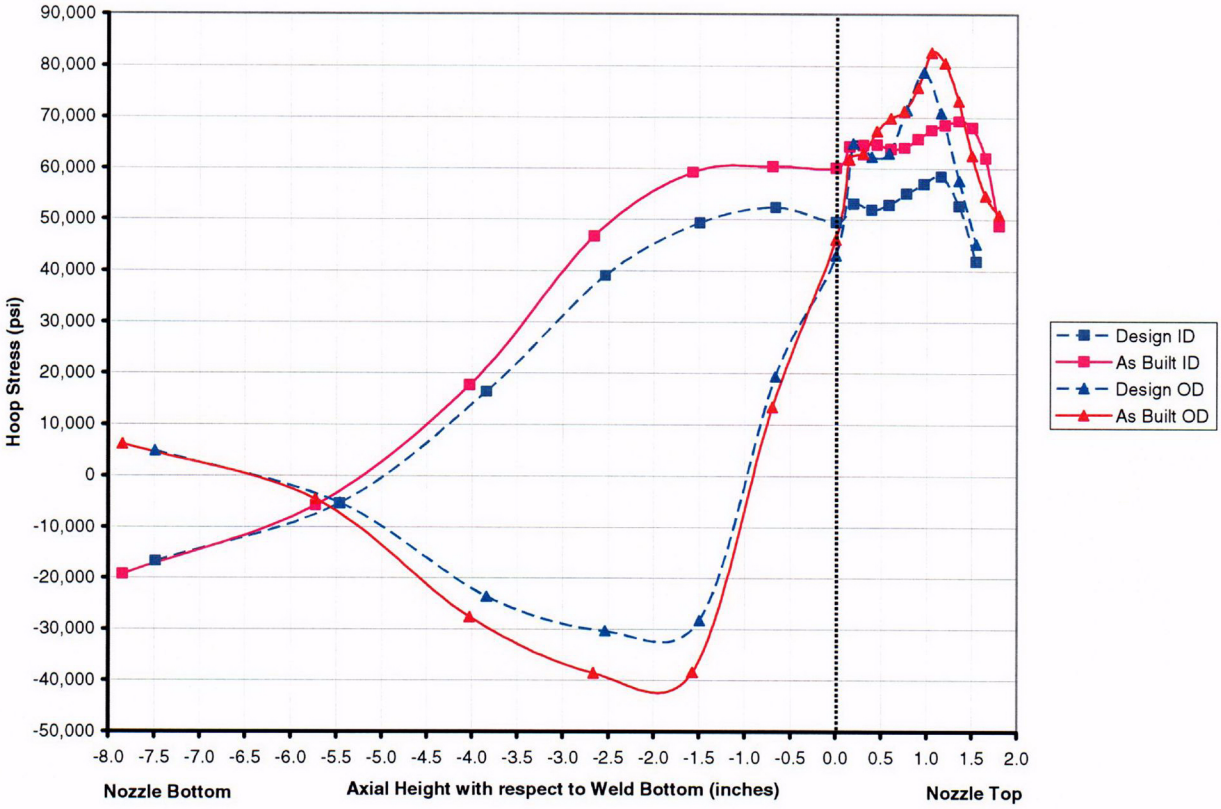

C32

Figure B-8
Nozzle ID and OD Hoop Stress (55.3° ICI Nozzle Downhill Case)

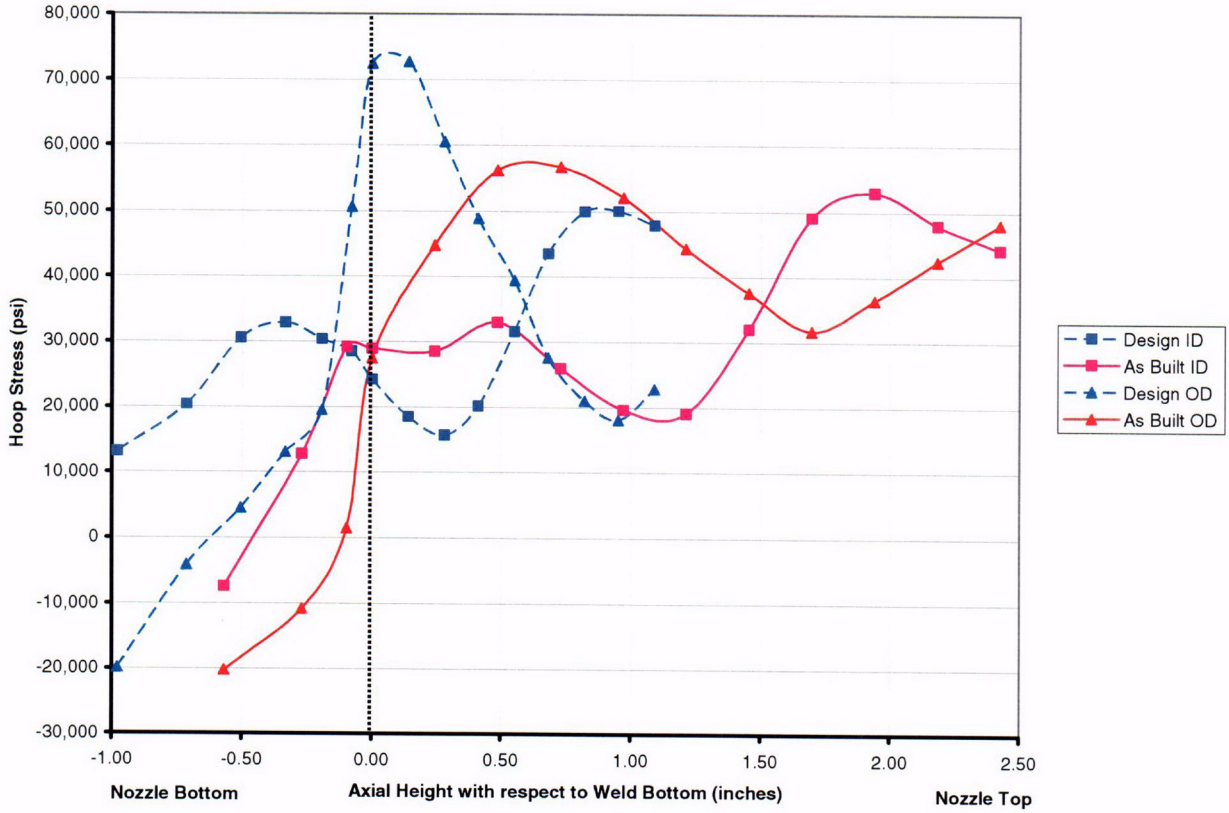

C33

Figure B-9
Nozzle ID and OD Hoop Stress (55.3° ICI Nozzle Uphill Case)

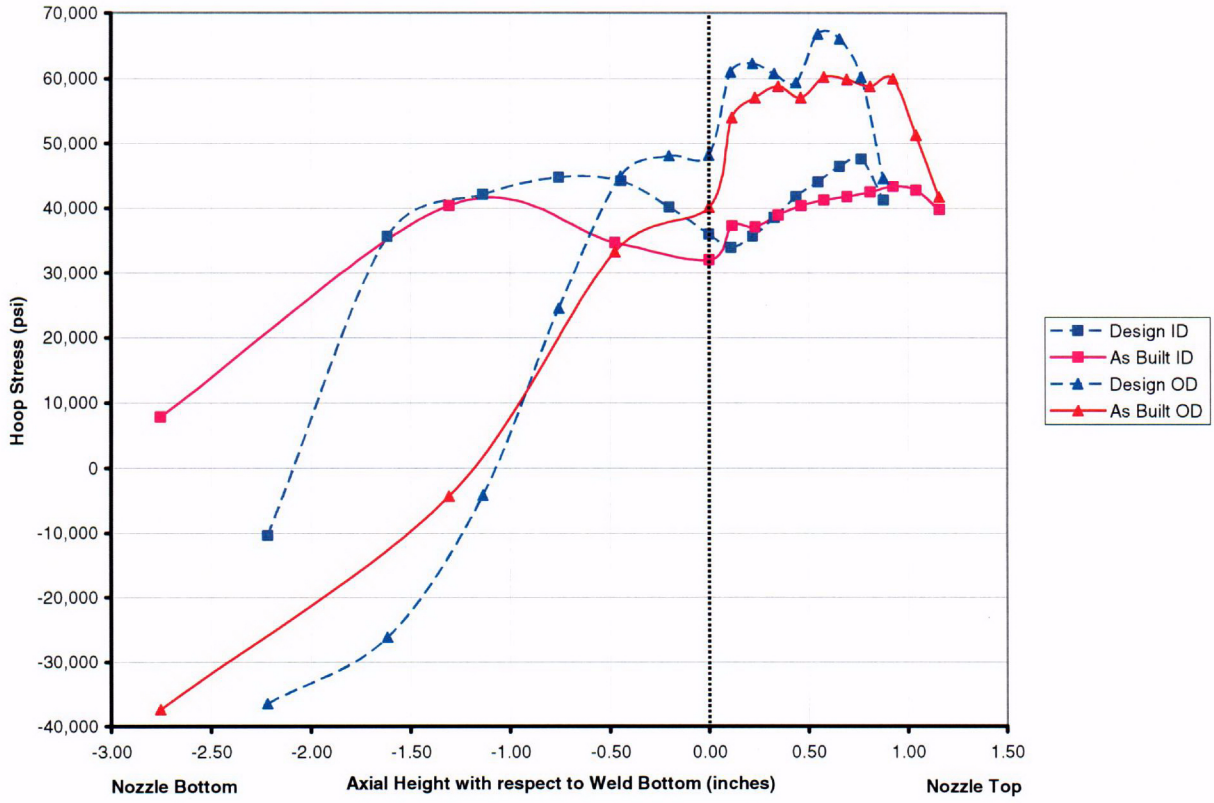

C34

APPENDIX C

THROUGH-WALL FLAW GROWTH BELOW THE WELD CHARTS

(LIMITING CASE)

Note that in Figures C-1 through C-5, the initial through-wall flaw size is determined by assuming that the lower extremity of the flaw is located on the penetration nozzle where either the inside or outside surface hoop stress drops below 0 ksi.

Figure C-1
Through-Wall Axial Flaws Located in the Center CEDM (0.0 Degrees) Penetration

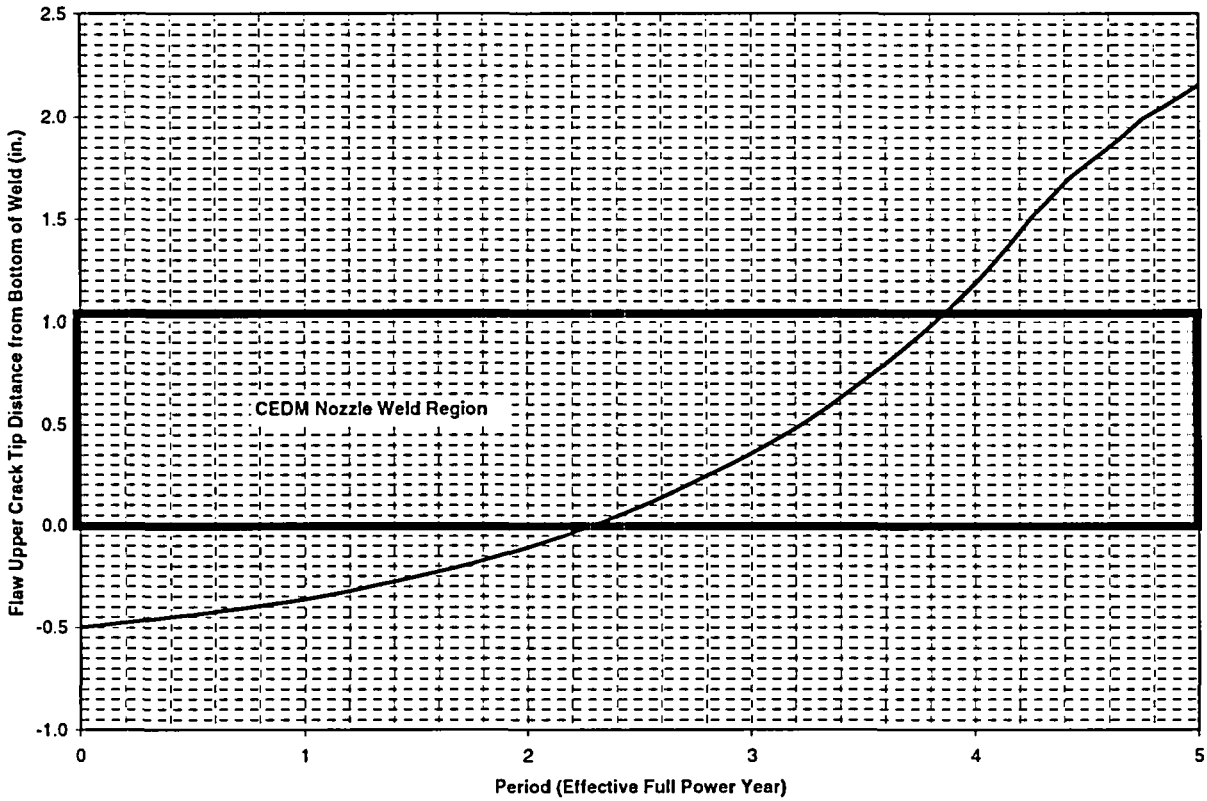

Figure C-2
Through-Wall Axial Flaws Located in the 7.8 Degrees Row of CEDM Penetrations Downhill Side

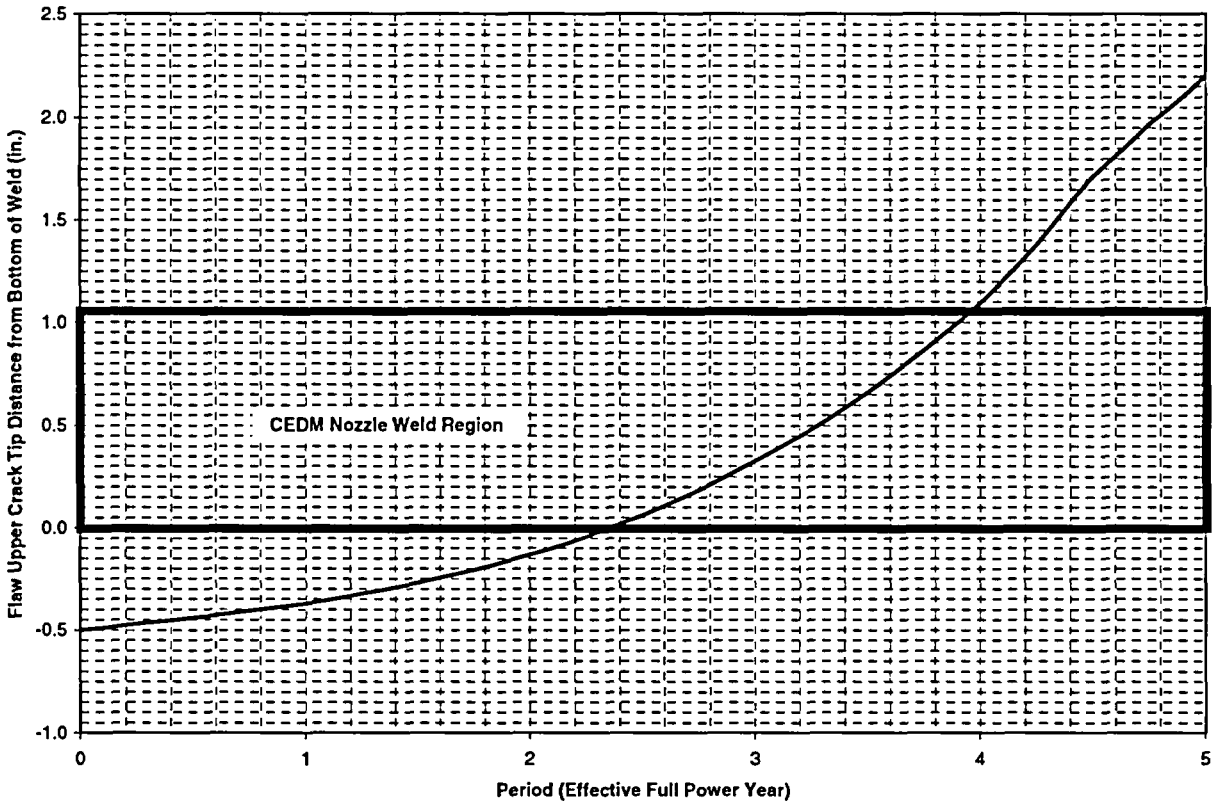

Figure C-3
Through-Wall Axial Flaws Located in the 29.1 Degrees Row of CEDM Penetrations
Downhill Side

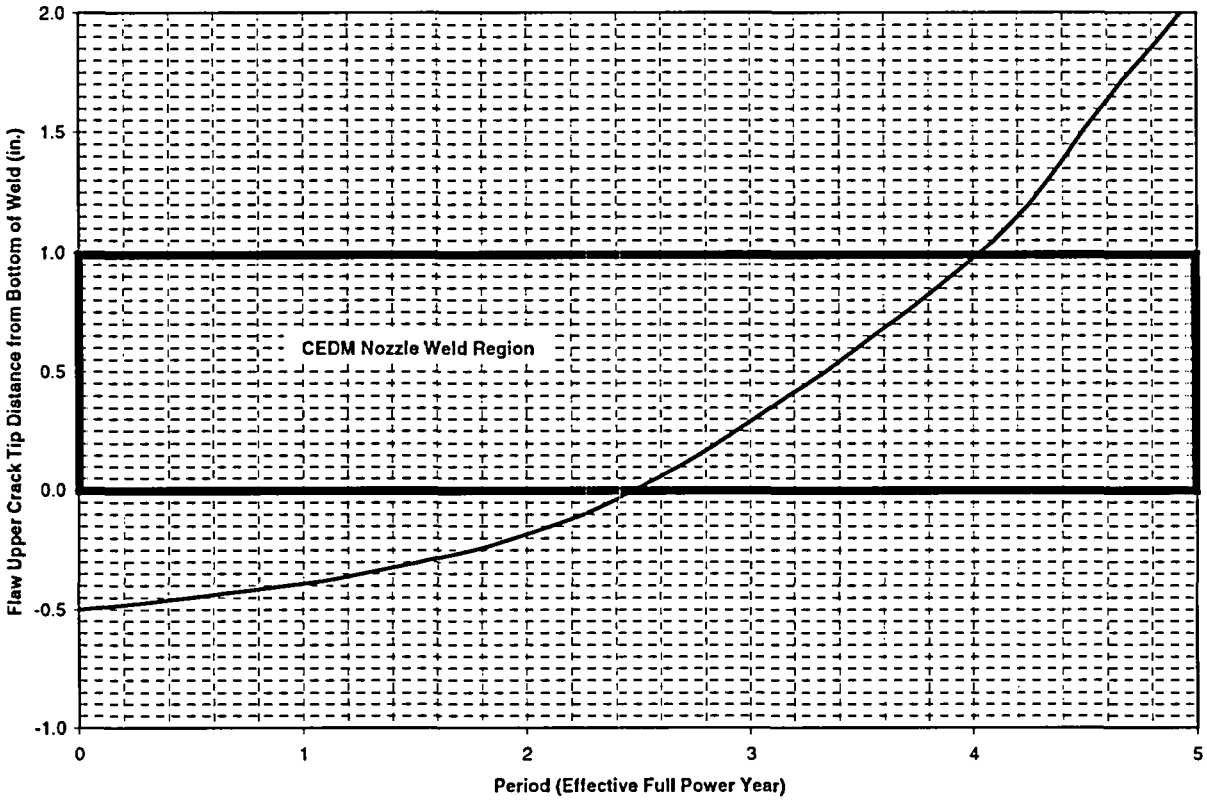

Figure C-4
Through-Wall Axial Flaws Located in the 49.7 Degrees Row of CEDM Penetrations
Downhill Side

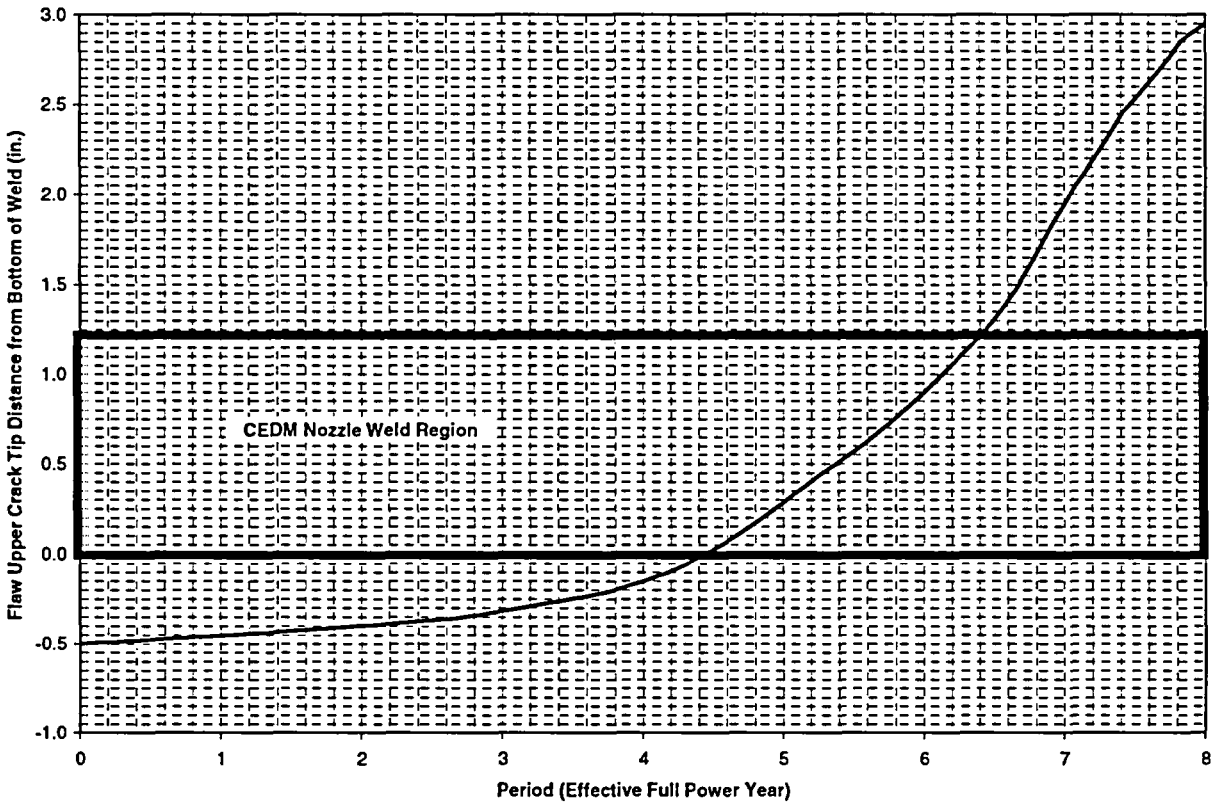

Figure C-5
Through-Wall Axial Flaws Located in the 55.3 Degrees Row of ICI Penetrations
Downhill Side

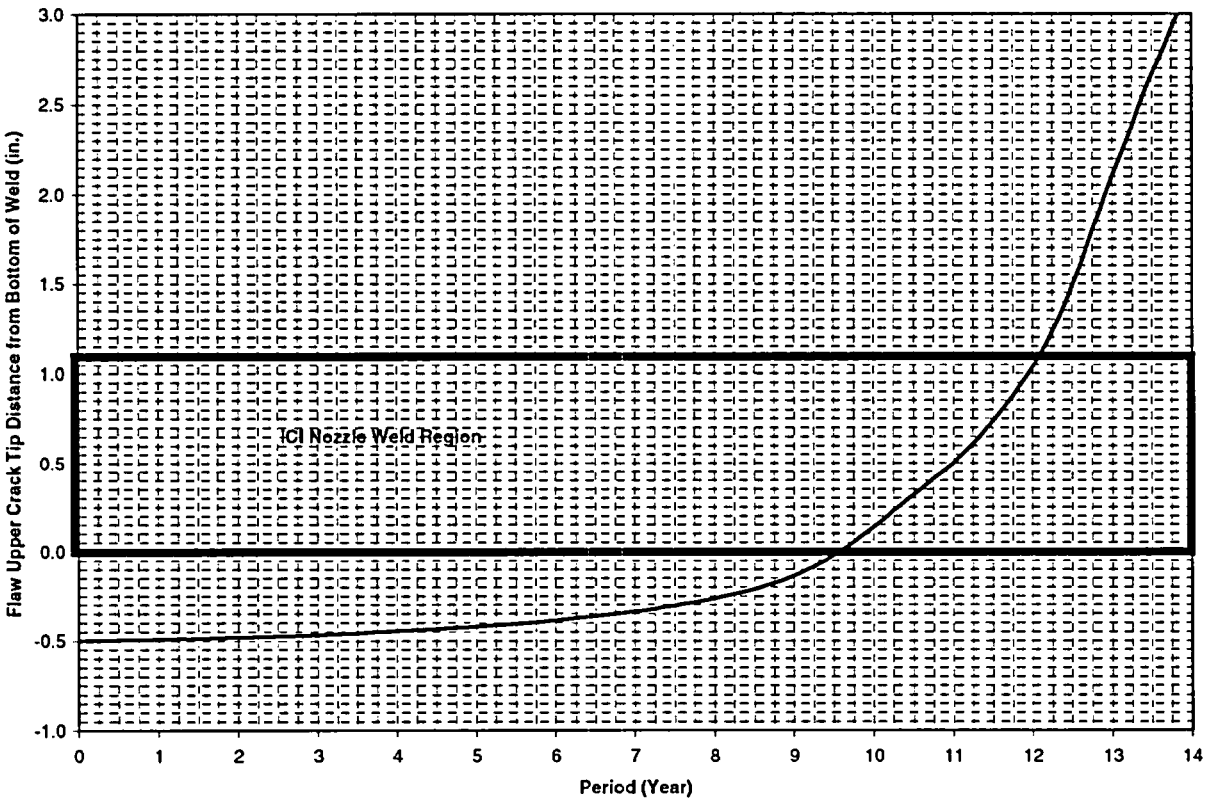

Figure C-6
Through-Wall Axial Flaws Located in the 55.3 Degrees Row of ICI Penetrations
Uphill Side

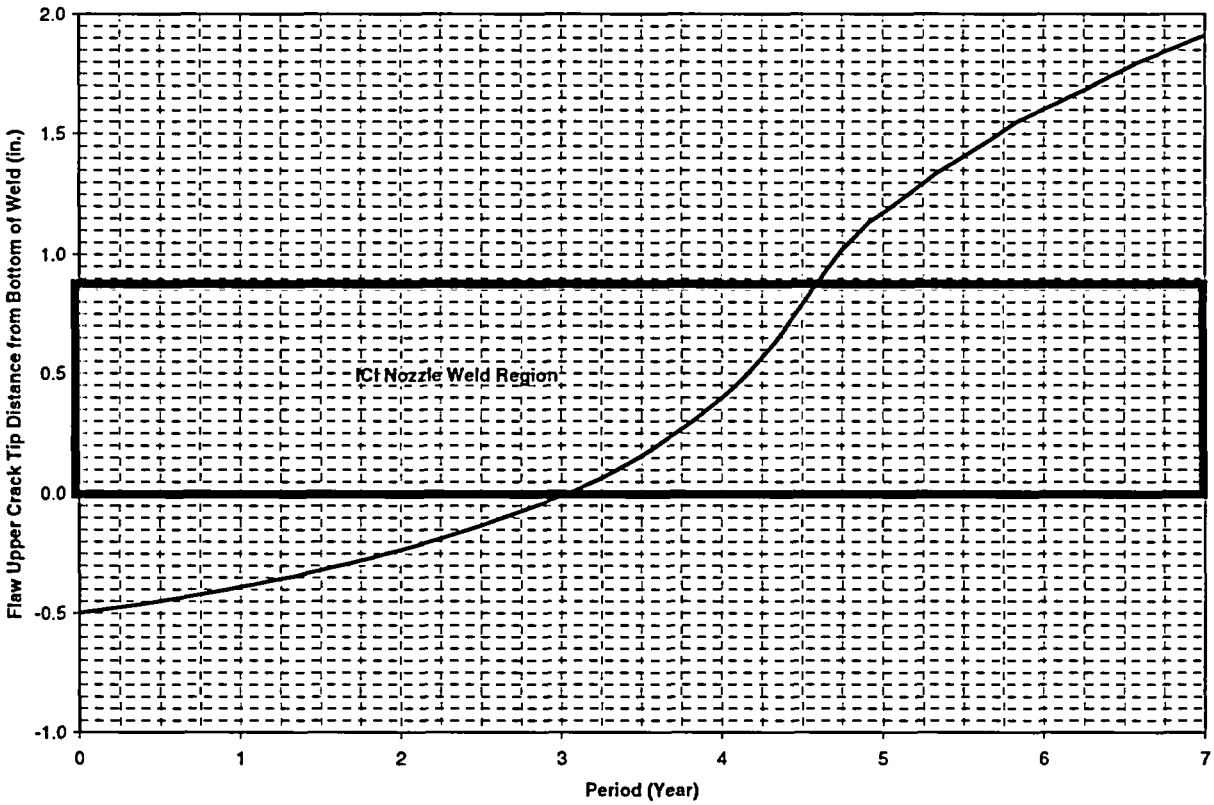

Attachment 4

SCE Responses to NRC Request for Additional Information Summary Information Regarding Relaxation Requests 1 and 2

SCE Drawing SO23-901-89

THIS PAGE IS AN OVERSIZED DRAWING OR FIGURE,

THAT CAN BE VIEWED AT THE RECORD TITLED: DRAWING NO. 234-582, "CLOSURE HEAD INSTRUMENT NOZZLE DETAILS"

WITHIN THIS PACKAGE... OR BY SEARCHING USING THE DOCUMENT/REPORT NO. 234-582

D-01

Attachment 5

SCE Responses to NRC Request for Additional Information Summary Information Regarding Relaxation Requests 1 and 2

SCE Drawing SO23-901-225

REVISIONS

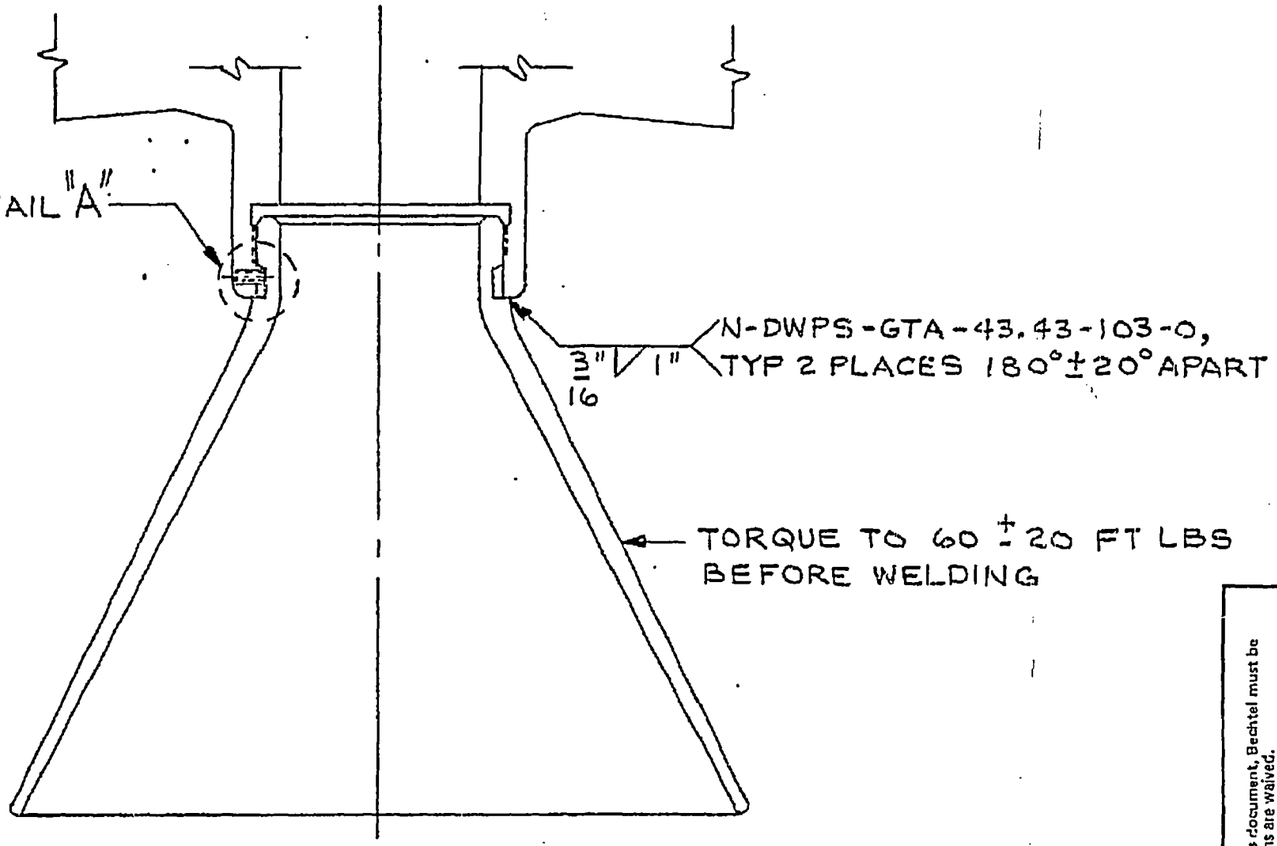

GUIDE CONE ATTACHMENT

SCALE 6" = 12"

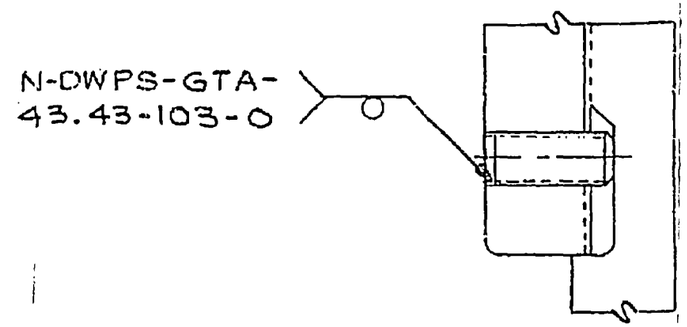

DETAIL "A"

SCALE 24" = 12"

☐ This revised Vendor Document incorporates changes associated with a Design Change Package (DCP).

DCP Number _____

☐ This Vendor Document revision does not reflect any physical plant modification and is not associated with a DCP or FCR.

Explain change New submittal

Reviewed by Brian Ward Date 5/8/86

PF-6183 (10072) 9/83

MICROFILM QUALITY ACCEPTABLE

S023-901-225-0

CONTRACT 71170

IMPORTANT
If the price or schedule is affected by this document, Bechtel must be notified prior to fabrication or such claims are waived.
Permission to proceed does not constitute acceptance or approval of documents involving design details, calculation, analysis or test report and is only an acceptance of the method used by the supplier. Supplier retains full responsibility for design.
Issuance of this document does not relieve the supplier from full responsibility for contract or purchase order requirements including, but not limited to, adequacy and suitability of materials and/or equipment represented thereon for the intended function.

DATE RECEIVED 5-22-85

DOC STATUS BY Brian Ward

DATE 5/8/86

DOCUMENT STATUS
1 ☒ Manufacturer may proceed
3 ☐ Exceptions as noted. Make changes and resubmit. Manufacturer may proceed.
4 ☐ Correct and resubmit.
7 ☐ Information only. ☐ Distribution required.

PF-1218 (10079) 8/82

GUIDE CONE MODIFICATION

FOR SAN ONOFRE II
172" ID PWR

SCALE AS NOTED
DRAWN BY J. STEWART
TRACED BY

DATE 10-5-84
CHECKED BY J.K. CLEMONS
APPROVED R.W. Scott

COMP. CODE:

DRAWING NO. B-246-857-0